The role of intraflagellar transport in cilia maintenance

Sascha Werner

Dissertation presented to obtain the Ph.D degree in Cell Biology

Instituto de Tecnologia Química e Biológica António Xavier | Universidade Nova de Lisboa

Research work coordinated by:

FUNDAÇÃO CALOUSTE GULBENKIAN
Instituto Gulbenkian de Ciência

Oeiras, October, 2017

Table of Content

Declaration 7
Declaração 7
Acknowledgements 9
Abbreviations 11
Summary 13
Sumário 17
Chapter I – Introduction: From the advent of cell theory to the problem of cilia maintenance 21
Introduction to the cytoskeleton – a historical perspective 23
The beginnings of cell theory and the cytoskeleton 23
Microtubules – not just for mitosis 28
Actin – contraction and expansion 31
Intermediate filaments – Stability and organization 32
What makes a cytoskeletal element and are there more? 33
Centrosomes and cilia – From rudimentary organelles to master regulators of cellular function 35
The discovery of centrosomes, cilia and their relationship 37
Centrosomes – Appropriate numbers and structures 42
Centrosome-associated diseases 45
Cilia – Structure and function 47
Intraflagellar transport – Essential for ciliogenesis? 50
Cilia assembly and disassembly 55
Cilia and the cell cycle – Can cilia block cell proliferation? 57
Cilia and the signalling pathways – A hub for everything? 58
Ciliopathies – What happens when cilia (functions) are lost? 62
Evolution of centrioles and cilia 66
The cilia maintenance problem 68

Maintenance in molecular and cell biology 68
What do we know about maintenance of cilia? 69
Drosophila as a model to address cilia maintenance 73
Drosophila chordotonal neurons – Development, architecture and function 76
A role of IFT88 in the maintenance of the photoreceptor ciliary signalling compartment 78
Introduction to cGMP signalling 80
Photoreceptor cGMP signalling in health and disease 81
Main objectives of this thesis 84
Chapter II – IFT88 as a case study for the role of IFT in cilia maintenance 85
Author contribution 87
Summary 87
Ciliated sensory neurons in adult *Drosophila* as a system to study cilia maintenance 89
Current understanding of IFT in *Drosophila* 90
Goals 91
Experimental strategy 92
Material and methods 93
Bioinformatic analysis of DmIFT88/NompB 93
Cryosectioning and immunolabeling of *Drosophila* antennae 94
mRNA isolation from adult antenna and reverse transcription 95
Cloning of DmIFT88/NompB and generation of transgenic flies 97
Live imaging of chordotonal cilia in L3 larvae 99
Quantification of NompB expression levels from adult antennae 100
Biophysical recordings from adult antennae 101
Electron microscopy: Sample preparation and image acquisition 102

Behavioural assessment of gravitaxis defects 102
Cuticle clearing and imaging of antennae whole-mounts 104
Results 105
Bioinformatic analysis of IFT88 reveals sequence divergence, but suggests structural conservation..... 105
DmIFT88/NompB expression and protein localisation in adult antenna 107
DmIFT88/NompB expression and protein localisation in adult antenna 109
IFT88 undergoes IFT in chordotonal neurons of L3 larvae 109
Validation of DmIFT88/NompB hairpin for mRNA knockdown 114
Inducible knockdown of DmIFT88/NompB causes gravitaxis defects without obvious structural defects in chordotonal cilia 116
Discussion and conclusions 121
Acknowledgements 126
Chapter III – Insights into the transport of the evolutionary conserved guanylyl cyclase CG34357 suggest disease mechanism 127
Author contribution 129
Summary 129
Introduction 130
Known roles of guanylyl cyclases in sensory cilia 131
Leber congenital amaurosis (LCA) and Gucy2d transport 132
Goals 134
Experimental strategy 134
Material and methods 135
Bioinformatic analysis of guanylyl cyclase sequences 135
Screen for potential Gucy2d homologue using gravitaxis assays 136
Detection of CG34357 gene expression 138

Cryosectioning and immunolabeling of *Drosophila* antennae 140
Cloning of CG34357 and generation of transgenic flies 140
Cell culture and immunoprecipitation experiments 143
Results 144
CG34357 is a potential homologue for mouse Gucy2e 144
CG34357 is expressed in chordotonal neurons 148
CG34357 shows specific localisation in chordotonal neurons 152
CG34357 binds NompB in cultured cells 154
NompB-binding domain on CG34357 is involved in localisation of the cyclase 156
Lethality caused by CG34357 overexpression is caused by the cyclase domain 159
Sequence comparison reveals strong conservation of the CG34357 DmIFT88/NompB-binding domain with potential disease relevance 160
Discussion and conclusions 164
Chapter IV – Final discussion 171
Regulation of IFT waiting time and remodelling 175
Does IFT have different roles in ciliogenesis and cilia maintenance? 176
A refined transport model for Gucy2d/CG34357 transport 179
Role of CG34357 in chordotonal cilia function 181
Implications of findings for maintenance and turnover in general 182
Final remarks 184
References 185

Declaration

I declare that this dissertation and the data presented are the result of my own work, as developed between 2013 and 2017 in the laboratory of Dr. Mónica Bettencourt-Dias at the Instituto Gulbenkian de Ciência in Oeiras, Portugal. Specific contributions are indicated in each chapter.

Financial support was granted by Fundação para a Ciência e a Tecnologia, doctoral fellowship SFRH/BD/52176/2013.

Declaração

Declaro que esta dissertação de doutoramento e os dados nela apresentados são o resultado do meu trabalho, desenvolvido entre 2012 e 2017 no laboratório do Dr. Mónica Bettencourt-Dias no Instituto Gulbenkian de Ciência em Oeiras, Portugal. As contribuições são indicadas em cada capítulo.

O apoio financeiro foi concedido pela Fundação para a Ciência e Tecnologia, através da bolsa de doutoramento SFRH/BD/52176/2013.

Acknowledgements

Many people were crucial for me to get to this point. It will be difficult to do all of them justice, but I will try.

I have to thank the person that allowed me develop this thesis - Mónica. Being a PhD student has a lot in common with coming of age. At the start there is a scientific infant and at the end, hopefully, a tolerable scientist. And then there is a lot of struggling in between. It was not always easy, but I am glad you embarked on this journey with me! I learnt with you and I owe you a lot. Obrigado.

Staying with the theme, I want to thank my scientific godparents next - Raquel and Miguel. Thank you for your patience and your input and thank you for pushing me a little further every year. I think it was necessary.

I want to thank the CCR lab. I truly was the “stubborn student”, but you all supported me along the way. I cannot help, but express special thanks to two members of the lab – Ana and Sihem. Ana, because we wrote “that thing” together. It was not easy, but I am proud of it now. And Sihem, because without your confidence in my work and your golden hands, I would not have these results.

Extending out from there, I have to thank the entire IGC community: Starting with Élio and Manuela, who were always there when I needed them. But there were so many more that I could always count on. Sometimes when I least expected it. I cannot name everyone, but being at IGC was truly a special experience.

We save the best for last (almost). I am forever indebted to my “support system” to steal a word from Ojas. Without you, without the craziest nights, without your company I would not have made it to the end. You accepted me, you supported me, you contradicted me and fought with me and when necessary you carried me. Thank you!

Der letzte Dank geht an dich, Micha. Eigentlich müsstest du ganz oben stehen. Danke, dass du mir dieses Abenteuer erlaubt hast. Es war hart und hat manchmal sehr weh getan. Es hat einiges gekostet, aber es gab auch viel zurück. Und ich freue mich auf so viele weitere Abenteuer mit dir. Ich liebe dich.

Abbreviations

ADP	Adenosine diphosphate
ATP	Adenosine triphosphate
CDK1	Cyclin-dependent kinase 1
Cep290	Centriolar protein 290
cGMP	Cyclic guanosine monophosphate
DmIFT88	Drosophila melanogaster IFT88
eIF-1A	Eukaryotic translation initiation factor 1A
FoxJ1	Forkhead Box J1
GC	Guanylyl cyclase
GDP	Guanosine diphosphate
GLI	Glioblastoma transcription factor
GTP	Guanosine triphosphate
Gucy2d	Guanylyl cyclase 2d
HDAC 6	Histone deacetylase 6
Iav	Inactive (TRP channel - vanilloid type)
IFT	Intraflagellar transport
LCA	Leber congenital amaurosis
LECA	Last eukaryotic common ancestor
MAPs	Microtubule-associated proteins
MT	Microtubules
MTOC	Microtubule organizing centre
Nan	Nanchung (TRP channel - vanilloid type)
NompB	No membrane potential B (IFT88 homologue)
NompC	No membrane potential C (namesake of the TRPN subgroup)
PCM	Pericentriolar matrix
PDE	Phosphodiesterase

PLK1	Polo-like kinase 1
PLK4	Polo-like kinase 4
PLP	Pericentrin-like protein (PCM component)
Rfx	Regulatory factor X
Smo	smoothend
Su(Tpl)	Suppressor of Triplo-lethal locus
TBP	TATA-binding protein
TRP	Transient receptor potential channel

Summary

Cilia are microtubule-base protrusions from the surface of most cells in the human body. They can be found in species from all branches of the eukaryotic tree of life and were probably already present in the last eukaryotic common ancestor (Carvalho-Santos et al., 2011). In all ciliated species, cilia are crucial for the development and physiology of the organism, and they carry out many different functions ranging from motility to sensing (Choksi et al., 2014).

In some cells cilia can persist for long periods of time, which is the case for the connecting cilium in vertebrate photoreceptors. Photoreceptors turn over their ciliary compartment within days (Besharse and Hollyfield, 1979), but in the green alga *Chlamydomonas* there is evidence for significant turnover of ciliary proteins within hours (Song and Dentler, 2001). Protein turnover is energetically costly for a cell. The fact that it occurs anyway at a high rate suggests that it is necessary to maintain the function of the ciliary compartment.

Cilia are distinct in their protein composition from the rest of the cell. The ciliary proteome is estimated to consist of up to 600 different proteins (Mick et al., 2015). This results from the activity of a protein complex called intraflagellar transport (IFT) that imports proteins specifically into the ciliary compartment (Taschner and Lorentzen, 2016). IFT is essential for the formation of most cilia. We still know little about how individual IFT complex members contribute to ciliary properties. Deactivating IFT in a fully formed cilium in a mouse photoreceptor leads to retina degeneration and blindness (Jiang et al., 2015). Furthermore, mutations in genes involved in ciliary trafficking can give rise to retina-specific ciliopathies such as Leber congenital amaurosis (LCA). The onset of the disease, however, can

vary between patients (den Hollander et al., 2008). This variability suggests that in some cases a functional photoreceptor was built but could not be maintained. Understanding the mechanisms underlying ciliary maintenance could hence help to predict the outcome of mutations in cilia genes as well as help to develop therapy options. It is now accepted that ciliary function needs to be actively maintained by IFT (Eguether et al., 2014; Fort et al., 2016; Jiang et al., 2015; Kozminski et al., 1995), but it is not clear how maintenance is regulated.

Ciliated sensory neurons in the fruit fly *Drosophila melanogaster* are a great model for cilia maintenance. The cilia are formed at the beginning of each developmental stage, and the cells are not replaced. They are essential for sensing (e.g. gravitaxis or olfaction), and perturbations in cilia function can easily be monitored in behavioural assays. Here I provide evidence that the evolutionary conserved IFT subunit IFT88 (called NompB in the fly) undergoes continuous trafficking in fully formed cilia. The contribution of the protein to maintenance of cilia function was investigated in knockdown experiments. In depletion of DmIFT88/NompB, flies show defects in gravitaxis behaviour. These findings indicate that IFT is required in the fly to maintain cilia function. Analysis of cilia compartmentalisation and morphology indicates changes in the cilia upon depletion of DmIFT88/NompB. The underlying molecular mechanism, however, remains unclear. In the search for a distinct DmIFT88/NompB cargo, I discovered the fly homologue (CG34357) of an evolutionarily conserved cGMP-generating enzyme (Gucy2d). Gucy2d was previously shown to be trafficked to cilia by IFT88 in the mouse retina (Bhowmick et al., 2009). Through truncation experiments it was possible to define the binding side for DmIFT88/NompB on CG34357. Sequence comparisons revealed that the binding side is strongly conserved and is also the site for

mutations found in patients with LCA. Taken together these data suggest that the trafficking mechanism is similar in humans and flies, and the work presented here suggests a novel disease mechanism for LCA. Additionally, the work provides the first evidence for a role of cGMP signalling in mechanosensation and gives a clear example of a molecular property in cilia that is maintained by IFT. Little is still known about how IFT cargos are loaded and unloaded onto the complex and how trafficking is regulated. The identification of new cargos allows us to test and generalize hypotheses about IFT regulation and cargo interaction. After *Trypanosoma* (Fort et al., 2016), *Drosophila* seems to be the second species that does not use IFT for structural maintenance. Taken together these observations put into question whether all ciliary proteins and perhaps even ciliary structures in general depend on IFT for maintenance in those species.

Sumário

Os cilios são estruturas compostas maioritariamente por microtúbulos que crescem na superfície da maioria das células do corpo humano. Observa-se a sua existência em diferentes espécies dos vários ramos da árvore evolutiva dos eucariotas, o que sugere que estas estruturas já estavam presentes no antepassado eucariótico comum (Carvalho-Santos et al., 2011). Em todas as espécies ciliadas, os cílios são essenciais para o desenvolvimento ou para a fisiologia do organismo e desempenham variadas funções, desde motilidade até funções sensoriais (Choksi et al., 2014).

Em algumas células, os cílios podem persistir por longos períodos de tempo, como por exemplo, em fotorreceptores de vertebrados, que se estima levarem dias a renovar os componentes do seu compartimento ciliar (Besharse e Hollyfield, 1979). Por outro lado, há evidências de que em Chlamydomonas - uma alga verde - a renovação das proteínas ciliares pode levar sómente algumas horas (Song e Dentler, 2001). Este processo involve um grande dispêndio de energia para a célula, e o facto de mesmo assim ocorrer com elevada frequência, sugere que é essencial para a manutenção da funcionalidade do compartimento ciliar.

A composição proteica dos cílios é geralmente distinta do resto da célula. Prevê-se que o proteoma ciliar é constituído por cerca de 600 proteínas distintas (Mick et al., 2015). O complexo de transporte intraflagelar (IFT) é responsável pela importação selectiva de proteínas para o compartimento ciliar (Taschner e Lorentzen, 2016), sendo que a sua funcionalidade é essencial para a formação da maioria dos cílios. Ainda não são conhecidos todos os componentes do IFT; no entanto, a sua inactivação nos cílios fotoreceptores de

ratinho já totalmente formados, induz a degeneração da retina e consequente cegueira (Jiang et al., 2015). Além disso, mutações em genes envolvidos no tráfego ciliar podem originar ciliopatias específicas da retina, como a atrofia ótica de Leber (AOL). O estabelecimento da doença pode, no entanto, variar entre diferentes pacientes (den Hollander et al., 2008). Essa variabilidade sugere que, em alguns casos, um fotorreceptor funcional foi formado, mas não pôde ser mantido. A compreenção dos mecanismos subjacentes à manutenção ciliar poderá, portanto, ajudar a prever o resultado de mutações em genes ciliares, bem como a desenvolver alternativas terapêuticas. O princípio de que a função ciliar necessita de ser activamente mantida pelo IFT é actualmente aceite (Eguether et al., 2014; Fort et al., 2016; Jiang et al., 2015; Kozminski et al., 1995), não sendo no entanto claro como é regulada esta função.

Os neurónios sensoriais ciliados na mosca da fruta - *Drosophila melanogaster* - são um bom modelo de manutenção ciliar: os cílios formam-se no início de cada estadio do desenvolvimento e as células não são mais substituídas; são elementos sensoriais da célula (por exemplo, gravitaxia ou olfatação) e perturbações na função ciliar podem ser facilmente monitorizadas através de ensaios comportamentais.

Neste trabalho, são fornecidas evidências de que a subunidade evolutivamente conservada do IFT denominada IFT88 (NompB na mosca) é continuamente renovada em cílios já totalmente formados. A contribuição desta proteína para a manutenção da função do cílio foi estudada através de experiências de mutação do gene. Na ausência de DmIFT88 / NompB, as moscas apresentam comportamentos de gravitaxia defeituosos. Estas descobertas indicam que o IFT é necessário na mosca para manter a função de cílio já formado. A análise da compartimentalização dos cílios e da sua morfologia mostra alterações nos cílios após a depleção de

DmIFT88 / NompB. O mecanismo molecular subjacente, no entanto, permanece por esclarecer. Em estudos desenvolvidos na identificação de novos componentes transportados por DmIFT88 / NompB, descobri o homólogo em mosca (CG34357) de uma enzima evolutivamente conservada sintetizadora de cGMP (Gucy2d). Gucy2d foi anteriormente identificada como uma proteína que é transportada para cílios por IFT88 na retina do ratinho (Bhowmick et al., 2009). Estudos com a proteína truncada em diferentes zonas permitiram-me definir a região através da qual CG34357 se liga a DmIFT88 / NompB. Estudos comparativos das sequências de aminoácidos de Gucy2d e CG34357 revelaram que a zona de ligação a IFT88/NompB é altamente conservada. De notar que pacientes com AOL apresentam mutações nessa zona de Gucy2d. Em conjunto, estes dados sugerem que o mecanismo de tráfego ciliar é semelhante entre seres humanos e a mosca e o trabalho descrito nesta tese revela um novo mecanismo pelo qual se pode desenvolver AOL. Adicionalmente, este trabalho fornece a primeira evidência para a existência de um papel da sinalização sensorial de estímulos mecânicos via cGMP. Esclarece também mais um processo molecular pelo qual a função ciliar é mantida via IFT. Pouco se conhece ainda sobre como as cargas do IFT são transportadas para dentro ou fora do cílio, ou como este tráfego é controlado. A identificação de novas cargas permitirá testar e generalizar hipóteses existentes sobre a regulação do IFT e a interação com a sua carga. Tal como Trypanosoma (Fort et al., 2016), Drosophila parece não utilizar IFT para manutenção estrutural (uma vez que se depletado após a montagem do cílio, este não perde integridade estrutural). Em conjunto, estas observações levantam a dúvida de se nas espécies referidas, as proteínas ciliares e talvez até as próprias estruturas ciliares dependem do IFT para a sua manutenção estrutural.

Chapter I – Introduction: From the advent of cell theory to the problem of cilia maintenance

Introduction to the cytoskeleton – a historical perspective

In this first section I will briefly summarize the main historical events that led to the formulation of cell theory and our current understanding of the cytoskeleton. I will then give a short account of our modern view of the cytoskeleton.

The beginnings of cell theory and the cytoskeleton

Scientific progress often appears saltatory - periods of stagnation are interrupted by technological advances followed by great productivity in that area. Technological advances drive the production of a large body of knowledge in a given area in a relatively short period of time, which might eventually lead to a unifying concept ideally encompassing individual observations. One example of such an advance in cell biology is the invention of the electron microscope (Harris, 2015; Masters, 2009), which allows us to study the structure of cells in unprecedented detail. Suddenly, questions could be answered that were previously out of reach. Understanding how genetic information is stored and used, and that it is amenable to manipulation opened a new door to unravel how cells function. First through random mutagenesis (using radiation or chemical mutagenesis) and later directed through RNAi and CRISPR (Housden et al., 2017), we are now able to manipulate cellular components with incredible spatial and temporal precision. This makes it possible to test hypotheses about how the individual pieces that are encoded in the genome come together to achieve cell function. The ability to sequence the entire transcriptome of individual cells might now mark the start of the next revolution with the potential to force us to rethink what a “cell type” actually is (Nowogrodzki, 2017; Trapnell, 2015).

In the early hours of cell biology, however, none of these techniques existed. The key advance that paved the way to a unifying cell theory was the invention of the light microscope. One prominent figure in the earlier days of light microscopy was Antoni van Leeuwenhoek (1632-1723). He discovered and described a plethora of previously unknown microorganisms (many of those are now grouped as protozoa). The term “cell”, however, was coined by the English physicist Robert Hooke (1635-1702). Reoccurring structures in thin slices of cork reminded him of the “small rooms” that monks live in (*cella* in latin). Matthias Jakob Schleiden (1804-1881) and Theodor Schwann (1810-1882) recognized cells as the basic design principle of all organisms and formulated cell theory. Robert Remak (1815-1865), Robert Virchow (1821-1902) and Albert Kölliker (1817-1905) all independently found that all cells are derived from other cells, a principle for which Virchow coined the phrase *omnis cellula e cellula* (every cell comes from a cell) (Mazzarello, 1999). Only neurons were long regarded as an exception to cell theory. Initially, all neurons were thought to be interconnected instead of forming discrete cellular entities. Neurons are difficult to visualize in their entirety due to their intricate morphology and the way they are entangled with each other. A protocol (“black reaction”) developed by Camillo Golgi (1843-1926) allowed visualizing individual nerve cells, which led Santiago Ramón y Cajal (1852-1934) to propose that neurons also followed the general cell theory. Definite proof for this idea, however, only came with the advent of electron microscopy, which made it possible to visualize the ultrastructure of the termini of neurons (Masters, 2009; Mazzarello, 1999).

With the gradual improvement of microscopes and staining techniques, more and more cellular details became apparent inside cells. The Scottish botanist Robert Brown (1773-1805) was the first to describe the nucleus in the leaves of orchids, which is probably

the first example of a subcellular compartment (Mazzarello, 1999). Structures within the nucleus could be stained easily, which led Walter Flemming (1843-1905) to name them “chromatin”. He was also the first one to describe mitosis in 1882 (Mazzarello, 1999). Prior to Flemming, Friedrich Miescher (1844-1895) had already discovered nucleic acid, and Albert Kossel (1853-1927) reported histones shortly after, but only about 40 years later could Frederick Griffith demonstrate a “transforming principle” underlying the Mendelian principles. Another 16 years later Oswald Avery (1877-1955) finally proved that the carrier of genetic information is DNA.

With the continuous discoveries of cellular components and behaviours came the “need” for a cellular apparatus that would account for these. The French biologist Felix Dujardin (1802-1860) postulated that there is a water-insoluble substance in cells, which he called “sarcode”, that would contribute to cell motility and structure. The first one to use the word cytoskeleton, however, was the French embryologist Paul Wintrebert (1867-1966). He introduced the concept to explain why different components of the cytoplasm of eggs would maintain their position (Zampieri et al., 2014). At the time it was already possible to visualize mitosis. Theodor Boveri (1862-1915) proposed that problems in organizing the mitotic spindle could lead to chromosomal segregation errors, which in turn could be at the origin of malignant tumours (Boveri, 2008), but there was no conclusive evidence that the “fibres” that constitute the mitotic spindle (now known as microtubules) would in fact generate the pulling force required to separate sister chromosomes. On the contrary, only certain staining protocols allowed for visualisation of the spindle, which raised concerns that they were mere artefacts. Proof came from the Japanese cell biologist Shinya Inoue (1921-), who developed in 1947 a technique using polarized light. The optical properties of microtubules allowed for the first time to demonstrate

that the mitotic spindle indeed pulled chromosomes apart in living sea urchin eggs (Dell and Vale, 2004). Six years later, the Swiss botanist Albert F. Frey-Wyssling described “microscopic chords” (which later turned out to be actin filaments) that would form a network in the cytoplasm and might account for its behaviours (Zampieri et al., 2014). The Canadian-American cell biologist Keith Porter (1912-1997) provided additional evidence for these different types of networks through the use of electron microscopy (Satir, 2005). Extraction experiments and biochemical analyses conducted by Duncan L. McCollester demonstrated another decade later that cells indeed have an insoluble fraction that could correspond to the cytoskeletal network. He also showed that this fraction is composed of subunits. Eventually, the biochemical purification of actin, myosin and an actin decorating protein called meromyosin from slime mold allowed the recognition of the actin filaments in electron micrographs (Zampieri et al., 2014). Once the individual components of the cytoskeleton were known, scientists could start using reconstitution experiments (Pollard, 2003). Reconstitution of components *in vitro* is a tremendously powerful approach that led to our current understanding on how the cytoskeletal elements interact to bring about the vast variety of cellular behaviours (Vale, 2014).

Today we have a detailed understanding about the subunits of the cytoskeleton; we know much about their evolution and how they function. We can manipulate them and even change their dynamics and composition to treat diseases. In the following, I will briefly describe the different cytoskeletal elements (microtubules, actin filaments and intermediate filaments) and their functions (Fig. 1.1). More recently, other cytoskeletal elements have been proposed that I will touch upon briefly at the end of this section.

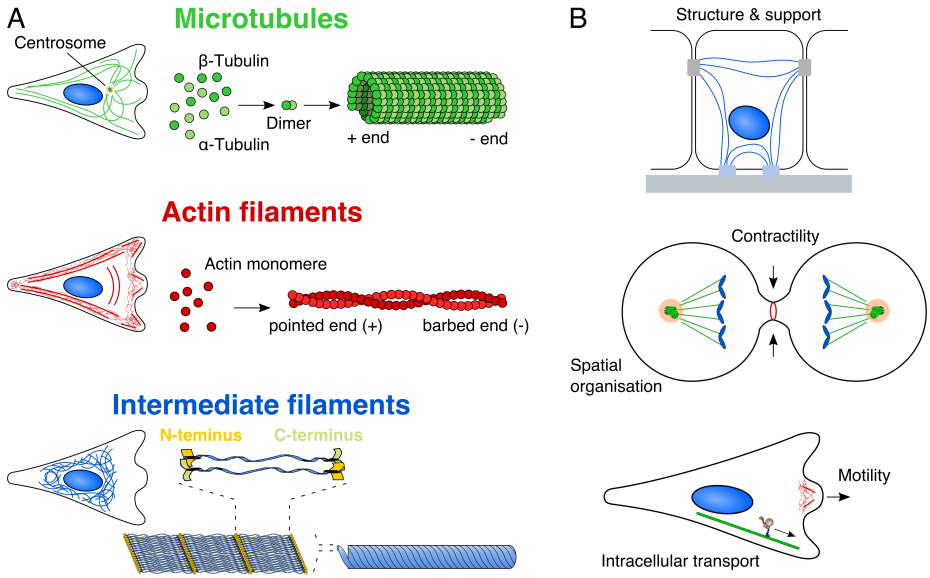

Fig. 1.1: **Overview of the three classical types of cytoskeletal elements in the eukaryotic cell and their main functions**. (A) Representation of the most studied types of cytoskeletal elements (microtubules, actin filaments and intermediate filaments) in the eukaryotic cell. Filaments are self-assembled from protein subunits. Actin and tubulin form polarized filaments due to the interaction of their subunits. Intermediate filaments do not have any intrinsic polarization. The schematic representations of cells on the left-hand side indicate the normal distribution of the respective cytoskeletal element in mammalian cultured cells. (B) The cytoskeletal elements carry out five different functions: (1) They generate structure and support the mechanical properties of cells, (2) generate contractile forces, (3) organise the cell's architecture in space and time, (4) transport molecules within the cell and (5) are required for cell movement. These functions are often not carried out by a single cytoskeletal element and the illustrations are only examples for the respective functions. *Top*: Intermediate filament (e.g keratin) connecting to desmosomes (cell-cell contact) and hemidesmosomes (cell-matrix contacts). *Middle*: Microtubules organise mitotic spindle; actin ring generates contractility required for cytokinesis. *Bottom*: Motor-driven protein transport uses microtubule for directionality. Actin polymerisation can cause membrane protrusion as a first step in generating cell motility.

Microtubules – not just for mitosis

Fibrillar structures had been observed in the mitotic spindle and in eukaryotic flagella (the words cilia and eukaryotic flagella will be used interchangeably throughout this thesis) already in the early 1900s. Novel light microscopy techniques demonstrated in the late 1950s that the mitotic spindle in fact separates the chromosomes, which was under debate before (Dell and Vale, 2004). Only in the 1950s and 1960s, however, through the use of electron microscopy did it gradually emerge that the filaments in these structures were actually the same (Wells, 2005a). Although initially mistaken in some cells as part of the endoplasmatic reticulum, these filaments were found to form tubular structures and to be widespread in cells. The tubular architecture also gave them eventually their name. Again, a technical advancement made it possible to compare the different microtubule arrangements in cells. Early electron microscopy protocols required cold treatment of the samples, which led to the loss of cytoplasmic microtubules, a problem that was only overcome with the invention of glutaraldehyde fixation (Satir, 2005; Wells, 2005a).

Gary Borisy discovered that the subunits that form microtubules are colchicine-binding proteins in the late 1960ies. Colchicine (a metabolite extracted from plants of the genus *Colchicum*) was known to destroy the mitotic spindle, but had a high affinity to cells that were rich in microtubules (Wells, 2005b). Today we know that microtubules are made up of heterodimers of α- and β-tubulin. Both have GTP-binding capacity, but only β-tubulin freely exchanges GTP with the cytoplasm when present in dimers. The tubulin heterodimers polymerize into tubes in a stereotypical fashion (Fig. 1.1A), which gives the resulting tube polarity (i.e. a microtubule has two distinguishable ends called a plus- and a minus-end). In polymerized microtubules the GTP bound by β-tubulin hydrolyses over time to

GDP. The amount of GDP bound by tubulin is hence a relative measure for the age of a given microtubule. Excess of GDP in tubulin can cause rapid depolymerisation of microtubules (also known as catastrophe) (Hancock, 2015). Today we know that cold treatment depolymerizes certain microtubule populations, which explains why cytoplasmic microtubules were not found in early electron microscopy preparations. In living cells most microtubule populations are very dynamic. They undergo growth and shrinkage events, experience catastrophes (i.e. rapid depolymerisation) and recover. This incredible dynamicity (also found in the actin cytoskeleton) is the reason why cells can rapidly respond to environmental cues through remodelling of their cytoskeleton and changing their properties.

Microtubule dynamicity is controlled and read out by many different microtubule-associate proteins (MAPs), which are expressed in a cell-type specific manner and contribute to the properties of individual cells. MAPs regulate microtubule growths and shrinkage but also control interaction with other cytoskeletal elements as wells as influencing the direction of microtubule growth (Akhmanova and Steinmetz, 2015). The interaction with a wide range of MAPs explains why microtubules can organize in very different ways (e.g. mitotic spindle, cilia and flagella, antiparallel arrays in axons of neurons). MAPs such as the minus- and plus-end tracking motors enable the self-organization of microtubules to execute their functions (Karsenti, 2008). Plus- and minus-end tracking motors are also what generates the force in the mitotic spindle that drives chromosomes apart during mitosis. Additionally, their directed movement is used to deliver cargoes to different compartments of cells (Fig. 1.1B). In order to guarantee the functionality of this delivery mechanism, cells need to build stereotypical microtubule networks.

In most animal cells microtubules are nucleated by the centrosome. The centrosome consists of two microtubule barrels (Fig. 1.3A) called centrioles, which are embedded in a proteinaceous matrix known as the pericentriolar matrix (PCM). Centrosomes are usually positioned near the nucleus and function as the dominant microtubule-organizing centre (MTOC, Fig. 1.1A). The nucleation capacity is generally associated to a third tubulin isoform known as γ-tubulin. Together with other MAPs it forms a ring-like structure that binds the minus-end of microtubules and promotes their nucleation (Akhmanova and Steinmetz, 2015). Microtubules radiate out from the centrosomes in most interphase cells (Fig. 1.1A). It was proposed recently, however, that cells inactivate their centrosomes in order to build alternative microtubule arrangements upon differentiation (Muroyama and Lechler, 2017).

Additional layers of regulation of microtubules come from posttranslational modifications of tubulin. These modifications seem to be specific for different microtubule populations and can be read out specifically by certain MAPs. This led to the preposition of the “tubulin code” (in reference to the “histone code”), which is used to give microtubules different properties. These modifications such as detyrosination, glutamylation, acetylation and glycylation are established and erased by dedicated enzymes. They are correlated with properties such as mechanical stability of the microtubules or the interaction with MAPs such as molecular motors (Gadadhar et al., 2017). Other tubulin isoforms were discovered more recently (e.g. δ-, ε-, ζ-, and η-tubulin). Some of them have been associated with flagella function and centriole stability, but little is still known about them (Dutcher, 2003).

Actin – contraction and expansion

Contractility was one of the first properties that led Felix Dujardin to propose that a cytoskeleton must exist. It was also from the beginning associated with motility (Zampieri et al., 2014). The most astonishing contractile cells in animals are probably muscles, and the first description of a contractile substance in those cells dates back to 1859. In 1942 Bruno Straub was able to demonstrate that this contractility is due to the interaction of actin and myosin (Schleicher and Jockusch, 2008). Once it was possible to purify actin and interacting proteins and to reconstitute their filaments *in vitro*, it enabled the detection of actin networks in all other cells through electron microscopy (Zampieri et al., 2014).

Similar to microtubules, actin filaments are built from subunits. The actin monomers assemble into two strands that form a helix (Fig. 1.1A). Another commonality with microtubules is the polarity of the filaments, which allows for coordinated movement through the action of molecular motors (all belong to the myosin super family). Due to their appearance in electron microscopy, the two ends of an actin filament are called pointed end (plus end) and barbed end (minus end). Analogous to tubulin, actin also interacts with nucleoside triphosphates, in this case, ATP. ATP is also hydrolysed to ADP in a time-dependent manner (Pollard, 2003). Additionally, actin is also associated with a wide variety of proteins (60 actin-binding protein families are known) that modulate growth and shrinkage of the actin filaments. They also determine the architecture of the actin network, which in turn regulates the force that is generated by the network (Fletcher and Mullins, 2010). Very recently it was shown that centrosomes can also nucleate actin filaments (Farina et al., 2016).

Another prominent function of actin associated to contractility is the force-generation that underlies the separation of the two daughter

cells during cytokinesis. Additionally, actin-based contractility is also required in the formation of extracellular vesicles (Kalra et al., 2016). The actin cytoskeleton, however, can also exert pushing forces through local polymerisation. Growing actin filaments are the driving force in the formation of membrane protrusions underlying amoeboid movement (Fig. 1.1B) (Pollard, 2003). The family of RhoGTPases coordinates the local activity of actin polymerisation through promotion of polymerisation at the leading edge of a moving cell and through inhibition at the rear end. Interestingly, RhoGTPases also provide an interface for crosstalk between the actin and the tubulin cytoskeleton (Wojnacki et al., 2014). Moreover, actin-based membrane protrusions are not just used for cell motility; they increase cell surface such as in the case of microvilli (Revenu et al., 2004) and in protrusion formation for phagocytosis (Fletcher and Mullins, 2010). Finally, actin has been found in the nucleus of cells, where it might be involved in trafficking between the nuclear compartment and the cytoplasm, as well as in transcription directly (Schleicher and Jockusch, 2008).

Intermediate filaments – Stability and organization

In the late 1960s a third filament was discovered in chicken embryo cells that was of intermediate diameter between actin and myosin (hence the name). As opposed to actin filaments and microtubules, intermediate filaments are formed by at least five protein families (e.g. keratins, lamins, vimentins). Within a given tissue, however, only a subset of intermediate filament proteins is usually expressed. This property seems to persist in tumour cells and is used to determine the tissue of origin of a tumour (Zampieri et al., 2014). Intermediate filaments are made from antiparallel arranged monomers that assemble into higher order structures (Fig. 1.1A). Like actin filaments and microtubules, intermediate filaments

contribute to the mechanical properties of the cell, but they have no intrinsic polarity nor do they exhibit dynamicity. Instead, they form stable connections between neighbouring cells (through desmosomes) as well as with the extracellular matrix (through hemidesmosomes, Fig. 1.1B) and mostly contribute to the resistance against tension (Fletcher and Mullins, 2010; Pollard, 2003).

Like actin, intermediate filaments exist inside and outside of the nucleus. Nuclear intermediate filaments (i.e. lamins) form the main component of the nuclear cytoskeleton. They interact with the chromatin and are involved in its organisation as well as its regulation (Eriksson et al., 2009).

Intermediate filaments are not found outside of metazoa, but insects have a very reduced set and only encode nuclear lamins in their genome. *Drosophila* seems to lack cytoplasmic intermediate filaments. Recent reports, however, suggest that the springtail *Isotomurus maculatus* also forms cytoplasmic intermediate filaments, which raises interesting questions about why intermediate filaments have been lost in higher insects (Herrmann and Strelkov, 2011).

What makes a cytoskeletal element and are there more?

In his Harvey Lecture given in 1957, Keith Porter discussed the need of a cellular "'elastic' framework" that would account for the behaviour and shape of cells. He thought that this "framework" would be below the limits of optical resolution, but that electron microscopy would allow him to find evidence for it. He was hesitant to use the word cytoskeleton, however (Satir, 2005). The biochemist Rudolph A. Peters (1889–1982) had previously cautioned against the use of the word because it might imply the "rigidity of bones" (Zampieri et al., 2014). It was already clear at that point that the cytoskeleton has to account for both the rigid properties of the cells as well as its capacity to change its shape rapidly. When Porter, however,

described the microtubule arrangements in flagella from the static point of view of an electron microscopist, he largely viewed them as the framework that establishes and maintains flagella shape (Satir, 2005). Today we know from the understanding of the behaviour of their subunits, that actin filaments, microtubules and intermediate filaments account for dynamic, as well as static, properties of the cell. It is also generally accepted that the properties of the cytoskeleton emerge from the way these subunits dynamically self-assemble into filaments and networks with the help of interacting proteins and molecular motors (Karsenti, 2008).

More recently, other types of proteins were reported to possess similar properties and assemble into filaments. One example is the protein family of septins that form rings during cytokinesis (Mostowy and Cossart, 2012). The evolutionary conserved enzyme CTP synthase was also shown to form filaments (Lynch et al., 2017). It is less clear though how these filaments contribute to the mechanical properties of the cell. There is an interesting connection, however, to the actin cytoskeleton as actin is believed to have evolved from an enzyme as well (a prokaryotic hexokinase (Pollard, 2003)).

In the future, it will be important to understand how the different cytoskeletal elements interact to achieve cellular function. RhoGTPases mediate crosstalk between the different cytoskeletal elements by modulating the polymerisation of actin and tubulin in a reciprocal manner (Wojnacki et al., 2014). All three classical cytoskeletal elements are also connected through crosslinking proteins and molecular motors (Huber et al., 2015). Actin and tubulin are nucleated from the centrosome (Farina et al., 2016), but the role of actin at the centrosome is not clear. More recently, actin, first discovered as a cytoskeletal element, has been implicated in processes such as regulating transcription in the nucleus, which are not classically viewed as cytoskeletal functions (Schleicher and

Jockusch, 2008). Now is therefore a prime time to attempt to understand the cytoskeleton as a whole, because we have overcome many of the technical difficulties that initially hindered investigation of their properties.

Centrosomes and cilia – From rudimentary organelles to master regulators of cellular function

Centrosomes and cilia have been known for centuries now. Both are microtubule-based structures, but they were originally regarded as separate cellular entities. Cilia were first known for their role in generating movement as flagella. Much later, centrosomes were first described independently as organizers of the mitotic spindle. For a long time, however, many of their functions and the relationship with each other were obscure and heavily debated (see “Microtubules – not just for mitosis”). This was partly due to the difficulties in visualizing and manipulating them. A detailed description of their structure became possible first with the advent of electron microscopy (Guichard et al., 2013; Li et al., 2012; Satir, 2005) and later superresolution microscopy (Lawo et al., 2012; Sonnen et al., 2012; Yang et al., 2016). Very recently, the combination of the two methods (correlative electron and light microscopy) has also become available to study these organelles (Kong and Loncarek, 2015). Their protein composition was mostly unknown until RNAi- and mass spectrometry-based methods became available (Andersen et al., 2003; Balestra et al., 2013; Dobbelaere et al., 2008; Gönczy et al., 2000; Goshima et al., 2007; Ishikawa et al., 2012; Jakobsen et al., 2011; Kamath et al., 2003; Kim et al., 2010, p. 201; Lukinavičius et al., 2013; Mick et al., 2015; Pazour et al., 2005; Sönnichsen et al., 2005; Wheway et al., 2015). I will first briefly summarize the

historical events that led to the discovery of these two organelles and their associate functions. Subsequently, I will discuss our current knowledge about their structure and function, their roles in physiology and disease and their evolutionary history.

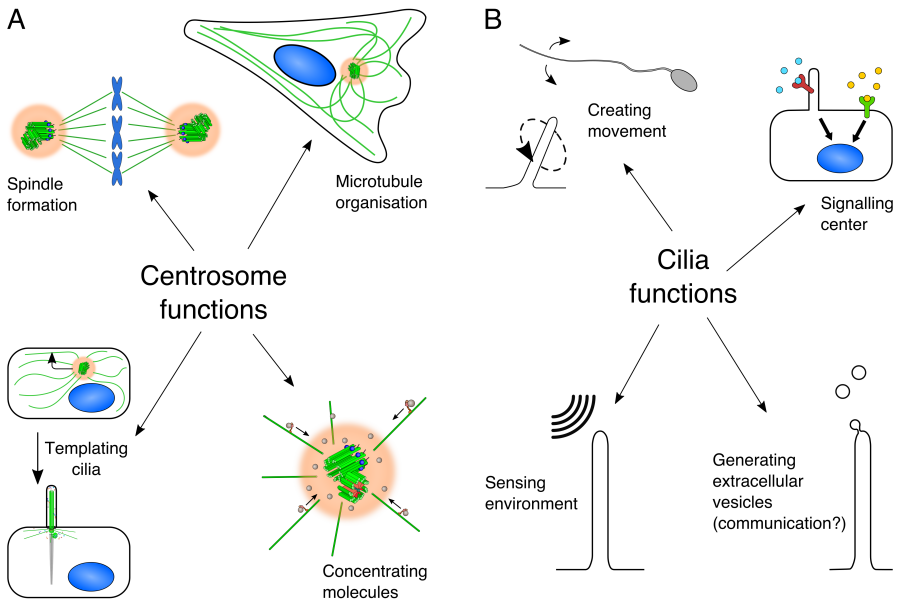

Fig. 1.2: **Cilia and centrosomes are microtubule-based structures that carry out various functions in the eukaryotic cell**. (A) Centrosomes consist of microtubule-based barrels; the centrioles are embedded in a protein matrix called pericentriolar material. They organize the microtubule network in most animal cells. The microtubule minus ends are nucleated and anchored at the centrosomes, while the plus ends radiate out. Molecular motors walk along microtubules in a stereotypical direction. They can transport other molecules and complexes along with them. Many components concentrate at the centrosome in the MT-minus ends. Due to the polarisation that centrosomes impose on the microtubule network, they are able to concentrate molecules. Centrioles are necessary to form cilia, and they organize the mitotic spindle. (B) Cilia are antenna-like protrusions from the cell surface. They are templated by centrioles that dock to the cell membrane and extend their microtubules. Cilia can generate motility by propelling the cell forward or move the fluid surrounding the cell. Cilia can sense cues from the environment in

various ways (e.g. respond to mechanical forces or to molecules in the extracellular medium). They can act as signalling centres by specifically concentrating receptor proteins on their membrane. More recently, they were also found to form extracellular vesicles that might be used in communication (see for example (Wang et al., 2014)).

The discovery of centrosomes, cilia and their relationship

Centrosomes consist of microtubule-based barrel-like structures (called centrioles) that are embedded in a proteinaceous matrix called pericentriolar material (PCM). Initially described at the poles of mitotic spindles (McIntosh and Hays, 2016), we know today that centrosomes carry out four functions (Fig. 1.2A): They organize and orient the mitotic spindle, coordinate the microtubule network in most animal cells, template cilia and flagella and act as concentrators of molecules. When part of a cilium, centrioles are called basal bodies.

The first descriptions of centrosomes at the spindle pole come from Edouard Van Beneden (1846-1910) and Walter Flemming. Van Beneden studied centrosomes first in animal parasites of cephalopods and later also found them in mitosis in *Ascaris megalocephala.* Shortly after, Theodor Boveri reported similar observations in *Ascaris*. He proposed the names centrosomes and centrioles, and he observed that centrosomes are inherited by daughter cells during cell division very much like chromosomes. Finally, he postulated that the centrosome copy number is important and its deregulation could drive tumour formation (Bloodgood, 2009; Sluder, 2014). Today we know that most animal cells either have one or two centrosomes (each harbouring two centrioles) depending on the cell cycle stage and deviations from these numbers can be fatal (see also “Centrosome-associated diseases”).

The tight regulation of centriole numbers seemed to suggest very early on that existing centrioles can template the formation of new centrioles. The idea arose that centrioles are self-replicating entities.

This view was later supported by reports of DNA localising to the basal bodies of *Chlamydomonas* (Hall et al., 1989; Hall and Luck, 1995), very much like other organelles such as mitochondria. Others suggested that DNA or RNA at centrioles could have a structural role (like in ribosomes) and could organize the formation of a new centriole following its own duplication, but those ideas were subsequently refuted (Sluder, 2014). Our current view on canonical centriole duplication is that polo-like kinase 4 (PLK4) triggers the process in tight connection with the cell cycle, but the protein components are encoded in the nuclear DNA. The new centriole appears next to a pre-existing one, because the centrosome acts as a concentrator of the necessary building blocks (Lopes et al., 2015; Zitouni et al., 2016). Although a new centriole normally forms next to a pre-existing one, centrioles can form template-free, i.e. *de novo*, under the appropriate conditions (see also “Centrosomes – Appropriate numbers and structures”) (Meunier and Spassky, 2016).

Cilia had already been described long before the first description of centrosomes (Dobell and Leeuwenhoek, 1932). The relationship between the two, however, was much debated (Bloodgood, 2009). Cilia are antenna-like protrusions that can be found on most cells in the human body. Their formation is templated by centrioles that dock to the cell membrane and extend their microtubules. Their functions can be broadly categorized into four groups: movement generation, signalling, transduction of environmental signals and more recently they were found to also emit signals (Fig. 1.2B).

Cilia and flagella were given various names throughout history depending on their properties, numbers and the cell type, because for a long period of time it was not clear that they are equivalent structures. The number of cilia on a single cell can range from one to hundreds. Cilia were probably first described by Antoni van Leeuwenhoek in protozoa. He immediately connected their function

with the swimming movement of these organisms (Dobell and Leeuwenhoek, 1932). Ecker (1844) was probably the first one to report non-motile cilia, but Zimmermann (1989) is very often credited with their discovery. He certainly described them in several mammalian cells (including humans) and proposed that their function would be to sense the cellular environment. Sorokin (1968) was the first to call them primary cilia (Bloodgood, 2009). Sometimes specific cilia on certain sensory neurons are regarded as modified primary cilia (Satir et al., 2010), but Sorokin considered primary cilia transitory and also used the term “abortive cilia”. According to him, these cilia would be reabsorbed again during development (Bloodgood, 2009).

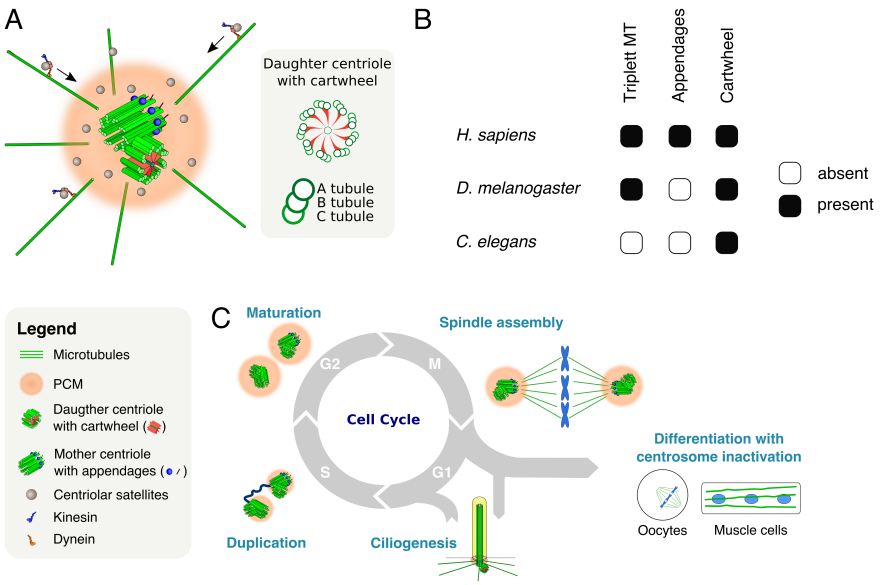

Fig. 1.3: **Centrosome structure and life cycle**. (A) Centrosomes are comprised of centrioles, barrel-shaped microtubule-based structures that are embedded in a protein matrix called the pericentriolar material (PCM). They are surrounded by protein aggregates (centriolar satellites) that are involved in protein transport to the centrosomes and cilia. Centriolar satellites are concentrated at the centrosomes through the activity of molecular motors. Centrioles are nine-fold symmetric structures. This conserved symmetry is generated by a protein complex called the

cartwheel (shown in the grey box). Centriolar microtubules are usually organized in triplets (A, B and C-tubule, only the A tubule is fully closed). Centrioles duplicate once per cell cycle, the older one is called the mother centriole and the younger one is called the daughter centriole. Mother centrioles acquire additional structures called subdistal and distal appendages, which are involved in microtubule anchoring and cilia formation. Centrosomes are proposed to represent a distinct cellular compartment without a membrane (Zwicker et al., 2014). (B) Centriole structure varies in different species. Appendages have not been reported so far in *D. melanogaster* and *C. elegans*. *C. elegans* centrioles can have singlet or doublet microtubules depending on the cell type. (C) Two centrosomes form the opposite poles of the mitotic spindle contributing to spindle assembly and ensuring each daughter cell inherits one and only one of those structures. Centrosomes are duplicated in the following S-phase to restore the necessary numbers for mitosis. Subsequently, centrosomes acquire additional PCM, and mothers form appendages in a process called maturation in G2-phase. After duplication and maturation, cells can form a bipolar spindle again. Alternatively, cells can leave the cell cycle in G1 and form cilia in G0 phase. Some cells also inactivate the microtubule-nucleating capacity of their centrosomes or lose them entirely as part of their differentiation process (e.g. oocytes and muscle cells).

For a long time the relationship between centrioles and cilia was a matter of debate. In 1898 already, Henneguy and Lenhossek proposed in separate publications that these two organelles are related. They based their proposal on observations such as the similar shape and size of centrioles and basal bodies and that both structures can be stained with iron–hematoxylin. Additionally, centrioles template sperm flagella, although it was not universally agreed upon whether the sperm flagellum was equivalent to cilia found on other cells. Furthermore, in insect spermatogenesis the basal bodies (a term introduced by Engelmann in 1880) would be part of the meiotic spindle. Finally, ciliated cells did not seem to have independent centrioles. This hypothesis led to interesting predictions such as that most cells cannot undergo mitosis without disassembling their cilia and that multiciliated cells have to amplify

their centrioles prior to ciliogenesis. The Henneguy-Lenhossek hypothesis met a considerable amount of opposition. One argument against it at the time was that many plant species do not possess centrosomes, but can form multiflagellated sperm cells. Today we know that those species form centrioles *de novo* prior to flagella biogenesis (see also "Centrosomes – Appropriate numbers and structures"). Definite proof for centrioles and basal bodies being the same structure only came from electron microscopy (by deHarven and Bernhard in 1956) and from experiments demonstrating that basal bodies purified from sperm flagella can induce aster formation in *Xenopus* extracts (Heidemann and Kirschner in 1975) (Bloodgood, 2009). Eventually, in 2001 Praetorius and Spring finally demonstrated that deflection of primary cilia of canine kidney cells leads to a rise in the intracellular calcium levels and showed for the first time that Zimmermann's prediction about the role of primary cilia in sensing was correct (Praetorius and Spring, 2001). The only other non-motile cilium that was associated with a particular function before was the connecting cilium in photoreceptor cells. Already in 1911, Bach and Seefelder proposed that the photoreceptor outer segment develops as a modification of a primary cilium (Bloodgood, 2009). However, the confirmation that the connection between the inner and the outer segment in photoreceptors is formed by a cilium came only later with the advent of electron microscopy (Satir, 2005). It was known for more than a century that most cells in mammals have cilia. The field of cilia research, however, only experienced a massive expansion with the discovery that primary cilia are associated to human disease (Pazour et al., 2000; Qin et al., 2001). Today cilia are well known to be involved in development, physiology and can cause many different diseases when their function in impaired (see also "Ciliopathies – What happens when cilia (functions) are lost?").

Centrosomes – Appropriate numbers and structures

Centrosomes, as stated above, are composed of centrioles and PCM. Centrioles vary in size and structure depending on cell type and species, but they share common features. They have a diameter of approximately 250 nm and depending on the species can be up to 500 nm long in vertebrate (Winey and O'Toole, 2014). Their size is at the limit of optical resolution, which presented considerable problems for their visualisation and the study of the spatial distribution of centrosome components before the invention of superresolution microscopy. Centrioles are nine-fold symmetrical. This symmetry is generated by a structure at the proximal end of the centrioles called a cartwheel. The cartwheel emerges first in centriole biogenesis (Fig. 1.3A). In vertebrates the centriole consists of nine triplet microtubules. Only one of the microtubules in a triplet is a full tube (called A tubule), the other two (B and C tubule) are open tubes (Fig. 1.3A). Some species such as *Drosophila* or *C. elegans*, however, have singlet or doublet microtubules (Fig. 1.3B) (Winey and O'Toole, 2014), although in the fly, some cells also form triplet centrioles (Riparbelli et al., 2009). This is the case in the germ line and in sensory neurons (Gottardo et al., 2015). In the beginning of the G1 phase of the cell cycle, the centrosome contains two centrioles embedded in PCM. The PCM was originally described as an amorphous electron density in electron microscopy. Through the use of superresolution microscopy, however, it became apparent that the PCM has an intrinsic structure (Woodruff et al., 2014). The PCM also accounts partly for the microtubule-nucleation capacity of the centrosomes because it concentrates tubulin locally (Woodruff et al., 2017).

In canonical centrosome biogenesis, one new centriole is formed in close proximity of a pre-existing centriole and stays in close association with it until the end of the next cell cycle. Consequently,

one centriole in a pair is at least one cell cycle older (referred to as mother centriole) than the other one (referred to as daughter centriole). Mother and daughter can be distinguished from one another by the presence of appendages. The appendages are acquired in a process called centrosome maturation that occurs in late S-phase and G2. Distal appendages are required for cilia formation (Tanos et al., 2013) while subdistal appendages have been associated with the ability of the centrioles to anchor microtubules (Delgehyr et al., 2005). They have not been found, however, in cycling cells in *Drosophila* or *C. elegans* (Fig 1.3B). During the process of maturation, centrosomes grow due to the addition of PCM. Finally, the two centrosomes separate at the onset of mitosis to organize the mitotic spindle, and each is inherited by one daughter cell in cytokinesis.

The duplication of centrioles occurs in coordination with the cell cycle. Zitouni and colleagues substantiated the existence of a licencing complex similar to the DNA replication licencing complex. In this model, centriole duplication is prevented in mitosis by the cyclin-dependent kinase 1 (CDK1). At the end of mitosis, CDK1 activity levels drop, which allows Plk4 to bind and phosphorylate STIL on a domain called CC motif that was previously occupied by CDK1. STIL is subsequently able to form a complex with Sas6, which allows for the formation of the cartwheel (Zitouni et al., 2016). Sas6 establishes the nine-fold symmetry of the cartwheel of the newly formed centriole (Kitagawa et al., 2011; Nakazawa et al., 2007; van Breugel et al., 2011). The cartwheel was also associated to centriole stability in motile cilia (Bayless et al., 2012; Pearson et al., 2009). After the initiation of centriole biogenesis, the centriole extends to a defined length in a process that is not well understood yet. The cartwheel is lost in vertebrate cells prior to mitosis and has been proposed that this event serves as a licencing event. If the

cartwheel is retained, centrioles cannot support duplication. Other proteins (e.g. Cep295), however, have to substitute the stabilizing function of the cartwheel perhaps through the recruitment of PCM, otherwise the newly formed centriole will not be maintained (Izquierdo et al., 2014; Wang et al., 2011). The site of centriole biogenesis as well as the number of newly formed centrioles is dictated by the localisation and the cellular levels of Plk4 (Lopes et al., 2015).

In the process of differentiation, certain cell types deviate strongly from normal centrosome numbers. Some cell types such as oocytes lose their centrosomes. The elimination mechanism seems to differ between species, however (Borrego-Pinto et al., 2016; Pimenta-Marques et al., 2016). In muscle cells, epithelial cells and neurons it is less clear whether centrosomes disappear completely or if they only lose their microtubule nucleation activity (Sanchez and Feldman, 2017). Loss of centrosomal microtubule activity is correlated with alternative microtubule arrangements in order to achieve different mechanical properties and cell shapes (Muroyama and Lechler, 2017). Cells that form multiple cilia rapidly amplify their centrioles. In those cells, the otherwise strongly controlled rule of “only one new centriole per pre-existing one” is abrogated. Daughter centrioles form in rosette-like structure around mother centrioles. Additionally, those cells form additional structures called deuterosomes that initiate centriole biogenesis in a similar configuration. It is now established that the deuterosomes are first formed by the daughter centriole. The daughter can give rise to several deuterosomes, which in turn gives rise to several centrioles leading to exponential amplification of the centrioles (Al Jord et al., 2014). Interestingly, in those cells centriole amplification is uncoupled from DNA synthesis. Centriole numbers are also altered

in pathological conditions, which will be discussed in the following section.

Centrosome-associated diseases

Here I will focus on diseases that arise from problems in centrosomal functions. Since one function of centrosomes is to template cilia formation (Fig. 1.2A), defects in centrosomes can also cause diseases related to cilia function. Those will be, however, discussed in the separate section (see “Ciliopathies – What happens when cilia (functions) are lost?”).

The first function that was associated with the centrosome is organizing the mitotic spindle. Any mutation that deregulates centrosome numbers or interferes with their ability to form a bipolar spindle can have devastating consequences. Boveri already linked multipolar mitotic spindles to the formation of cancer in 1914 (Boveri, 2008). Amplification of centrosomes has now been shown to cause chromosome instability and promotes the invasive capacity of cancer cells but results often in cell death (Ganem et al., 2009; Godinho et al., 2014). It was also shown recently, that cells with supernumerary centrosomes can spontaneously from tumours in mice (Levine et al., 2017). Some cells have, however, the ability to cluster centrosomes in order to form a pseudo-bipolar spindle (Godinho, 2014). The loss of centrosomes in cycling cells leads to p53-mediated G1-arrest (Fong et al., 2016; Lambrus et al., 2016; Meitinger et al., 2016). If cells without a centrosome proceed to mitosis, aneuploidy can also arise, depending on the ability of the cells to form acentriolar spindles (Nano and Basto, 2016). In early divisions in mouse development, mitosis occurs without centrioles (Howe and FitzHarris, 2013). Later in development, however, the absence of centrioles in mitosis causes apoptosis induced by p53 (Bazzi and

Anderson, 2014). This shows that the consequences of deviations from normal centrosome numbers are strongly context dependent.

Centrosomes are also involved in the orientation of the mitotic spindle. Spindle-orientation is known to contribute to the formation of the architecture of a developing tissue as well as the maintenance of stem cell capacity (Tang and Marshall, 2012). In Pericentrin mutant mice it was proposed that spindle orientation defects cause microcephaly as well as septal defects in the developing heart (Chen et al., 2014). Additionally, randomisation of spindle orientation affects cell differentiation from stem cells in the developing mouse brain (Falk et al., 2017). Besides mutations, viruses can also impair centrosome structure and function. This was demonstrated in the case of ZIKA in brain organoids. Cells infected with ZIKA show signs of centrosome defects and altered division planes (Gabriel et al., 2017).

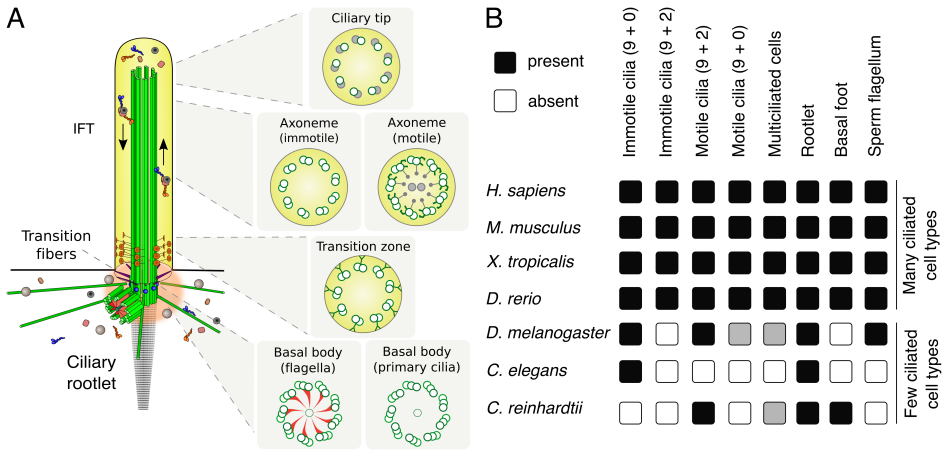

Fig. 1.4: **General cilia structure and variation between cilia types and different species**. (A) Cilia are microtubule-based protrusions from the surface of animal cells. They are templated by the mother centrioles (now called basal bodies), with the daughter centriole often in the vicinity. The distal appendages of the mother form membrane connections (transition fibres). The cilium consists of doublet

microtubules called the axoneme that extend out from the mother centriole and are engulfed by the cell membrane. At the base of the axoneme, the cilium forms additional membrane connections (Y-links, based on their appearance in cross sections in electron microscopy). This ciliary compartment is called the transition zone. The centrioles are still embedded in a protein matrix made up of proteins of the pericentriolar material (shown here in orange). The typical organisation of the different ciliary compartments is shown in cross sections in grey boxes. The basal bodies retain a cartwheel in some cilia types and lose it in others, a trait correlated with motility of cilia and flagella. In motile cilia the microtubule doublets interact with each other through dynein arms (which are not present in immotile cilia). Motile cilia usually possess a central pair of microtubules (9 + 2 type). Additionally, radial spokes extend from the nine doublet microtubules in the direction of the central pair. They are also involved in motility and influence the shape in which flagella beat. The central pair and the radial spokes are not always present in motile cilia (9 + 0 type, e.g. Nodal cilia, hence depicted in grey). At the ciliary tip microtubules can be present as doublets or singlets (hence B tubule shown in grey). (B) Summary of different cilia types and features which are present or absent in humans as well as several model organisms (grey box indicates that *D. melanogaster* and *C. reinhardtii* have cells with two cilia, table was adapted from (Carvalho-Santos et al., 2011; Choksi et al., 2014). Of note, chordotonal cilia in *Drosphila* show dynein arms in cross section, which are required for their function (Karak et al., 2015). Cilia movement, however, has never been visualized in this system.

Cilia – Structure and function

Depending on their function, cilia can vary strongly in their architecture between tissues and species. In a conventional cilium, the mother centriole is docked to the apical cell membrane (now called basal body). The A and B tubule are extended. This cytoskeletal portion of the cilium is called the axoneme. The axoneme is engulfed in a specialized cell membrane. The B tubule does not, however, always extend until the tip of the cilium (Fig. 1.4A). Classically, cilia are categorized into motile and immotile cilia. In cross sections of the ciliary axoneme, these two types of cilia can be distinguished by the absence or presence of dynein arms (Fig. 1.4A). Additionally, motility is often correlated with a central pair

of microtubules (9 + 2 cilia). This central pair is usually absent from immotile cilia (9 + 0 cilia). This is not a strict rule, however. Non-motile cilia of the 9 + 2 type can be found in the olfactory bulb of mice, while motile cilia in the node do not have a central pair. The node is an organ found at the posterior end of the developing vertebrate embryo that is required for the establishment of left-right asymmetry. (Satir and Christensen, 2007). Many cilia extend a striated rootlet (as defined by its appearance in electron microscopy) into the cell body. At the base of the cilium the axoneme is characterised by the presence of Y-shaped electron densities visible in electron micrographs of cross sections (Fig. 1.4A). These electron densities are called Y-links. The area of the axoneme containing Y-links is called the transition zone. Centrioles lose the cartwheel in the maturation process (see “Centrosomes – Appropriate numbers and structures”). Consequently, many basal bodies do not have a cartwheel. The cartwheel is however, retained in the basal bodies of motile cilia/flagella of many different species (Hirono, 2014). In the multiciliated unicellular alga *Tetrahymena,* it was proposed that the cartwheel stabilizes the basal body against the mechanical forces caused by the movement of the flagella (Bayless et al., 2012).

The blueprint of cilia architecture outlined above is remarkably variable. In many mammalian primary cilia the daughter centriole is arranged in a 90º angle with respect to the mother. This association is not present, however, in multiciliated cells (Garcia and Reiter, 2016). This could be due to the particular centriole biogenesis pathway in multiciliated cells (see “Centrosomes – Appropriate numbers and structures”). All centrioles acquire mother centriole characteristics and dock to the membrane (Al Jord et al., 2014). In ciliated sensory neurons of arthropods, the two centrioles are usually linearly arranged (Keil, 2012). In mature cilia in *C. elegans*, centrioles are lost entirely (Fig. 1.4B) (Serwas et al., 2017).

Multiciliated cells generally have a structure attached to the basal body called the basal foot. The basal foot organizes the apical microtubule network in those cells and is involved in coordinated cilia beating (Clare et al., 2014). Basal feet are absent, however, in cilia of *C. elegans* and *Drosophila* (Fig. 1.4B) (Carvalho-Santos et al., 2011).

The protein composition of the ciliary compartment is distinct from the cytoplasm and the cell membrane, which suggests diffusion barriers and dedicated transport mechanisms. I will proceed next to describe how the ciliary transport was discovered.

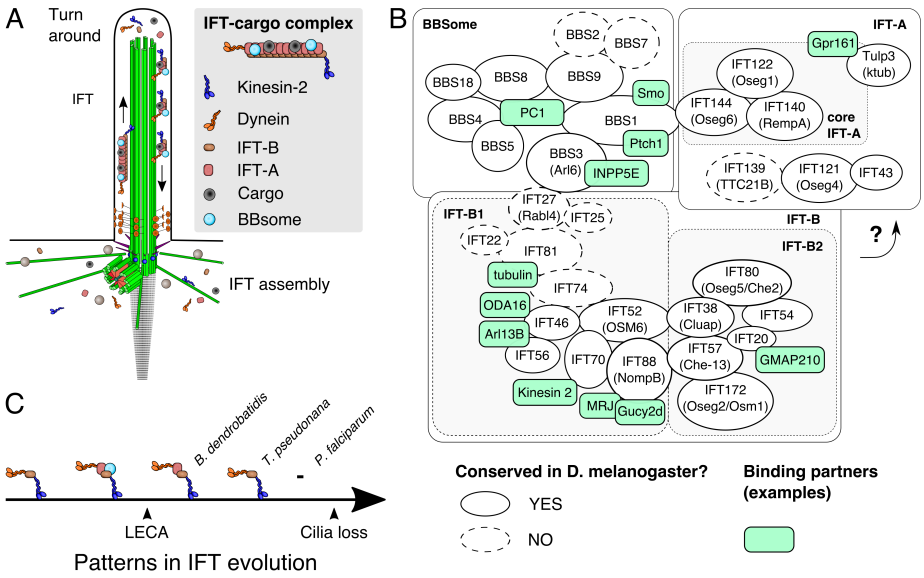

Fig. 1.5: **Intraflagellar transport (IFT) complex architecture and evolution**. (A) IFT is a multiprotein complex that assembles at the ciliary base. It moves in an anterograde direction through the use of kinesin-2. The complex is partly disassembled at the ciliary tip, before it moves in a retrograde direction using dynein-2 (a cartoon of an IFT train and its main components is shown in the grey box). IFT trains serve to transport, accumulate and remove proteins specifically to and from the cilium. (B) IFT consists of three complexes: A, B and the BBsome. IFT-A and –B can be further divided based on their genetic features and biochemical

properties. The scheme depicts the overall IFT complex together with the BBsome as it can be found in *C. reinhardtii* and humans. For the IFT-A and –B proteins the *C. reinhardtii* nomenclature is used here (numbers correspond to the molecular weight of the individual IFT proteins, modified from (Mourão et al., 2016). Proteins not conserved in *D. melanogaster* are shown as circles with dashed outlines. The scheme shows where the three complexes interact and highlight some known binding partners (green boxes). (C) Genome analysis of various ciliated species of all eukaryotic domains suggests that the whole IFT complex was already present in the last eukaryotic common ancestor (LECA). Similarities to other protein transport systems suggest that IFT-B emerged first and IFT-A and the BBsome resulted from gene duplication and modification events of IFT-B (van Dam et al., 2013). In taxa that eventually lose cilia, the BBsome seems to disappear from the genome first. This is followed by the loss of IFT-A and then IFT-B (example species for each intermediate step are given, scheme modified after (van Dam et al., 2013)). Interestingly, *P. falciparum* forms cilia but does not encode IFT components in their genome.

Intraflagellar transport – Essential for ciliogenesis?

According to Satir, the discovery of intraflagellar transport (IFT) marks a transition in cilia research (Satir, 2017). Before, work on cilia was mostly focused on motile cilia, and immotile cilia were largely ignored. IFT connected immotile cilia to physiology and disease (Pazour et al., 2000; Qin et al., 2001). Manipulating IFT also turned out to be a powerful approach to study cilia physiology. After 2000, the field of cilia research exploded, and what Bloodgood calls the "Golden Age of Primary Cilia" began (Bloodgood, 2009).

IFT was discovered as a curiosity in the biflagellated green alga *Chlamydomonas reinhardtii.* In 1993 Kozminski reported a "motility" along the flagellar axoneme (Kozminski et al., 1993). Robert Bloodgood had previously shown that polystyrene balls attached to the membrane of *Chlamydomonas* flagella would move along the flagellum (Bloodgood, 1977; Kozminski, 2012). Using a novel microscopy technique (high-resolution, video-enhanced, differential interference contrast microscopy), Kozminski was able to show that

the movement Bloodgood had reported corresponds to an intraflagellar motility. This motility moves anterogradly, as well as retrogradely. He correlated the moving particles that he had observed with light microscopy with electron densities he found between the axoneme and the flagellar membrane along the flagellum (Kozminski et al., 1993). Through the use of temperature-sensitive kinesin mutants, Kozminski was able to show that this movement is kinesin-dependent (Kozminski et al., 1995). He concluded already at the time that IFT must be essential for cilia biogenesis as well as maintenance. *Chlamydomonas* turned out to be a good system to study IFT. A collection of temperature-sensitive mutants was available that would inactivate the corresponding proteins rapidly upon temperature shift (Huang et al., 1977). Live-imaging of the flagella was possible (Kozminski et al., 1993), and flagella could be isolated easily for biochemical analysis (Witman et al., 1972). Soon after, it was demonstrated that the retrograde movement of IFT is mediated by dynein (Pazour et al., 1998), but the real breakthrough came when Pazour showed that IFT is conserved in other species, and IFT mutant mice exhibit phenotypes similar to human diseases (Pazour et al., 2000, 2002). Analysis of the *Chlamydomonas* temperature-sentitive IFT mutants showed that IFT is involved in tubulin turnover at the flagella tip and that this transport mechanism was involved in regulation of the flagella length (Marshall et al., 2005; Marshall and Rosenbaum, 2001). Only 20 years after the initial discovery of IFT, however, was it demonstrated that IFT transports tubulin in several species (Bhogaraju et al., 2013).

Nowadays it is known that IFT is a multiprotein complex that move anterogradely and retrogrately along the ciliary axoneme, transports cilia specific cargoes and has 22 complex members (Fig. 1.5A,B). The individual IFT proteins are named after the molecular weight of the corresponding protein in *Chlamydomonas*. Biochemical analysis

of the IFT particles purified from *Chlamydomonas* flagella showed that it can be separated into two subcomplexes (i.e. IFT-A and IFT-B, Fig. 1.5B) (Cole et al., 1998). Additional analysis demonstrated that the IFT-B subcompex in turn consists of two subcompexes (i.e. IFT-B1 and IFT-B2, Fig. 1.5B) (Lucker et al., 2005). The IFT-B complex mediates binding to kinesin (movement towards the ciliary tip), whereas the IFT-A complex binds dynein (movement towards the ciliary base). Consequently, many IFT-B mutants do not form cilia, because of the inability to transport proteins into cilia (Fan et al., 2010; Han et al., 2003; Pazour et al., 2000, 2002; Tsujikawa and Malicki, 2004). Loss of some IFT-A members, however, leads to bulging of the ciliary tip presumably due to the accumulation of protein and the lack of export from the cilium (Iomini et al., 2009; Tran et al., 2008). Additionally, the IFT complex is associated with a complex called the BBSome, which is composed of eight proteins. All members of the BBSome were found mutated in patients with the ciliopathy Bardet-Biedl syndrome (BBS, hence the name, see "Ciliopathies – What happens when cilia (functions) are lost?"). The BBSome binds to several proteins involved in ciliary signalling (Fig. 1.5B). Some authors have also suggested that the BBSome mediates binding between IFT-B and IFT-A and is involved in the assembly of the IFT complex. These proposals regarding the role of the BBSome in IFT complex architecture are, however, still under debate (Taschner and Lorentzen, 2016). The full reconstitution of IFT-A, -B and the BBSome complex and the determination of the complex structure are still missing.

Several IFT cargos are now known or have been proposed (Fig. 1.5B). Evidence for these cargoes does not always come from protein-protein binding assays, but is sometimes based on live-imaging results showing that a putative cargo moves in cilia at the same speed as IFT (Mourão et al., 2016). Some IFT proteins seem

to be absolutely essential for cilia formation (e.g. IFT88), whereas others seem to give rise to phenotypes that are more cargo specific when perturbed (e.g. IFT27). In the case of IFT88, loss of the protein seems to destabilize at least parts of the complex (Fort et al., 2016; Pazour et al., 2000). Loss of IFT27, however, does not impair cilia formation nor does it seem to impair ciliary movement of other IFT complex members (Eguether et al., 2014, p. 25), which suggests that this protein is less involved in the architecture of the IFT complex. Mouse mutants for IFT27 exhibit severe development defects, which shows that IFT27 is involved in trafficking of important ciliary cargos (Eguether et al., 2014). Little is still known about how many of the ciliary proteins are actually transported by IFT. Proteomics studies suggest that the cilium is composed of about 200-600 proteins (Ishikawa et al., 2012; Mick et al., 2015; Pazour et al., 2005). Given that that ciliary transition zone functions as a size-dependent diffusion barrier, it is expected that many of these proteins have to be transported actively into the ciliary compartment (Takao and Verhey, 2016). Only very few of those proteins, however, have been connected to IFT directly. We also know little about the contribution of IFT to the formation of a tissue-specific cilium. Furthermore, it is unclear how IFT complex assembly, cargo loading, complex disassembly and cargo release are regulated.

More recently, some reports have suggested cilia-independent functions for IFT proteins, which makes the analysis of IFT function even more difficult. Several IFT proteins were found to localise to the mitotic spindle in vertebrate systems, and data from IFT88 mutant mice and from zebrafish suggest that the protein is involved in spindle orientation (Delaval et al., 2011). IFT88 mutant flies, however, do not show obvious phenotypes associated with spindle orientation defects (Han et al., 2003). Experiments in *Drosophila* provided, however, evidence that IFT-A proteins are involved in

canonical Wnt signalling. The canonical Wnt signalling pathway when activated leads to accumulation of β-catenin in the nucleus and transcription of appropriate target genes. Upon depletion of IFT-A proteins in imaginal discs of the fly during development, the wings show patterning defects. Since there are no cilia in imaginal discs during development, this must be a cilia-independent function of IFT-A (Balmer et al., 2015). Wnt signalling in zebrafish does not seem to require cilia either (Huang and Schier, 2009). A cilia-independent role of IFT-A proteins in Wnt signalling in vertebrates, however, is not known. Taken together, these findings suggest that cilia-independent IFT functions have evolved secondarily and are probably not generalizable between different species. Comparative studies could hence be very powerful in understanding the cilia-specific roles of IFT.

Evolutionary analysis suggests that LECA (last eukaryotic common ancestor) already possessed the full IFT complex consisting of IFT-A, -B and the BBsome (Fig. 1.5C). According to sequence analysis and comparisons with similar protein complexes, IFT-B evolved first. IFT-A and the BBSome resulted from gene duplication events followed by modifications. It is not clear, however, in which order IFT-A and the BBSome evolved. Cilia were lost in several eukaryote taxa (Carvalho-Santos et al., 2011). Sister groups to those taxa can be informative about the order in which ciliary proteins are lost. In the case of IFT, it appears that that BBsome is always lost before IFT-A (van Dam et al., 2013). *Plasmodium falciparum* represents an interesting exception. The unicellular parasites forms flagella, but does not encode IFT proteins in its genome (van Dam et al., 2013). Ciliogenesis can occur without IFT such as in the case of insect spermatogenesis (as discussed below). It should be pointed out here that more recently it was proposed that additionally IFT-independent protein transport occurs in the flagella of Chlamydomans (Harris et

al., 2016). These observations suggest that some ciliary properties might be established and maintained through IFT-independent mechanisms.

Cilia assembly and disassembly

Cultured cells form cilia upon growth factor withdrawal (i.e. in serum starvation) in coordination with cell cycle exit (Fig. 1.3C). It is not clear, however, how the absence of mitogens in the medium triggers ciliogenesis. We know little about what induces ciliogenesis in organisms (Sánchez and Dynlacht, 2016). Often ciliogenesis seems to be a programmed consequence of acquiring a particular cell linage. It is, however, not a universal consequence of differentiation as not all cell types develop cilia. Lymphocytes, hepatocytes and mature adipocytes and skeletal muscle cells are some prominent exceptions (Fu et al., 2014; Sánchez and Dynlacht, 2016; Stinchcombe et al., 2015; Wheatley et al., 1996). Several transcription factors are known to be required for ciliogenesis and involved in specification of cilia sub-types (e.g. Rfx2, Rfx3, Foxj1) (Choksi et al., 2014). That ciliogenesis is under the control of a genetic program can be demonstrated through the ectopic expression of prociliogenic transcription factors. Injection of FoxJ1 mRNA into Xenopus embryos induces ciliogenesis even in cells that are normally not ciliated (Stubbs et al., 2008).

During canonical ciliogenesis, the mother centriole forms the cilium. The mother centriole can be distinguished from the daughter in electron micrographs through the presence of distal appendages (Fig. 1.3). The distal appendages mediate docking to a Rab11-positiv vesicle, which mediates fusion to the cell membrane (centriole-to-basal-body conversion) (Sánchez and Dynlacht, 2016). Depending on the cell type, the centriole either starts elongating already prior to docking to the cell membrane or only after (Sorokin,

1962, 1968). After docking to the membrane, the distal appendages are referred to as transition fibres (Reiter et al., 2012; Tanos et al., 2013). Interestingly, *Drosophila* centrioles do not seem to possess appendages in cycling cells (Fig. 1.3B) (Lattao et al., 2017). Cilia in the fruit fly, however, have transition fibres (Vieillard et al., 2016). This suggests that in *Drosophila*, distal appendages are only formed upon induction of ciliogenesis.

Once the centriole has docked to the membrane, the transition zone is formed. The transition zone is characterized in electron microscopy by the presence of Y-shaped electron densities that connect the microtubules to the membrane (Fig. 1.4A). The transition zone acts as a diffusion barrier called the ciliary gate that separates the ciliary compartment from the cytoplasm (Reiter et al., 2012). Once the transition zone is established, the cilium requires IFT for axoneme extension. This can be seen for example in *Drosophila* mutants for the IFT anterograde motor kinesin. In these mutants, early steps of ciliogenesis take place and the transition zone starts to form, but the axoneme is not extended. Presumably, continuous axoneme growth cannot be supported sufficiently by passive diffusion of building blocks into the cilium (Sarpal et al., 2003). The insect sperm flagellum, however, develops intracellularly and does not require IFT (Avidor-Reiss et al., 2017; Han et al., 2003; Sarpal et al., 2003).

Cilia disassembly is less understood than cilia assembly. Many terminally differentiated cells probably never undergo cilia disassembly. In the case of the cells that disassemble their cilia, the axoneme has to be disassembled, which involves destabilizing the axonemal microtubules. Work in *Chlamydomonas* suggests that flagella length is maintained through a IFT-mediated dynamic equilibrium of tubulin addition and removal at the tips (Marshall et al., 2005; Marshall and Rosenbaum, 2001). One consequence of

triggering cilia disassembly should hence be the deviation from that equilibrium. Work in human cultured cells suggests that ciliary microtubules are destabilized through the tubulin deacetylase HDAC6. Acetylation is a posttranslational modification of tubulin that is associated with microtubule stability. Ciliated cultures cells can be promoted to disassemble their cilia through the addition of serum to the culture medium. The addition of serum promotes re-entry into the cell cycle, which leads to a rise in the activity of the cell cycle kinase Aurora A. Aurora A in turn activates HDAC6 through phosphorylation (Pugacheva et al., 2007). HDAC6 null mice, however, show hyperacetylated tubulin, but develop normally (Zhang et al., 2008), which suggests the existence of redundant cilia disassembly mechanisms. Others have proposed that microtubule-depolymerizing kinesins such as Kif2a and Kif24 are activated similarly to HDAC6 in coordination with cell cycle re-entry (Kim et al., 2015; Miyamoto et al., 2015). It is unclear, however, to what extent the mechanisms proposed in cultured cells apply to cell cycle re-entry in developing organisms or in cancer formation.

Cilia and the cell cycle – Can cilia block cell proliferation?

The idea that cilia have an inhibitory effect on the cell cycle is not recent. As early as 1989, Henneguy and Lenhossek proposed that cells could only undergo mitosis when they disassemble their cilia. Already at the time, however, some exceptions to this rule were known (e.g. basal bodies form the meiotic spindle in insect spermatogenesis) (Bloodgood, 2009). Today it is generally accepted that most cells exit the cell cycle in G1 prior to ciliogenesis (Fig. 1.3C) (Avasthi and Marshall, 2012). Cycling cells might even use active mechanisms to suppress ciliogenesis (Goto et al., 2017). Some evidence supporting this hypothesis comes from cancer research. Inhibition of HDAC6 prevents cilia disassembly and slows

down tumour growth (Gradilone et al., 2013; Xiang et al., 2017). The role of cilia in cancer progression is puzzling, however. In some cancer types the presence of cilia was reported to have both promoting and inhibiting effects. It was argued that in those cases the role of cilia depends on the underlying genetic make-up of the cancer. In mouse models expressing a constitutively active form of the hedgehog pathway member Smoothend (Smo, see also "Cilia and the signalling pathways"), cilia are deleterious. Smo depends on localisation to cilia to promote cell cycle progression. Inhibition of ciliogenesis can hence rescue the phenotype in those mice. In the case of a constitutively active downstream molecule in the same pathway that act outside of cilia (e.g. Gli2), however, the presence or absence of cilia does not affect cancer progression (Han et al., 2009; Wong et al., 2009). In the last decade several signalling pathways have been found to act at least partially through cilia (Bangs and Anderson, 2017; Christensen et al., 2007, 2017). Other signalling pathways have a similar potential to cause cell cycle progression when signalling through cilia. I will next briefly discuss signalling through cilia and how different pathways might be integrated.

Cilia and the signalling pathways – A hub for everything?

It was puzzling for a long time why immotile cilia appear so frequently in the human body. The first experimentally supported role for immotile cilia was in mechanosensation in kidney cells. Bending of cilia on kidney cells elicits an increase in intracellular calcium levels (Praetorius and Spring, 2001). This and other findings led to the idea that cilia are mechanosensors that can detect shear stress and fluid flow (Praetorius, 2015). Very recently, however, it was shown that the calcium signal does not originate inside the cilium (Delling et al., 2016). The primary signal transduction event in ciliary

mechanosensation and how this translates to elevated calcium levels in the cell is now once again an open question.

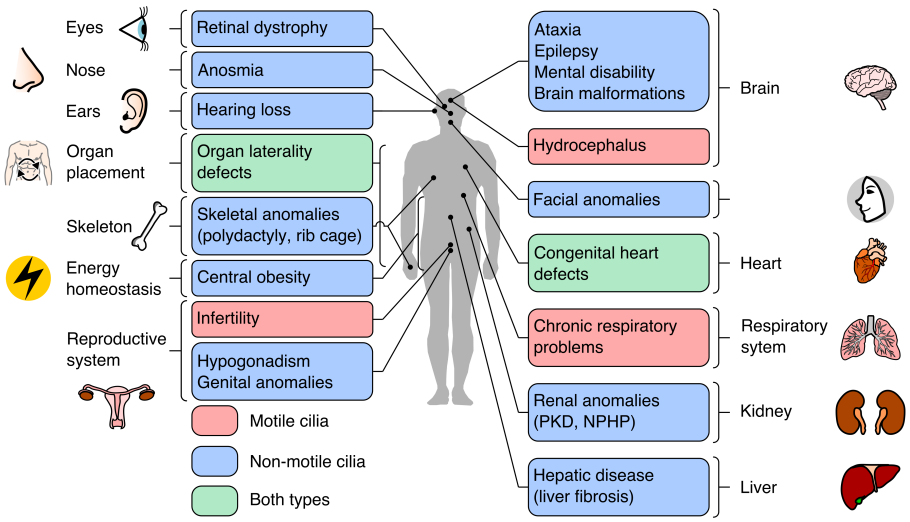

Fig. 1.6: **Mutations affecting motile vs. non-motile cilia largely give rise to distinct but overlapping phenotypes**. The majority of ciliopathy phenotypes are caused by defects in non-motile cilia. Mutations in both cilia types can affect the same organ, but often in different ways. For example, motile as well as immotile cilia can cause brain defects when their function is impaired, but the associated phenotypes might be different. Organ laterality defects and congenital heart defects can be caused by mutations in both cilia types. Particular mutations affecting one specific cilia type do not necessarily give rise to all phenotypes depicted here (see also Fig. 1.7, figure adapted from (Reiter and Leroux, 2017).

Another answer for the frequency of immotile cilia in the human body came from a genetic screen conducted in mice with developmental patterning defects. The screen recovered several genes required for intraflagellar transport. The mice, however, had phenotypes resembling mutations in the hedgehog-signalling pathway (Huangfu et al., 2003). The hedgehog signalling pathway was originally discovered in the fruit fly (Nüsslein-Volhard and Wieschaus, 1980).

Ironically, in *Drosophila* development, cilia do not play a role in hedgehog signalling (Han et al., 2003; Sarpal et al., 2003). There is evidence, however, that hedgehog signalling in *Drosophila* modulates the function of olfactory cilia (Kuzhandaivel et al., 2014; Sanchez et al., 2016). The hedgehog pathway in mammals is involved in many different developmental processes (e.g. neural patterning, bone and limb development). Upon activation of hedgehog signalling the transmembrane protein Smo translocates to the cilium where it causes the phosphorylation of the Gli transcription factors. This phosphorylation in turn promotes nuclear transport of the Glis and activation of Gli responsive genes (Bangs and Anderson, 2017). It is now established that the IFT-B proteins IFT25 and IFT27 together with the BBSome (Fig. 1.5B) are required to export Smo from the cilium when the pathway is not activated (Eguether et al., 2014). Mutations in IFT25 or IFT27 can hence cause constitutive activation of the hedgehog pathway leading to developmental defects also found in human patients. Given the importance of the hedgehog pathway for development, it is not surprising that a complete loss of cilia function is lethal in midgestation (Bangs and Anderson, 2017). Interestingly though, IFT25 and IFT27 are not conserved in the fly (Fig. 1.5B) (van Dam et al., 2013), which might have to do with the uncoupling of the hedgehog pathway from cilia during *Drosophila* development.

In addition to the hedgehog pathway, receptor tyrosine kinases (RTKs) and Tumour-transforming growth factor-β (TGF-β) receptor were found to localise to the cilium (Christensen et al., 2007; Labour et al., 2016; Schneider et al., 2005). In some tissues such as the developing heart, these different pathways are known to contribute together to cell differentiation and tissue morphogenesis (Koefoed et al., 2014). It is well established that there is a considerable amount of crosstalk between different pathways (Christensen et al., 2017).

Provided that many pathways initiate signalling at least in part in the cilium, it is possible that some of the crosstalk already occurs in this cellular compartment prior to propagation. How much of this crosstalk actually occurs inside cilia and depends on cilia is not known, however. Understanding cilia function in cell signalling might also help to further understand the role of cilia in cell proliferation in cancer (see “Cilia and the cell cycle – Can cilia block cell proliferation?”). It might also help to understand the role of cilia in other diseases.

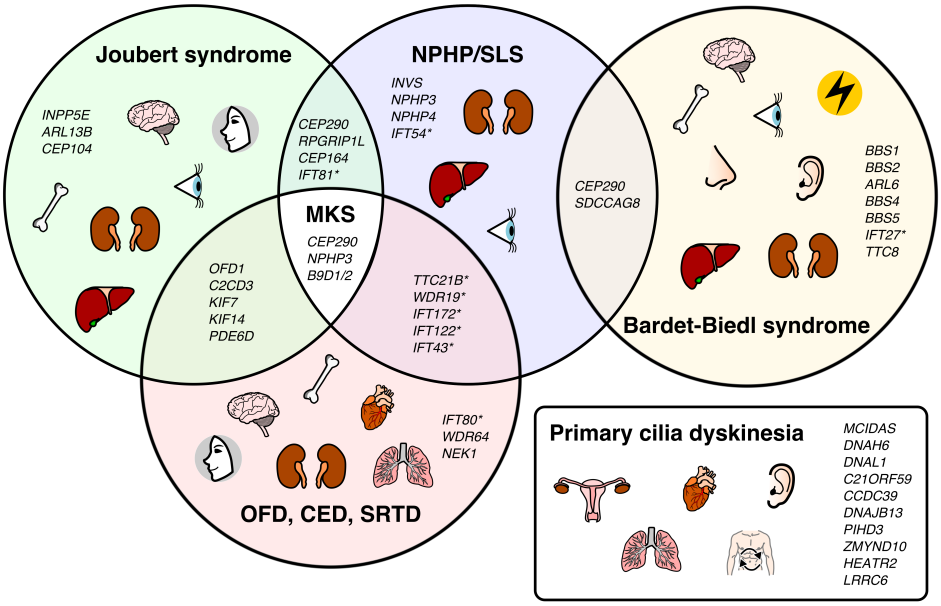

Fig. 1.7: **Shared and distinct features of various ciliopathies**. Various disease-causing mutations have been found in patients with certain ciliopathies (only selected ciliopathies are shown here, CED – Cranioectodermal Dysplasia, MKS – Meckel Syndrome, NPHP – Nephronophtisis, OFD – Orofaciodigital Syndrome, SLS – Senior-Løken-Syndrome, SRTD – Short-Rib-Thoracic Dysplasia). Mutations in the same gene can give rise to one or several ciliopathies depending on the gene and the mutation. Organs involved in the respective ciliopathy are shown as symbols (for a detailed legend refer to Fig. 1.6). No organ involvement was indicated for MKS,

because affected patients die before birth or shortly after. There is almost no overlap between primary cilia dyskinesia (PCD) and the other ciliopathies with respect to genes as well as organs, likely because (PCD) is caused largely by mutations in genes that specifically affect cilia motility. The list of genes displayed here was considerably shortened for the sake of clarity. Genes were picked to highlight that several ciliopathies can be caused by mutations in the IFT machinery (IFT genes were marked with an asterisk, figure was modified from (Braun and Hildebrandt, 2017).

Ciliopathies – What happens when cilia (functions) are lost?

Ciliopathies can be classified according to which cilia type (motile versus immotile) is affected. Given that almost all cells on the human body bear cilia at least at some developmental stage, it is not surprising that cilia defects can impact almost every organ in the human body. Interestingly, defects in motile cilia mostly affect a different set of organs from defects in immotile cilia. Even when they cause defects in the same organs, for example in the case of the brain, the defects are distinct (Fig. 1.6). Cilia defects can also cause global problems when they impair the endocrine system or organ laterality (Reiter and Leroux, 2017). Complete loss of cilia in mammals, however, is embryonic lethal, because of their role in hedgehog and probably other signalling pathways (Huangfu et al., 2003). Most disease-causing mutations in human patients are hence probably hypomorphic or affect only a certain population of cells (Reiter and Leroux, 2017).

In 1976, Afzelius proposed a syndrome based on the loss of ciliary motility (Afzelius, 1976). This syndrome is now called primary ciliary dyskinesia. It is caused by the loss of function in genes specifically involved in the generation of ciliary movement, such as the dynein arms directly, or genes that are required specifically in the assembly or the transport of the dynein arms (Fig. 1.7). Typical symptoms are infertility, respiratory problems, organ laterality defects and congenital heart defects.

The association of immotile cilia with human disease really only came at the beginning of 21st century (Pazour et al., 2000). Almost every organ can be affected by dysfunction in immotile cilia (Fig. 1.6). Today we know of a broad, but genetically and phenotypically overlapping group of diseases (Fig. 1.7). For example, Meckel-Gruber and Joubert syndrome are considered genetically related diseases. Both are autosomal-recessive and show vast phenotypic pleiotropy (Braun and Hildebrandt, 2017). Meckel-Gruber syndrome, however, is mostly embryonic lethal, whereas the life-expectancy for Joubert patience (often diagnosed by a brain malformation called “molar tooth sign”) ranges widely depending on the organs involved and its severity (Brancati et al., 2010). They overlap in many of the genes that are affected, which led to the proposal that in Meckel syndrome genes lose their function completely, whereas in Joubert syndrome the corresponding genes are present as hypomorphic alleles (Parisi and Glass, 2017; Reiter and Leroux, 2017). The considerable overlap between disease genes in various ciliopathies (Fig. 1.7) also suggests that the individual underlying mutations might have tissue specific consequences. This would explain why different mutations in proteins such as Cep290 can be found in patients with different ciliopathies (Fig. 1.7). They sometimes cause very distinct phenotypes such as in patients with the retina-specific ciliopathy Leber congenital amurosis (see “Photoreceptor cGMP signalling in health and disease”) (den Hollander et al., 2008). Additionally, it was proposed that certain mutations only lead to expression of the disease phenotype in the presence of additional mutations in modifier genes (Khanna et al., 2009), which might also restrict the tissue that is affected as well as the age of onset of the disease. Similar observations were made in a mouse model for polycystic kidney disease. The Tg373 allele of IFT88 behaves very differently

with respect to the onset of phenotype as well as severity, depending on the genetic background of the mouse strain (Lehman et al., 2008).

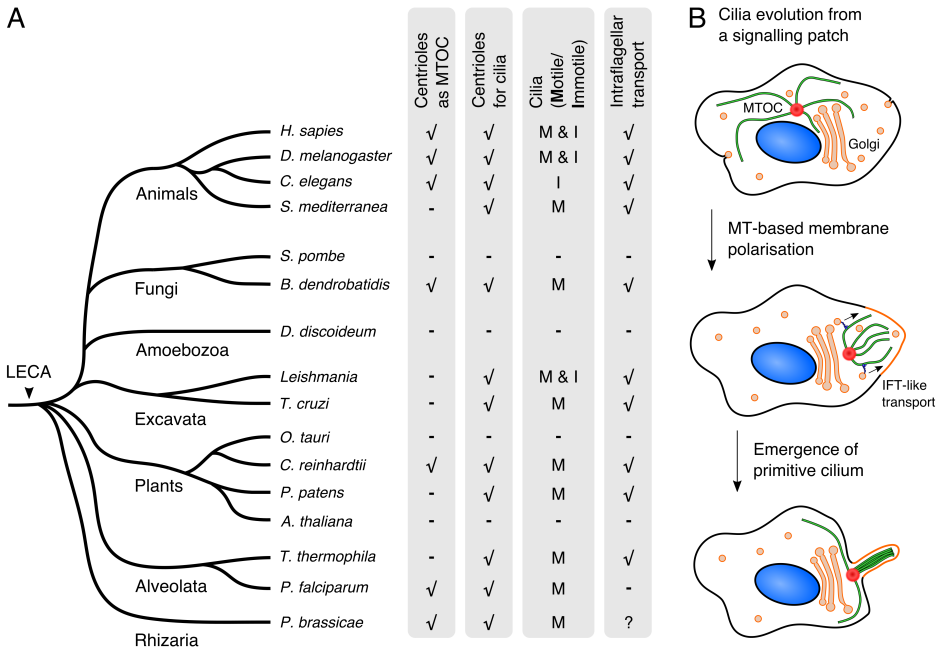

Fig. 1.8: **Distribution of cilia features in various eukaryotic species and a simplified model for cilia evolution**. (A) The phylogenetic tree shows all eukaryotic domains with example species for each domain and is rooted in the last common eukaryotic ancestor (LECA). The table indicates whether centrioles act as microtubule organising centres (MTOC) in the respective species and whether centrioles are formed to make cilia (tick) or not (minus). Some species form centrioles only to template cilia (e.g. *S. mediterranea*). It also displays whether the respective species possess motile (M) or immotile (I) cilia or both (M & I) and whether those species encode IFT proteins in their genome. The table suggests that the LECA had motile cilia and used IFT. It might have only formed centrioles to template cilia (table adapted from (Carvalho-Santos et al., 2011; van Dam et al., 2013). (B) The simplified scenario for cilia evolution shown here proposes that a primitive eukaryote already possessed an MTOC, but had no or very little polarisation in terms of its cell membrane composition. In the course of evolution IFT-like particles were employed in order to transport vesicles from the Golgi to one particular side of the cell using the microtubule network. This local concentration of molecules such as membrane receptors (“signalling patch”) might have made signal

amplification possible. Alternatively, local microtubule polymerisation could have helped to create forces to move the cell. In a subsequent step, the cilium could have emerged through closer attachment of the cell membrane to the microtubules to form a distinct compartment. This would have further strengthened signalling function or allowed for improved motility (modified from (Jékely and Arendt, 2006)). In this scenario the modern IFT complex would only appear in the last step once the cilium is a truly distinct compartment.

Obesity is one of the lesser-understood ciliopathy-related phenotypes. This is probably due to the fact that obesity is not just based on the dysfunction of one particular organ, but involves endocrine crosstalk between the central nervous system and the periphery (Vaisse et al., 2017). Already in 2007, it was shown that loss of cilia function can cause hyperphagia and obesity in mice (Davenport et al., 2007). This observation was exciting, because proteins mutated in patients with human obesity syndromes such as Bardet-Biedl syndrome localise to cilia, but had not been functionally explored. Seven of these proteins were then shown to form a complex (the BBSome) that is required for ciliary trafficking (Nachury et al., 2007). There are, however, still many open questions regarding the tissues involved in cilia-mediated obesity, as well as what can trigger it. Surprisingly, there seems to be very little overlap between the disease genes found in patients with primary ciliary dyskinesia and patients with defects in immotile cilia (Fig. 1.7) (Braun and Hildebrandt, 2017). Cilia and flagella are found on many different eukaryotic species, which allows us to study their function in various model systems and to gain new insights into disease mechanisms. In the following section, I will briefly review the evolution of cilia and centrioles.

Evolution of centrioles and cilia

Today it is generally accepted that centrioles and cilia must have been present in the last common eukaryotic ancestor (LECA). LECA most likely had a motile cilium that used IFT (Fig. 1.8A). Evidence for this comes from the presence of motile cilia and centrioles in all major branches of the eukaryotic tree of life (Carvalho-Santos et al., 2011; Hodges et al., 2010). According to this scenario, immotile cilia are the result of a secondary loss of the motility genes in the species that have no motile cilia such as *C. elegans*. In species that have motile and immotile cilia, motility genes must have become independent in their transcriptional regulation from more general cilia genes. As far as we know, centrioles are always required for the formation of cilia, but many species can undergo mitosis in the absence of centrioles, which led to the conclusion that centrioles evolved to template cilia and might have acquired their mitotic function later, potentially to guarantee that each daughter cells is able to rapidly form a cilium (Hodges et al., 2010; Marshall, 2009). The planarian species *Schmidtea mediterranea* (belonging to the platyhelminthes) most likely lost the mitotic function of centrioles secondarily, because the sister clade of the ecdysozoa (of which *Drosophila* and *C. elegans* are members) forms centriolar spindle poles. *Schmidtea* still forms centrioles *de novo* at the onset of ciliogenesis (Azimzadeh et al., 2012).

Three different hypotheses have been put forward to explain the evolution of cilia: (1) It was proposed that centrioles/basal bodies evolved from a virus. According to the authors of this theory, the virus hypothesis would explain the self-replication properties of centrioles and the interaction with membranes (analogous to basal bodies anchored to the cell membrane). Additionally, many virus particles are built symmetrically, and the virus hypothesis would also account for the absence of many centriole proteins from the

genomes of prokaryotic species (Satir et al., 2007). (2) In an alternative scenario, cilia have evolved from the endosymbiosis of spirochetes. Margulis and colleagues claim that the evolution of cilia required the coordination of a vast number of gene products, which can only be explained by endosymbiosis. According to this theory the endosymbiont would have gradually evolved into the modern cilium (Margulis et al., 2006). (3) The third hypothesis postulates that the cilium has gradually evolved from a signalling patch (Fig. 1.8B). Following this theory, cilia and centrioles would have evolved from existing precursor structures. The selective advantage in this scenario is the localisation of signalling components to one particular spot on the cell, which would improve signalling function. Directed trafficking would be enabled through microtubule-based transport reminiscent of modern intracilliary trafficking (related to IFT). Continued selection pressure on enhanced signalling function would finally lead to engulfment of the microtubules in the cell membrane in a cilia-like arrangement. Enhanced signalling function would result from local confinement of the signalling machinery. This scenario, however, requires the pre-existence of a microtubule organising centre (Jékely and Arendt, 2006).

Out of the three hypotheses summarized here, the third one seems currently the most likely. No virus particles have ever been described that would account for the nine-fold symmetry of the centrioles, and except for tubulin in bacteria, there are no ciliary proteins known that can be traced back to bacteria or viruses. It was, however, proposed that microtubule-base formation of membrane protrusions could have promoted cellular movement and therefore conferred a selective advantage in early cilia evolution (Jékely and Arendt, 2006). Furthermore, several phylogenetic analyses suggested that the ciliary transport machinery could have evolved from more ancestral transport mechanisms (Rout and Field, 2017; van Dam et

al., 2013). Additional credit for the signalling patch hypothesis comes from the behaviour of the mother centriole at the immunological synapse. In cytotoxic T cells the mother centriole docks to the membrane at the interaction site with other cells. There it mediates polarized trafficking to the membrane without forming a cilium (Stinchcombe et al., 2015). Since lymphocytes only appeared in the vertebrate lineage it is unlikely for the immune synapse to be ancestral (Vivier et al., 2016). It makes it more plausible that a primitive microtubule-organising centre could be associated to a membrane to support polarised membrane trafficking without the need to evolve the machinery for ciliary motility.

The cilia maintenance problem

The aim of this thesis is to explore the role of IFT in the maintenance of ciliary properties. The word maintenance, however, has been used in different ways in molecular and cell biology. I will first briefly review different maintenance concepts. I will then continue to review the literature on cilia maintenance before describing the model system I used in this study.

Maintenance in molecular and cell biology

I define maintenance as an active process that prevents the properties of a fully formed cellular element from deteriorating. These properties include structure as well as function. It should be pointed out that it is possible to lose structural components (e.g. cartwheel loss in centriole maturation) without losing function and *vice versa*. The maintenance mechanisms might be different depending how properties are lost, which can happen in two different ways: (1) The amount of cellular components drops as a consequence of physiological processes such as cell division or

vesicle formation. (2) Cellular components are compromised through factors such as cell stress.

The responses of a cell to loss of a property might be different depending how it is lost. Cells might be able to return the amounts of cellular components back to a set point in a process of homeostatic maintenance. This, however, implies that cells are able to measure the amount of the component in question or that the set-point is an intrinsically stable state to which cells return after perturbation. In order to test whether homeostatic maintenance exists for cilia, one would need to investigate the ability of the system to return to a set-point after perturbation (Avasthi and Marshall, 2012). The compensation for compromised function of cellular components I call reparative maintenance. This could happen potentially in two ways. Cells could have a dedicated machinery that detects damage and replaces compromised parts (e.g. DNA repair ionizing radiation (Le Guen et al., 2014)). In synapses, however, it was proposed that turnover is regulated in an activity-dependent manner to maintain neuronal function (Sheehan et al., 2016). In the latter case, as long as turnover is sufficiently faster than the frequency at which the damages occur, any given cellular structure should remain functional. This last scenario does not necessarily require a machinery that detects damage. Finally, in order to realize different cellular properties, maintenance of a given structure could be inactivated. This in turn might allow plastic responses of cells to changing environments or to a switch in cell type.

What do we know about maintenance of cilia?

As outlined above, maintenance involves replacement of building blocks of any given cellular structure. This entails production of new proteins through transcription and translation as well as transport of the newly synthesized proteins to that cellular structure.

IFT was always associated with cilia maintenance, because the acute inactivation of kinesin function through the use of temperature-sensitive mutants leads to disassembly of the flagella in *Chlamydomonas* (Kozminski et al., 1995). Removal of IFT in the mouse photoreceptors leads to disruption of the outer segment, suggesting that IFT also has a role in cilia maintenance in other systems (Jiang et al., 2015; Pazour et al., 2002). Photoreceptors are an interesting model to study cilia maintenance. Photoreceptors do not re-enter the cell cycle and hence do not normally disassemble their cilia. The photoreceptor outer segment, however, is entirely replaced within days, which requires the ciliary compartment to be continuously functional (Besharse and Hollyfield, 1979). IFT has also been implicated in dynamically maintaining ciliary properties such as flagella length in *Chlamydomonas* (Marshall et al., 2005; Marshall and Rosenbaum, 2001) or the signalling capacity in primary cilia in mice (Eguether et al., 2014). In the case of hedgehog signalling, the maintenance role of IFT lies in the export of Smo from unstimulated cilia to prevent inappropriate pathway activation (see “Cilia and the signalling pathways”, (Eguether et al., 2014)). More recently, it was demonstrated in *C. elegans* that IFT can also selectively enrich GTP-bound Rab28 (Jensen et al., 2016). Rab28 is a small GTPase associated with the membrane function of cilia. The protein is small enough to escape the barrier function of the transition zone (see “Intraflagellar transport – Essential for ciliogenesis?”). IFT is hence not required for ciliary localisation of Rab28, but selectively enriches GTP-bound Rab28 over GDP-bound Rab28 and contributes to the activity of the GTPase in cilia (Jensen et al., 2016). The role of IFT in cilia maintenance might, however, be species-specific. As outlined above (“Intraflagellar transport”), the lack of IFT88 in *Chamydomonas* and mice leads to cilia disassembly. In the unicellular parasite *Trypanosoma*, however, IFT88 is required for

flagella biogenesis. Its depletion does not maintain the structure of a fully formed flagella, but causes functional defects (e.g. flagella beating frequency is reduced), which might have to do with the deregulation of signalling components (Fort et al., 2016).

Besides transport, the maintenance of a structure also implies novel synthesis of its building blocks. This requires continuous transcription of cilia genes. The loss of the Van-Hippel-Lindau (VHL) transcription factor leads to the loss of cilia in kidney cells. It was proposed that in the absence of cilia, the cells undergo proliferation and form cystic kidneys (Thoma et al., 2007). It is unclear, however, which genes are under control of VHL, and how the loss of VHL causes cilia disassembly. Additionally, the modulation of transcriptional activity through miRNAs was shown to be required specifically for the maintenance but not biogenesis of mouse photoreceptors (Busskamp et al., 2014).

Posttranslational modifications of tubulin are known to affect ciliary stability. It is not always clear, however, how this is achieved. They might increase the intrinsic stability of microtubules or recruit MAPs that stabilize the cilium. Loss of tubulin modifiers were shown to cause progressive phenotypes in mouse photoreceptors as well as sensory cilia in *C. elegans*, but do not seem to affect cilia biogenesis (Bosch Grau et al., 2017; O'Hagan et al., 2011). Those tubulin-modifying enzymes might be specific maintenance factors, although it is not quite understood how they maintain the cilium. Additionally, the loss of rootletin, the main component of the ciliary rootlet, leads to degeneration of sensory cilia in mice and *C. elegans* (Mohan et al., 2013; Yang et al., 2005). The work in *C. elegans* suggests that rootletin is involved in IFT assembly, but the exact role of rootletin in cilia maintenance is not clear (Mohan et al., 2013).

The mouse photoreceptor and sensory neurons in *C. elegans* are great systems to study cilia maintenance, because these cells do not

disassemble their cilia. Additionally, findings in the mouse photoreceptor can be easily related to retina-associated ciliopathies in humans. Both systems, however, do not allow for the study of motility property maintenance. In the fruit fly there is a type of sensory neuron that forms cilia with dynein arms (chordotonal neurons, see “Drosophila chordotonal neurons – Development, architecture and function”). *Drosophila* could hence be good system to address the maintenance of a different set of features.

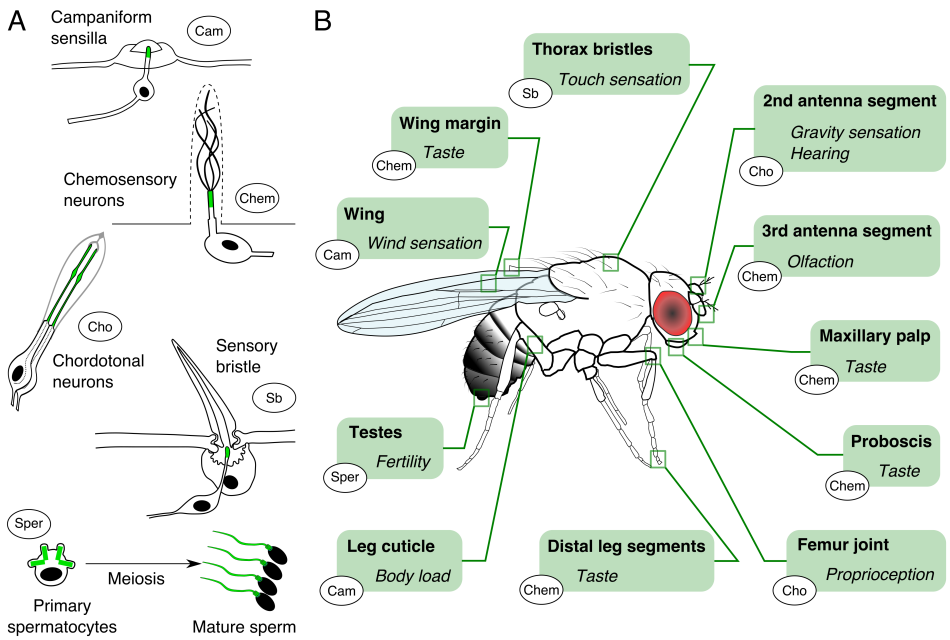

Fig. 1.9: ***Drosophila* forms diverse cilia in sensory neurons and in spermatogenesis**. (A) Schematic representations of the ciliated cell types in *Drosophila* (the cilia are highlighted in green): Campaniform sensilla (Cam) sit near the cuticle. The cilium connects to a membranous cap. It generates action potentials in response to the cap being moved by wind or other forces acting on the cuticle (such as mechanical load). Chemosensory neurons (Chem) project cilia into hair-like structures in the cuticle. They contain chemosensory receptors on the ciliary membrane that allow them to respond to specific molecules from the environment. Chordotonal neurons (Cho) usually occur in groups of up to 5 neurons engulfed by

support cells. They project to connections between body segments of the fly. When two neighbouring body segments move with respect to each other, the cilia of the Cho are bent. This results in activation of the neurons. Sensory bristles contain usually one ciliated neuron that is activated in response to the bristle being deflected. Finally, primary spermatocytes form four cilia. After two meiotic divisions, each of them will be converted into the flagellum of an individual sperm cell. (B) Ciliated cells can be found all over the body of adult flies. With the exception of sperm, all those cells are involved in sensing the environment. The schematic representation of a male *Drosophila melanogaster* shows where ciliated cells can be found and which ciliated cell type is present there (the respective function is given in italic).

Drosophila as a model to address cilia maintenance

The fruit fly only forms cilia on a few cells during spermatogenesis and on type I sensory neurons (Fig. 1.9A) (Lattao et al., 2017). I will briefly describe the different ciliated cell types in the fly first and then justify and explain the system I used in this study.

During spermatogenesis *Drosophila* centrosomes elongate and attach to the cell membrane to form a non-motile cilium (dynein arms are absent at this stage) that also nucleates the mitotic spindle. Each of the four centrioles will form a flagellum. Every primary spermatocyte hence gives rise to four sperm cells. During flagella elongation the axoneme is not fully engulfed by the cell membrane. Spermatogenesis in *Drosophila* is IFT-independent (Han et al., 2003; Sarpal et al., 2003). At the tip of the growing flagellum, however, there is a transition zone-like compartment that forms a diffusion barrier that is important for flagella formation (Basiri et al., 2014). The authors argue that axoneme assembly might need to occur in a distinct compartment.

Type I neurons require the formation of a multicellular unit for their function. These ciliated neurons always form one cilium at the apical end of a dendrite, which are always of the 9 + 0 type and associate with the cuticle. They are involved in different types of chemo- and

mechanosensory behaviours (Fig. 1.9B). The type I sensory neurons are mostly regarded as immotile, but otherwise share many features with cilia in other animals (e.g. rootlet, transition zone, extend an axoneme as doublet microtubules). Ciliated sensory neurons occur at every developmental stage in the fly. The cilia in campaniform sensilla and in sensory bristles are very short. Chemosensory cilia lose the axonemal arrangement towards the tip and form several membrane branches (Fig. 1.9A).

These neurons are postmitotic, and it has not been reported whether they can disassemble their cilia. Together with the genetic tools available in this model system, it is hence possible to manipulate ciliary proteins in adult animals and to uncouple ciliogenesis from maintenance. Additionally, the cilia function can be monitored through the use of behavioural assays (Inagaki et al., 2010; Simonnet et al., 2014). Out of the different ciliated sensory neurons chordotonal neurons can be studied easily and cost-effective through the use of simple gravitaxis assays (Inagaki et al., 2010). Additionally, their structure and function are known and methods and tools are available to visualize them (Jana et al., 2016; Vieillard et al., 2015). I hence chose to focus on this system. I will next explain development and architecture of chordotonal neurons in more detail.

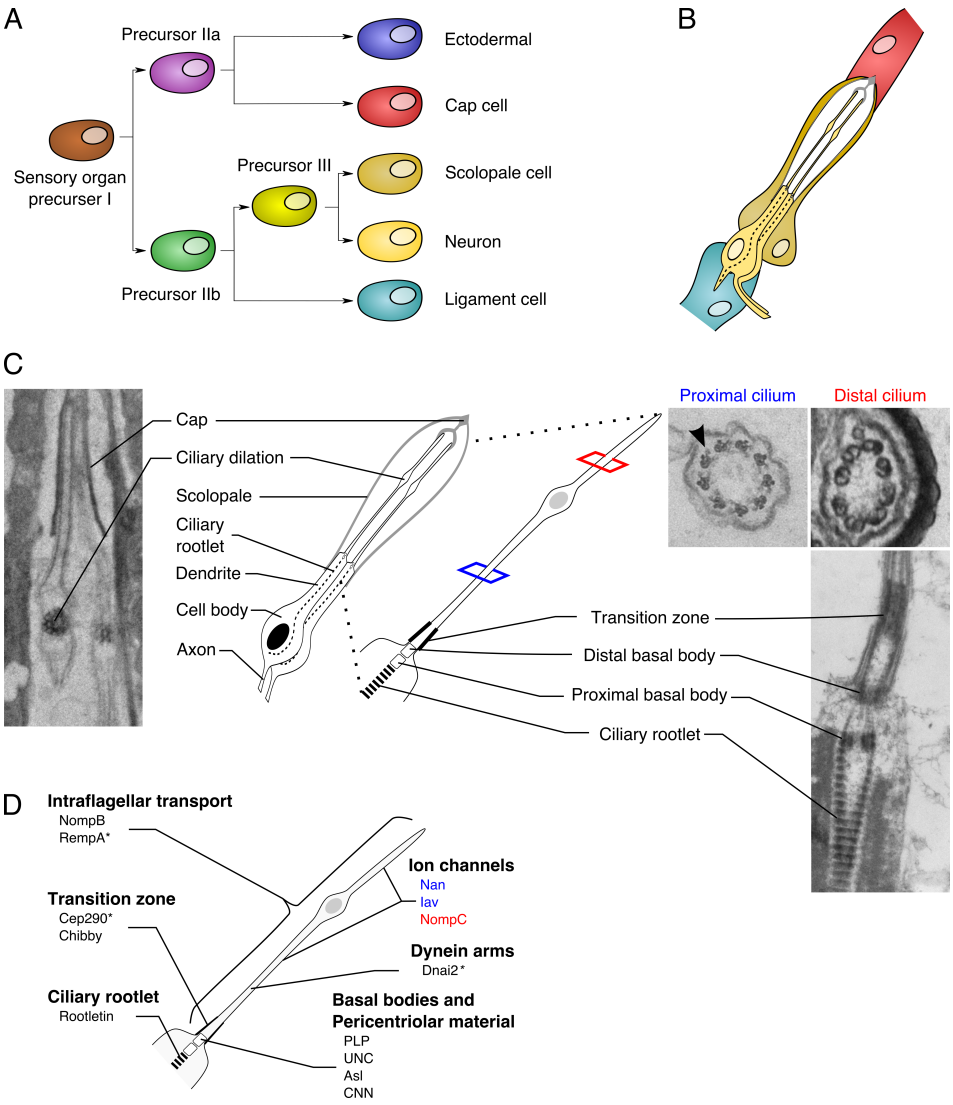

Fig. 1.10: **Development and architecture of chordotonal neurons**. (A, B) Graphic representation of the stereotypical lineage specification of chordotonal neurons and their support cells from a common precursor cell. The resulting arrangement of the cells within the tissue is shown on the right (modified after (Kernan, 2007)). (A) Chordotonal neurons are formed in three consecutive asymmetric cell divisions from a sensory precursor cell that also gives rise to other cells that form a functional unit with the chordotonal neurons. (B) Organisation of the different cells descendent from the common precursor is shown here. The cap cell connects the cilia to the cuticle and is therefore essential for the mechanotransduction function of these neurons. The scolopale cell forms an extracellular space around the cilia of the

neurons and is presumably involved in maintaining a particular ion composition in the extracellular space. (C) Detailed architecture of chordotonal neurons. Up to five neurons can be found to form a functional group. In the second antenna segment of *Drosophila,* two neurons project their cilia towards a cap cell. Each cilium is divided into a proximal and a distal zone by a particular structure called the ciliary dilation. They are distinct in their axonemal architecture. For example, the proximal cilium exhibits dynein arms in cross sections (arrow head) whereas the distal cilium does not (all electron micrographs shown here were generated by Susana Mendonça). (D) Chordotonal cilia possess many features of the cilia of animal cells and can hence serve as model for human cilia. The individual ciliary compartments can be visualized using specific markers (examples given here). Some of these proteins are conserved until humans, sometimes with relevance for human diseases (marked by an asterisk). The ion channels listed here localise specifically either to the proximal cilium (Nan and Iav) or the distal cilium (NompC).

Drosophila chordotonal neurons – Development, architecture and function

Like all type I sensory neurons, chordotonal neurons form a functional unit with several support cells. They all develop from a common sensory precursor cell and are specified through asymmetric cell division and the action of evolutionarily conserved transcription factors such as atonal, fd3f and Rfx (Fig. 1.10A (Boekhoff-Falk and Eberl, 2014; Dubruille et al., 2002; Jarman and Groves, 2013; Kernan, 2007; Newton et al., 2012)). Depending on the developmental stage and on the location in the animal, one to five cilia are engulfed by a support cell called a scolopale cell. Each neuron forms one cilium, and the cilia project jointly into a funnel-like structure generated by a cap cell (Fig. 1.10B). Chordotonal cilia respond to mechanical stimulation by generating action potentials. These are propagated through the axons directly into the brain of the animal. The cap cell connects the cilia to the cuticle. Mechanical deformation of the cuticle is transmitted to the cilia and results in opening of ion channels that localise specifically to the ciliary membrane of these neurons. The scolopale cell is thought to

generate and maintain a particular ion composition in the extracellular environment surrounding the cilia. It is also characterised by a large number of parallel actin rods, which probably contribute to the mechanical properties of the system (Boekhoff-Falk and Eberl, 2014).

I will mostly focus here on the chordotonal cilia in the second antenna segment of the flies, because they are the best understood. About 480 ciliated neurons can be found per antenna, but they fall into distinct subclasses required for different sensory functions such as hearing, gravitaxis and wind-sensation (Kamikouchi et al., 2009; Yorozu et al., 2009). The chordotonal cilium is compartmentalized. An electron dense protein matrix called the ciliary dilation is visible in electron micrographs and separates the proximal from the distal cilium (Fig. 1.10C (Bechstedt et al., 2010)). The proximal cilium bears dynein arms that can be observed in cross sections. These cilia are physically attached at the tip and it is currently unclear what type of movement they perform. The dynein arms are, however, essential for the mechanical amplification of sounds, which makes these neurons incredibly sensitive sound receivers (Karak et al., 2015). The proximal and distal segment are also distinct in their ion channel composition. Two transient receptor potential (TRP) channels called Nanchung and Inactive are of the vanilloid subtype and localise to the proximal cilium (Gong et al., 2004a). Another TRP channel called NompC localises to the distal cilium (Lee et al., 2010). In hearing, NompC was proposed to mediate signal transduction, whereas Nanchung and Inactive amplify and propagate the signal (Albert and Göpfert, 2015). In campaniform sensilla, NompC was found to form connections between the ciliary membrane and the microtubules underneath. Analysis from mutants unable to form these membrane tethers led to the proposal that they act similarly to the tip-link structures in vertebrate ears. If the membrane is moved

relative to the microtubules, this tether will pull the NompC channel open and lead to depolarization of the cell (Zhang et al., 2015). A similar mechanism might also apply in the auditory cilia. It is not, however, generalizable for all chordotonal cilia because NompC was found to be dispensible for gravity sensation (Sun et al., 2009).

Little is known about maintenance of the sensory neurons in *Drosophila*, but adult flies use chordotonal neurons for at least up to two weeks before age-related behavioural phenotypes can be observed (Grotewiel et al., 2005). In other systems such as *Chlamydomonas,* significant protein turnover in the cilia occurs within hours and days (Song and Dentler, 2001). It is hence expected that the *Drosophila* also requires transport mechanisms such as IFT in order to maintain ciliary function.

The role of IFT in cilia maintenance in the fly was never addressed specifically. Very few IFT proteins were studied in *Drosophila*. IFT88 in other ciliated species seems to have an important role in the formation of the IFT complex and to play a role in cilia maintenance. Loss of IFT88 function in *Drosophila* is incompatible with cilia formation (Fort et al., 2016; Han et al., 2003; Pazour et al., 2000, 2002). IFT88 is hence a strong candidate to be involved in cilia maintenance in *Drosophila* as well. Given that only a subset of the IFT complex is conserved in the fly (Fig. 1.5B), *Drosophila* might also be an interesting model to investigate evolutionary constraints on the IFT complex.

A role of IFT88 in the maintenance of the photoreceptor ciliary signalling compartment

This thesis is about the role of the evolutionary conserved IFT core component IFT88 in cilia maintenance. IFT88 was proposed to contribute to the maintenance of the cGMP signalling compartment in mammalian photoreceptors (Bhowmick et al., 2009). Johnson and

Leroux argued that there is an evolutionary relationship between cGMP signalling and cilia function (Fig. 1.11 (Johnson and Leroux, 2010)). In this section of the introduction, I will briefly summarize cGMP signalling and then discuss its association with IFT and its specific function in photoreceptor cilia.

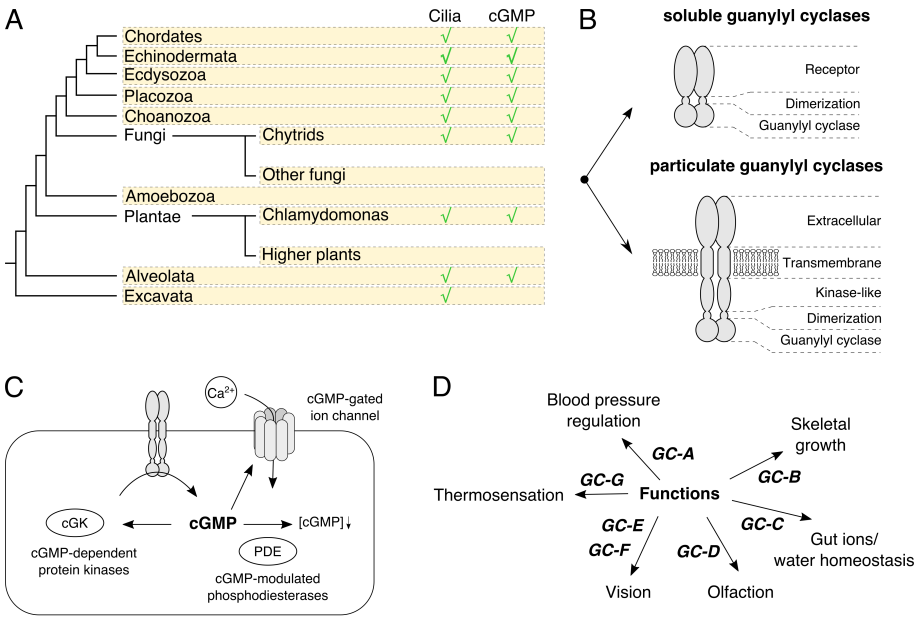

Fig. 1.11: **cGMP signalling is evolutionarily related to cilia and involved in various physiological processes in mammals**. (A) A correlation is shown here between the presence or absence of cilia (green tick mark for presence) in various eukaryotic species and cGMP signalling machinery (see C) encoded in the genome (modified from (Johnson and Leroux, 2010). The evolutionary distribution of the two traits suggests that they are correlated. (B) There are two classes of guanylyl cyclases – soluble and particulate. The first class can freely diffuse in the cytoplasm, whereas the latter is membrane-bound. Both have a cyclase domain to form cGMP and require dimerization for their activity. Soluble guanylyl cyclases have a receptor domain. Their activation depends on ligand binding to the receptor domain. Particulate guanylyl cyclases analogously have an extracellular domain that can respond to ligands, but this does not apply to all guanylyl cyclases. Exceptions are GC-E, -F and –G. The retinal GCs are activated through protein binding

intracellularly (modified from (Sharma and Duda, 2014)). (C) cGMP is generated by guanylyl cyclases and in turn modulates the activity of cGMP-dependent kinases (cGK) and opens cGMP-gated ion channels. The cellular levels of cGMP are controlled by a group of specific phosphodiesterases (PDE). (D) Overview of the various physiological processes that are regulated by guanylyl cyclases in mammals and their respective cyclases. GC-D and GC-G cannot be found in the human genome (Fig. 1.11C and D were modified from (Kuhn, 2016)).

Introduction to cGMP signalling

The small signalling molecule cGMP was first discovered in the urine of rabbits. It was subsequently shown that the production of urinary cGMP is under the control of the endocrine system (Kots et al., 2009). Biochemical analysis revealed that the soluble as well as the particulate (or membrane bound) fraction of cell lysates from lung tissue of rats contained cGMP-generating activity (Chrisman et al., 1975). Today we know that those correspond to two classes of cGMP-generating enzymes (Fig. 1.11B). Both protein classes form dimers to be active. Soluble guanylyl cyclases have a receptor domain that mainly binds nitric oxide. In humans they are involved in processes such as the regulation of the endothelial tissue in the blood vessels. All particulate guanylyl cyclases have one transmembrane domain, which separates the protein into an extracellular part and an intracellular part. Some particulate guanylyl cyclases respond to ligand binding, but ligands have not been identified for all of them. On the intracellular side the proteins usually have a kinase homology domain that is often found phosphorylated and involved in dimerization, but only a few were shown so far to have kinase activity. Dimerisation is also important for the activity of the cyclase domain (Kuhn, 2016).

Intracellular cGMP levels are regulated by guanylyl cyclases as well as cGMP-modulated phosphodiesterases that break down cGMP (Fig. 1.11C). Two groups of proteins respond to cellular cGMP

levels: cGMP-dependent kinases and cGMP-gated ion channels. cGMP-dependent kinases in turn modulate the activity of other molecules and are involved in hormone release and electrolyte homeostasis. cGMP-gated ion channels are mainly known to function in the sensory system (e.g. in olfaction and in vision).

Seven particulate guanylyl cyclases are known in mammals and six in Drosophila. *C. elegans*, however, encodes 27 particulate guanylyl cyclases in its genome, many of which have been linked to cilia function (Maruyama, 2016). The nomenclature of the mammalian particulate guanylyl cyclases is confusing. I follow here the recommendation of the International Union of Basic and Clinical Pharmacology and name the mammalian particulate guanylyl cyclases GC-A to G (Fig. 1.11D). I will deviate, however, when referring to GC-E, because in human patients the use of Gucy2d (Gucy2e in mice) is still more frequent. GC-D and GC-G are pseudogenes in humans (Kuhn, 2016). Four (GC-D to -G) of the seven particulate guanylyl cyclases were reported in cilia involved in olfaction and vision (Baehr et al., n.d.; Liu et al., 2009; Meyer et al., 2000). In the next section I will briefly discuss the function of GC-E/Gucy2d, because it has been suggested that this protein binds to IFT88 and requires IFT for ciliary transport (Bhowmick et al., 2009).

Photoreceptor cGMP signalling in health and disease

In photoreceptor cells the Gucy2d protein is required to maintain depolarisation of the cell in darkness (Fig. 1.12A). In the absence of light, cGMP levels are kept high by the protein, which leads to the opening of cGMP-gated ion channels and subsequent influx of calcium and sodium ions. Depolarized photoreceptors release the neurotransmitter glutamate onto the downstream neurons. When the photoreceptor is exposed to light, phosphodiesterase 6 is activated, which leads to rapid degradation of cGMP and closure of the

corresponding ion channels (Fig. 1.12B). As a consequence, the photoreceptor stops the release of glutamate (Baehr, 2014).

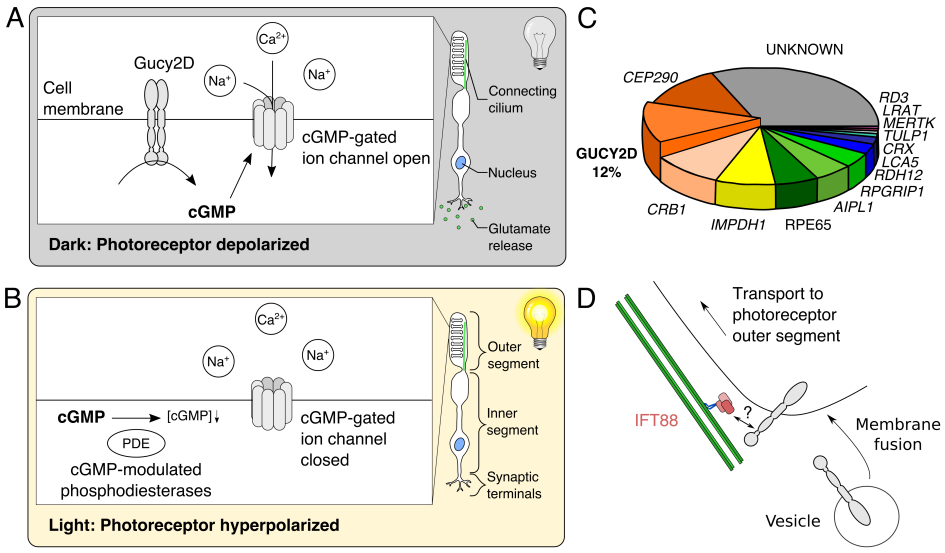

Fig. 1.12: **Gucy2d, essential for photoreceptor recovery and frequently mutated in human patients with Leber congenital amurosis (LCA), requires IFT88 for localisation**. (A) Gucy2d (GC-E, retGC1) generates cGMP in the outer segment of photoreceptors in the mammalian retina in the absence of light. This in turn opens ion channels permeable to calcium and sodium ions. The photoreceptors release glutamate (a synaptic transmitter) onto the downstream neurons as a result of the depolarisation. (B) Light-induced activation of a specific phosphodiesterase (PDE) reduces the intracellular cGMP levels. cGMP-gated ion channels close as a consequence which results in photoreceptor hyperpolarisation. This in turn blocks glutamate release. The compartmentalisation of the photoreceptor cells is depicted on the right side of the boxes (A and B are modified from (Kuhn, 2016)). (C) Gucy2d is frequently found mutated in patients with the retina-specific ciliopathy LCA (numbers from a large metastudy summarising 38 individual studies, graph adapted from (den Hollander et al., 2008). (D) The mouse and bovine homologues of Gucy2d are

transported to the outer segment of the photoreceptor cells. This transport requires binding to IFT88 (model adapted from (Bhowmick et al., 2009)).

The loss of ciliary function is known to cause photoreceptor degeneration and retina dystrophy mice (Jiang et al., 2015; Pazour et al., 2002). Retina involvement is known in several ciliopathies such as Joubert syndrome, Bardet-Biedl syndrome, Nephronophtisis and Orofaciodigital Syndrome (Fig. 1.7 (Braun and Hildebrandt, 2017)). In Leber congenital amaurosis (LCA) it is mainly the retina affected due to mutations in genes involved in cilia function. Mutations in this disease have been found in genes required for transition zone formation such as Cep290 or genes implicated in ciliary trafficking like Tulp1 (Astuti et al., 2016; Coppieters et al., 2010). The most commonly mutated gene in LCA, however, is Gucy2d (Fig. 1.12D (den Hollander et al., 2008)). From work in the mouse and bovine retina, it was proposed that IFT88 binds to Gucy2d and transports it to the cilium (Bhowmick et al., 2009). Recent work, however, suggests a more complicated model in which IFT is not sufficient for Gucy2d transport, and the protein requires co-transport with rhodopsin for photoreceptor localisation (Pearring et al., 2015). Most disease-causing mutations in Gucy2d are explained by a reduction in the ability of the protein to generate cGMP. It is an open question, however, if transport can also account for some of the mutations reported in LCA patients.

cGMP signalling has never been associated with cilia function in *Drosophila*. This work aims to demonstrate whether cGMP signalling is also used in sensory cilia in the fly and to investigate whether transport mechanisms of a putative cGMP-generating enzyme in the neurons are also IFT-dependent.

Main objectives of this thesis

The main objectives of this thesis are:

Understand whether IFT has a role in ciliary maintenance in *Drosophila*

1. Investigate whether IFT is still active and DmIFT88/NompB is still present in fully formed cilia in *Drosophila melanogaster* (Chapter II)
2. Set-up and establish tools to manipulate DmIFT88/NompB activity in fully formed cilia (Chapter II)
3. Describe behavioural and cellular consequences of removing NompB from fully formed cilia in sensory neurons (Chapter II)

Explore the role of Gucy2d as an IFT cargo with a role in ciliary maintenance in *Drosophila*

4. Identification of a particulate guanylyl cyclase that could be related to Gucy2d and that is involved in gravitaxis in *Drosophila melanogaster* (Chapter III)
5. Provide evidence for molecular interaction of that cyclase with DmIFT88/NompB, if possible establish binding site(s) on the cyclase (Chapter III)
6. Analyse the binding site(s) for evolutionary conservation, if possible, derive hypotheses for the implications of the mutations for the interaction of the two proteins, with focus on outcome in LCA patients (Chapter III)

Chapter II – IFT88 as a case study for the role of IFT in cilia maintenance

Author contribution

If not otherwise specified, I conducted all experiments. Christian Spalthoff from the Göpfert lab (Göttingen) acquired the electrophysiology data (Fig. 2.4). Samples for electron microscopy were prepared and sectioned by Susana Mendonça (Fig. 2.5). Images were acquired jointly with me. The clearing protocol to image whole antennae was developed with the help from Ânia Gonçalves from the IGC imaging facility (Fig. 2.7).

Summary

Cilia function is very important in development and disease. Hundreds of different proteins contribute towards forming this astonishingly versatile organelle. Little is known, however, about which and how individual proteins are involved in maintaining cilia function. This problem is especially interesting in long-lived cells such as photoreceptor cells in the human retina, that are only slowly or never replaced and depend on cilia for their function. If those cilia are not maintained properly, the individual will turn blind with time. In the mouse, the intraflagellar transport protein IFT88 is required for photoreceptor maintenance (Jiang et al., 2015). IFT88 is a very important molecule for cilia biogenesis in all species studied to date. It is not clear, however, what properties are maintained by IFT88 and what proteins it transports.

Here I use the *Drosophila* homologue of IFT88 (DmIFT88/NompB) to investigate if and how DmIFT88/NompB contributes to the maintenance of cilia in chordotonal neurons in in the antenna the fruit fly. My work shows that DmIFT88/NompB is continuously present in those cilia even when biogenesis is completed. Moreover, the protein persistently undergoes anterograde and retrograde transport. Removal of the protein after ciliogenesis is completed

causes ciliary dysfunction, suggesting that it is required for cilia maintenance in this system. The mechanism through which the protein contributes to cilia maintenance, however, remains elusive.

Introduction

Maintenance of cellular compartments and protein complexes is an important problem. Cells lose components through cell division or through the formation of extracellular vesicles. Additionally, molecules suffer insults from cellular stress such as the exposure to radical oxygen species or problems in protein folding due to heat stress (Kültz, 2005). One important aspect of maintaining cellular structures is to transport new building blocks to the appropriate cellular location to replace compromised subunits of a given structure. Most of our knowledge regarding cilia maintenance and cilia specific transport is derived from the Chlamydomonas rheinhardtii (see “What do we know about maintenance of cilia?“). Work on this unicellular algae led to the discovery of intraflagellar transport (IFT). IFT is a protein complex with 22 subunits that moves anterogradely and retrogradely along the ciliary axoneme (Taschner and Lorentzen, 2016). The results obtained in Chlamydomonas also demonstrated that IFT plays a main role in cilia maintenance (Huang et al., 1977; Kozminski et al., 1993, 1995; Marshall et al., 2005; Marshall and Rosenbaum, 2001). One role of IFT is to transport tubulin in Chlamydomonas and other species (Bhogaraju et al., 2013), but several other cargoes are known now as well (Taschner and Lorentzen, 2016). The continuous presence and activity of IFT in mammalian cilia suggests that it is also required to maintain properties of cilia in other species (Hu et al., 2010; Milenkovic et al., 2015; Trivedi et al., 2012; Ye et al., 2013). The role of IFT in maintenance is difficult to separate from its contribution to biogenesis, because most IFT mutants have compromised ciliogenesis. Informative results for the role of IFT in cilia

maintenance in vertebrates come from work carried out in the mouse retina. Vertebrate photoreceptors are an excellent model to study cilia maintenance, because the outer segment of the photoreceptor is a modified cilium that undergoes complete turnover within several days (Besharse and Hollyfield, 1979; Hsu et al., 2017). Complete removal of the IFT-B (the subcomplex required for antegrade IFT movement) through either inducible knockout of its motor or through removing the essential subunit IFT88 both lead to photoreceptor degeneration (Jiang et al., 2015). It is not known, however, whether there are differences in the cargoes transported by IFT in cilia of different species, or even between cilia types of the same species. Furthermore, it is important to understand the individual contribution of those cargoes in specific cilia for both stability and function. The unicellular parasite Trypanosoma uses flagella beating for motility. In Trypanosoma, IFT88 is not necessary for maintenance of cilia structure, but the beating frequency is changed (Fort et al., 2016). Deactivation of IFT in fully formed cilia could hence give rise to different structural and/or functional defects. This might in turn provide new hints as to which are relevant IFT cargoes. Here I use IFT88 to further investigate cilia maintenance.

Ciliated sensory neurons in adult *Drosophila* as a system to study cilia maintenance

One key problem in addressing the contribution of a protein to the maintenance of a structure lies in the difficulty of separate maintenance from biogenesis experimentally. For example, mutations in putative maintenance genes might also compromise biogenesis. Additionally, an experimental system in which cilia can be reabsorbed might further complicate the analysis of the data. The ideal system would permit perturbation of cilia over a reasonable period of time, during which the cells do not normally reabsorb their

cilia. Furthermore, it should be simple to assess cilia function to be able to test the role of different proteins at different time points. *Drosophila melanogaster* possesses several types of ciliated sensory neurons that are required for different sensory modalities (Fig. 1.9). These neurons can be found in all developmental stages of the fly. In adult animals, they are formed during pupae stage. Additional neurogenesis in the peripheral nervous system after eclosure has never been reported. Furthermore, many genetically encoded tools are available for *Drosophila melanogaster* to manipulate activity of a wide range of genes in specific tissues and at a time point of interest (Dietzl et al., 2007; Jenett et al., 2012; McGuire et al., 2003; Perkins et al., 2015). These properties make the fly an ideal experimental system to address the contribution of IFT to cilia maintenance.

Current understanding of IFT in *Drosophila*

Very little information is available about IFT in the fruit fly. IFT is required for cilia biogenesis in specific sensory neurons, but not for the formation of the sperm flagellum (Han et al., 2003; Sarpal et al., 2003). Cilia on those sensory neurons in *Drosophila* are an integral part of the signal transduction process (i.e. the conversion of a environmental stimulus to an electric signal). Since those cilia are required for sensation, behaviour can be used as a primary readout for cilia function. DmIFT88 (*Drosophila melanogaster* IFT88)/NompB is essential for cilia biogenesis in those neurons (Han et al., 2003), as well as for cilia in *Chlamydomonas* and mice (Pazour et al., 2000). Other IFT homologues have been identified through bioinformatics analysis and shown to be expressed in sensory neurons (Avidor-Reiss et al., 2004), but only DmIFT140/RempA has been described in more detail. RempA is a component of the IFT-A complex, which is required for retrograde IFT movement. It is only

involved in the formation of the distal segment of the sensory cilia (Lee et al., 2008). Two more IFT proteins have been shown to cause ciliary defects when mutated. DmIFT122/Oseg1 (IFT-A) and DmIFT172/Oseg2 (IFT-B) both are required for the sensory neurons to respond to stimulation, but the precise cilium defects are less clear (Avidor-Reiss et al., 2004).

IFT88 is required to maintain photoreceptor cilia in mice (Jiang et al., 2015). Moreover, the fly mutant for DmIFT88/NompB has the most severe phenotype of all IFT components studied so far in the fly, making it likely an essential part to the IFT complex. DmIFT88/NompB is, therefore, an interesting candidate to address the role of IFT in cilia maintenance. Furthermore, members of the IFT-A subcomplex have been found to be involved in Wnt signalling in non-ciliated cells in the developing *Drosophila* wing (Balmer et al., 2015). These roles of IFT proteins outside of the cilia might complicate the analysis of behaviour, because of the involvement of other organs in generating behavioural responses. IFT88, however, has not not found to have a role in Wnt signalling (Balmer et al., 2015), nor has it been previously associated to any other function unrelated to cilia. Another example for a non-cilia function would be the role of mammalian IFT88 in orientation of the mitotic spindle (Delaval et al., 2011, p. 88). It is not known whether DmIFT88/NompB localises to the mitotic spindle. It does not seem to have an essential function there, however, as the DmIFT88/NompB mutant flies do not exhibit any phenotypes suggesting mitotic defects (Han et al., 2003). Furthermore, it is the first IFT component that has been associated to human disease (Pazour et al., 2000).

Goals

1. Investigate whether IFT is still active and DmIFT88/NompB is still present in fully formed cilia in *Drosophila melanogaster*

2. Set-up and establish tools to manipulate DmIFT88/NompB activity in fully formed cilia
3. Describe behavioural and cellular consequences of removing NompB from fully formed cilia in sensory neurons

Experimental strategy

The Drosophila homologue of IFT88 (DmIFT88/NompB) has little conservation in terms of amino acid composition, but is conserved on the level of protein structure (Fig. 2.1). DmIFT88/NompB DmIFT88/NompB can be observed in fully formed cilia in tissue sections (i.e. fixed material) using a transgenic line that expresses a GFP-fusion protein under an endogenous promoter fragment (Han et al., 2003). This does not determine, however, if this protein population actually undergoes IFT-like movement (Fig. 2.2). The transgenic protein can only be observed upon antibody staining and is therefore not suitable for live-imaging. I therefore generated a new transgenic fly line to study the protein in living tissue. I also developed a preparation to image fully formed cilia in living larvae (Fig. 2.3).

Removal of DmIFT88/NompB through mutation leads to flies without cilia, but it does not impair the formation of the neuron otherwise, nor does it impact fly development in general as far as we can tell (Han et al., 2003). The resulting flies have motile sperm, but are unable to mate due to coordination defects. These phenotypes can be phenocopied through the use of RNAi (Fig. 2.4). With the help of the $Gal80^{ts}$ system (McGuire et al., 2003), I generated flies that express a hairpin specific for DmIFT88/NompB in the ciliated sensory neurons, through which the expression can be suppressed during neuronal development. This allows flies to develop with normal DmIFT88/NompB expression levels. DmIFT88/NompB knockdown is only induced in adult flies (Fig. 2.6). Using this strategy, NompB

activity can be removed specifically in adult flies to test the role of DmIFT88/NompB in fully formed cilia.

Material and methods

Bioinformatic analysis of DmIFT88/NompB

The gene model for DmIFT88/NompB was extracted from the Ensembl Genome Browser (Yates et al., 2016). The number of tetratricopeptide repeat domains (TPR) was predicted using the TPRpred tool (Karpenahalli et al., 2007). I compared the IFT88 protein sequences of eleven metazoan species (see Tab. 2.1). Whenever several IFT88 isoforms are reported for the same species, the largest one was chosen. The MegAlign program (Lasergene suite, Version 8.1.3, DNASTAR©) was used to generate a tree summarizing sequences similarities as a function of number of amino acid substitutions between sequences. Sequences were aligned using the ClustalW algorithm with default settings. Bootstrapping analysis was performed with default values to calculate the support of each branching point in the tree.

Multiple sequence alignment is presented as a heatmap (Fig. 2.1). I generated an alignment file in the fasta format using the web browser-based MUSCLE tool (Edgar, 2004). The percentages for sequence identity were also extracted from there. Subsequently, I used the ProfilGrid tool (Roca et al., 2008) with default settings to assign a similarity score to each position in the alignment. The score can reach values between 0 and 1. The results are presented as a heatmap. The heatmap was visualized with RStudio (RStudio®) and the ggplot2 package (Wickham, 2016).

Tab. 2.1: IFT88 sequence used for comparison

Species	Accession number
Aedes aegypti	EAT40549
Anopheles gambiae	XP_556988.3
Danio rerio	XP_005167586
Drosophila erecta	XP_001973983.2
Drosophila melanogaster	NP_724347.3
Drosophila simulans	EDX05743.1
Gallus gallus	XP_015134793.1
Homo sapiens	NP_001305422
Mus musculus	NP_033402
Tribolium castaneum	EFA00677
Xenopus tropicalis	F6W448

Cryosectioning and immunolabeling of *Drosophila* antennae

The protocol to section adult antenna was adapted from the literature (Mishra, 2015). If not stated otherwise, steps were carried out at room temperature. Flies were anaesthetized using CO_2 and decapitated. The heads were collected in pre-cooled fixation buffer (4% paraformaldehyde, 75 mM PIPES buffer (pH 7.6), 0.05% Triton-X, picric acid) and incubated for 40 minutes. Good fixation requires the heads to sink to the bottom of the reaction tube. Subsequently, the heads were washed three times in PBST (PBS with 0.05% Triton-X). The detergent in the buffer helps to overcome the hydrophobicity of the cuticle. The heads were then incubated on a rotator in PBST with 10% sucrose for one hour at room temperature and then overnight in 25% at 4°C. The heads were embedded and oriented appropriately in OCT (optimal cutting temperature formulation) and the OCT was frozen on dry ice. Blocks with *Drosophila* heads were kept on dry ice until sectioning. Head samples were sectioned in a Leica Cryostat CM 3050 S (Leica). Samples were sectioned at 12 µm thickness and slices were collected on Poly-lysine coated slides (Sigma). Sections were

washed with PBST (PBS with 0.05% Triton-X) several times for 10 minutes each, followed by incubation in blocking buffer (10% BSA in PBST) for one hour and subsequent incubation with the primary antibody diluted in blocking buffer overnight at 4°C (for details of the antibodies see Tab. 2.2). Samples were washed three times in blocking buffer and incubated for one hour with secondary antibody in blocking buffer. Finally, after three additional washing steps using PBS for 5 minutes each, samples were embedded in Vectashield supplemented with DAPI (Vector Laboratories). Images were acquired on a SP5 Live Upright microscope (Leica, Germany).

To test whether DmIFT88/NompB knockdown affects cilia compartmentalisation, antenna sections were stained for Inactive (Iav). Iav labels specifically the proximal cilium (Gong et al., 2004b). For quantification of Iav signal intensities, image stacks were deconvolved using the Huygens Deconvolution v17.4 software (Scientific Volume Imaging). Images were segmented using Imaris v6.4 software (Bitplane). The Iav signal was used to define volumes manually. The pixel intensities from the Iav staining were then extracted from those volumes. Statistical analysis and graphical representation of the data was done in RStudio (RStudio®, USA).

mRNA isolation from adult antenna and reverse transcription

Between 100 and 200 flies were decapitated per genotype. For quantification of mRNA levels, 50 to 70 heads can be sufficient. Heads were collected in Protein LoBind tubes (Eppendorf) on dry ice. Ten to 20 heads were collected at a time to avoid compromising the tissue due to long exposure to room temperature. Tubes were snap-frozen in liquid nitrogen. Antennae were dissociated from heads through mechanical force using a vortex mixer (three times for ten seconds, cooled in between again on dry ice). To separate heads from antenna, tubes were opened and inverted. Heads will fall

out, whereas the majority of the antennae will adhere to the wall of the tubes.

Tab. 2.2: Details of the antibodies used in this chapter

Antibody	Dilution	Species	Source
Primary antibodies			
anti-GFP	1:1000	rabbit	Invitrogen
anti-PLP	1:1000	chicken	Glover lab
GT335	1:500	mouse	Janke lab
anti-NompC	1:200	rabbit	Chung lab
anti-Iav	1:500	rat	Kim lab
anti-acet. tubulin	1:500	mouse	Sigma
Secondary antibody			
anti-rabbit Alexa488	1:500	goat	Molecular Probes
anti-rabbit Alexa647	1:500	donkey	Jackson
anti-chicken Rhod	1:500	donkey	Jackson
anti-rat Rhodamine	1:500	goat	Jackson
anti-mouse Alexa488	1:500	goat	Molecular Probes
anti-mouse Alexa647	1:500	goat	Life technologies

Total mRNA was isolated from antenna using the PureLink^{TM} RNA Mini Kit (Ambion). Antennae were lysed in 250 µl of lysis buffer. The protocol was carried out as described in the accompanying manual. No DNAse treatment was performed. The mRNA was always converted to cDNA immediately. For quantification of mRNA expression amounts as low as 150 ng of total mRNA in 20 µl of the reverse transcription reaction are sufficient to reliably detect gene expression. For cloning 1 µg of total mRNA was reverse transcribed. The reverse transcription reaction was performed with the Transcriptor First Strand cDNA Synthesis kit (Roche). For cloning

NompB, cDNA was generated using poly-dT primers included in the kit. The cDNA samples were stored at −20°C until further use.

Cloning of DmIFT88/NompB and generation of transgenic flies

The cDNA for cloning NompB was obtained from w^{1118} flies. NompB was amplified using the KOD polymerase kit (EMD Millipore) in 50 µl reaction volume (for PCR primers see Tab 2.3). PCR was set up as outlined by the kit. The reaction mix was supplemented with DMSO. The PCR product was purified using the DNA Clean & Concentrator™ kit (Zymo Research) and adenylated at the 5' ends through incubation with DreamTaq (Thermofisher) using the appropriate buffer and dNTPs at 70°C for one hour. Subsequently, the PCR product was ligated into pGEM-Teasy (Promega) following the manufacturer's instructions and plasmids were confirmed through sequencing (for sequencing primers see Tab 2.3). Using the Gateway system, the coding sequence was first cloned into pDONR 221 in a BP-reaction (Invitrogen), following the instructions for the kit and subsequently transferred to pTHW and pTGW in an LR-reaction (Invitrogen) to fuse the resulting protein to three HA-tags or one GFP-tag on the N-terminus, respectively (for details on pTHW and pTGW see Drosophila Genomic Resource Center). DmIFT88/NompB was tagged at the N-terminus, because the resulting protein fusion was previously shown to rescue the mutant phenotype and can hence be considered fully functional (Han et al., 2003). Plasmid DNA was amplified in *E. coli* DH5α and purified using ZR Plasmid MiniprepTM-Classic (Zymo research). For large scale DNA purification (for transfection experiments and fly transgenesis) the ZymoPURE™ Midiprep Kit (Zymo research) was used. Injections into *Drosophila* embryos and selection of positive transformants were outsourced (BestGene or IGC transgenics facility).

Tab. 2.3: Primers used for the experiments in this chapter, annealing temperatures (T_a) were used as stated here, the OligoCalc tool was used for prediction (Kibbe, 2007), extension times were chosen according to the length of expected product and the properties of the respective polymerase according to the manufacturer

Name	Purpose	Sequence	T_a
NompB_FL_gateway_fwd	Gateway cloning NompB	GGGACAAGTTTGTACA AAAAAGCAGGCTTCAT GACTTCTCAAATAACT GCTAACGGAACGC	52°C
NompB_FLS_gateway_rev	Gateway cloning NompB (with Stop codon)	GGGGACCACTTTGTAC AAGAAAGCTGGGTCTC AAATAGGCAATAAGCT TTCGGG	52°C
NompB_seq_fwd	For sequencing NompB coding sequence	GCAGCCACAGTGAAAC ATCG	--
NompB_seq_rev	For sequencing NompB coding sequence	AACTCAGGTTGGTCAG AGCG	--
NompB_seq_rev2	For sequencing NompB coding sequence	AGACGGGTGTATTCCG ATGC	--
NompB-RD_RT-PCR_fwd	Quantify mRNA expression of NompB-RD isoform	CCCCTACACGTCCATT CTGC	54°C
NompB-RD_RT-PCR_rev	Quantify mRNA expression of NompB-RD isoform	CCCCTACACGTCCATT CTGC	54°C
NompB_RT-PCR_fwd	Quantify mRNA expression of NompB-RC isoform	CGCTGGAATTAGGGGA CCTG	54°C
NompB-RC_RT-PCR_rev2	Quantify mRNA expression of NompB-RC isoform	AGGATCAAACTGCAGA AATCG	54°C
eIF-1A_RT-PCR_fwd	Quantify mRNA expression of eIF-1A (house keeping	GATATACTGGTTCCCC GCGA	54°C

	gene)		
eIF-1A_RT-PCR_rev	Quantify mRNA expression of eIF-1A (house keeping gene)	GGCTTGTTGGCGACCA ATTTT	54°C
Su(Tpl)_RT-PCR_fwd	Quantify mRNA expression of Su(Tpl) (house keeping gene)	AGCCACAAATCCATGC AGAG	54°C
Su(Tpl)_RT-PCR_rev	Quantify mRNA expression of Su(Tpl) (house keeping gene)	TGGACGTTGACTTCTT GTTGT	54°C
TBP_RT-PCR_fwd	Quantify mRNA expression of TBP (house keeping gene)	TTATGCGAATCCGAGA GCCC	54°C
TBP_RT-PCR_rev	Quantify mRNA expression of TBP (house keeping gene)	GTCGAGGAACTTTGCA GGGA	54°C

Live imaging of chordotonal cilia in L3 larvae

GFP::NompB was expressed in chordotonal neurons using iav-Gal4 (Gong et al., 2004b). Flies were reared at 25°C to the third larval stage. All experiments were performed with wandering L3 larvae. Larvae were collected and briefly washed in PBS. For imaging, larvae were immobilized between a coverslip and a slide in a drop of PBS (Zhang et al., 2013). The cover slip was held in place using transparent tape. Imaging was performed at the Roper Spinning Disc microscope (Nikon). Samples were kept at 25°C through the imaging process. To prevent artefacts from cell death, larvae were always imaged immediately after immobilization and for a maximum duration of two minutes. An image was acquired every 120 ms with 100 ms exposure time. Images were analysed using the FIJI software

(Schindelin et al., 2012) and kymographs were generated using the KymographClear plugin (Mangeol et al., 2016). Data plots were generated using RStudio (RStudio®).

Quantification of NompB expression levels from adult antennae

For measuring NompB expression levels, the total mRNA was isolated from antenna of adult flies up to four days after eclosure using Real-time PCR (RT-PCR). At least one primer in a pair was designed to span an exon-exon junction in order to avoid amplification of genomic DNA that might contaminate samples. The web browser-based Primer-BLAST tool (Ye et al., 2012) was used to design primers specific for a given transcript. All primers (see Tab. 2.3) used here were tested to only yield a single product and to not amplify genomic DNA. The NompB primers were proven to only amplify the respective isoform using cDNA (data not shown). 150 ng of total mRNA were reverse transcribed to cDNA in a reaction volume of 20 µl. The cDNA mix was diluted 1:10, and 4 µl of the dilutions were used in each reaction. iTaq™ Universal SYBR® Green Supermix (Biorad) was used to detect amplification of the PCR products. The reactions were set-up up according to the manufacturers protocol and run on the CFX384 Touch™ Real-Time PCR Detection System (Biorad). The total mRNA was isolated three times per genotype and each sample was measured in triplicates. Results were analyzed using RStudio (Rstudio®).

Tab. 2.4: Fly stocks used in this chapter

Name	Genotype	Source
tub-Gal4	y[1] w[*]; P{w[+mC]=tubP-GAL4}LL7/TM3, Sb[1] Ser[1]	Bloomington stock center, BL# 5138
tub-Gal80ts	w[*]; sna[Sco]/CyO; P{w[+mC]=tubP-GAL80[ts]}7	From Florence Janody's lab
mCherry RNAi	y[1] sc[*] v[1]; P{y[+t7.7]	Bloomington stock

	v[+t1.8]=VALIUM20-mCherry}attP2	center, BL# 35785
NompB RNAi	y[1] v[1]; P{y[+t7.7]	Bloomington stock
	v[+t1.8]=TRiP.JF03080}attP2	center BL# 28665
UAS-GFP::NompB	W[1];;UAS-GFP::NompB/TM6B	Our lab (IGC facility)
UAS-mCD8::GFP	w[*]; UAS-mCD8::GFP/CyO.Z;	From Elio Sucena's
	MKRS/TM6B	lab
Chat-Gal4	Chat-Gal4/CyO	From Swadhin Jana
Chat-Gal4, UAS-GFP	Chat-Gal4, UAS-GFP	From Swadhin Jana
Iav-Gal4	w[*];; Iav-Gal4	From Martin Göpfert's lab
endo-GFP::NompB	w[*]; endo-GFP::NompB	From Daniel Eberl

Biophysical recordings from adult antennae

All electrophysiological and mechanical recordings were carried out by Christian Spalthoff in the lab of Martin Göpfert in Göttingen, Germany. Recordings of mechanical and electrophysiological properties were performed as previously reported (Albert et al., 2006; Bechstedt et al., 2010). The hairpin for NompB knockdown was driven using tub-Gal4, a constitutively active promoter, to test whether the hairpin used for this study can mimic the hearing phenotype described for NompB mutant flies (Han et al., 2003). Adult flies were measured until up to six days after eclosure. Action potentials were recorded from head-fixed animals. For recording, a tungsten needle was inserted between head and antenna. The other antenna was immobilized to not elicit electric signals that might interfere with the recording. A reference electrode was positioned in the thorax. To determine maximum compound action potential, flies were stimulated using pure tones at the best frequency determine for every individual animal prior to measurement. Data was analyzed and graphs were generated using RStudio (RStudio®).

Electron microscopy: Sample preparation and image acquisition

All samples for electron microscopy were processed and sectioned by Susana Mendonça as previously described (Jana et al., 2016). Antennae were dissected from the heads and incubated in fixative (2% formaldehyde, 2.5% glutaraldehyde in 0.1 M sodium bi-phosphate buffer pH 7.2–7.4) overnight. Samples were washed several times in PBS and then incubated for 1.5 hours in 1% osmium tetroxide for postfixation. Subsequently, samples were washed several times in deionized water before incubating them in 2% uranyl acetate for 20 minutes on a rotator for *en bloc* staining. After this step, samples were dehydrated in a graded sequence of alcohol dilutions (from 50% to a 100%). Ethanol was removed through two incubation steps with propylene oxide for 30 min. Samples were embedded in resin overnight and transferred to a fresh batch of resin for 1h. Under a dissection microscope, the second segment of the antenna was separated from the third. The second segment is placed into mold with resin and polymerized. Samples were sectioned in the desired orientation. Sections were 70 nm thick. Sections were stained with 2% uranyl acetate followed by lead citrate staining. Finally, samples were air-dried and investigated using the Hitachi H-7650 transmission electron microscope.

Behavioural assessment of gravitaxis defects

For quantification of gravitaxis behaviour, flies were collected in 24 hour time windows and kept in groups of the same age. The animals were transferred to vials with fresh food every three days. Prior to the behaviour experiments, flies were separated according to sex into groups of ten animals that would be tested jointly. Flies were briefly anesthetized using CO_2 for sorting. Only healthy-looking and clean animals were considered for the assay. The flies were kept in

the room where the behavioural experiments were conducted for about one hour prior to the actual experiment. This time period was given to allow the animals to acclimatise to potentially different light and temperature regimes. Experiments were conducted in measuring cylinders made of glass. Animals were placed in cylinders a couple of minutes before the assay was started. Cylinders were sealed on top with perforated parafilm to prevent the flies from escaping. Cylinders were tapped until all flies were at the bottom of the cylinder and flies were subsequently allowed to walk up. All experiments were videotaped and analysed blindly only once a full data set (including control flies) was obtained. I always recorded the experiments for one minute, but the metric used for analysis was the number of flies above ten centimetres after ten seconds. I had previously established that flies expressing a hairpin against mCherry (negative control) pan-neuronally need on average ten seconds to perform this task in my set-up (data not shown). Videos were analysed for the whole duration of ten seconds after tapping the cylinder, to rule out that flies reached the ten-centimetre mark and walked back down again.

In order to test the maintenance role of DmIFT88/NompB, I generated flies that carried the pan-neuronal driver Chat-Gal4 on the second chromosome (Salvaterra and Kitamoto, 2001) and the constitutively expressed, but temperature sensitive, repressor tub-Gal80^{ts} (McGuire et al., 2003), on the third chromosome. Additionally, the second chromosome harboured a UAS-GFP insertion (UAS - Upstream activating sequence). These flies would express any construct under control of UAS in neurons of the central nervous system as well as the periphery when kept at 29°C. At 18°C Gal4 would be prevented from inducing expression through binding Gal80^{ts}. GFP would be expressed at 29°C under UAS control. This allows assessment of the general morphology of the neurons at

different time points of the experiment. Flies carrying these three insertions were mated to animals that encode hairpins corresponding to DmIFT88/NompB or mCherry (negative control) under the control of UAS.

I measured the behavioural performance of the flies in the assay for up to 15 days, but the control flies start to develop a gravitaxis phenotype around 12 days after eclosure, when kept at 29°C. This functional decline was previously reported (Grotewiel et al., 2005). This age-dependent gravitaxis phenotype might be unrelated to cilia function and could stem from function senescence in other organs such as the muscles. Therefore, data for experiments conducted at 29°C was only plotted until 9 days after eclosure.

Cuticle clearing and imaging of antennae whole-mounts

In order to image the GFP expressed in the chordotonal neurons in animals with knockdown of NompB and control animals, I had to overcome the problem of the cuticle covering the neurons. The cuticle is opaque and autofluorescent, which makes it generally unsuitable for imaging. With the help of Ânia Gonçalves, I developed a clearing method that made the cuticle transparent. It also allowed us to image the whole antenna without mechanical manipulation, which preserved the morphology of the cells. We compared several fixatives and clearing methods. Many treatments destroy the fluorescence of GFP (Kolesová et al., 2016). We obtained the best results by fixing whole heads in 4 % of paraformaldehyde in PBS (supplemented with 0.05 % Triton-X) for 40 minutes on ice. Heads were then transferred to a reaction tube containing FocusClear (CelExplorer, Taiwan) and incubated overnight. For imaging, heads were mounted on a slide in MountClear (CelExplorer, Taiwan). Several layers of clear tape were used as spacer between slide and coverslip. Images were acquired on a SP5 Live Upright microscope

(Leica, Germany). The size of the image stack was chosen to contain the whole antenna segment.

Results

Bioinformatic analysis of IFT88 reveals sequence divergence, but suggests structural conservation

Two isoforms are annotated for DmIFT88/NompB in the Ensembl Genome Browser (Yates et al., 2016). They vary very little in amino acid composition. Isoform NompB-RC uses two alternative splice site acceptors in exon 4 and in exon 5 leading to the insertion of seven and five additional amino acids, respectively (Fig. 2.1A). Isoform RD inserts one additional exon of 29 amino acids towards the C-terminus of the protein. Isoform RD is sufficient to rescue the known mutant phenotypes (Han et al., 2003). The mutations used by Han and collaborators (2003) affect both isoforms equally. The significance of isoform RC is presently unknown.

Ten tetratricopeptide repeat domains (TPR) can be predicted for each isoform (Fig. 2.1) using the TPRpred tool (Karpenahalli et al., 2007). TPR domains are frequently found in scaffold proteins. Usually, TPR domains consist of two antiparallel α-helices, and they are known to act as interfaces for protein-protein interactions involved in many different cellular processes ranging from transcriptional control and protein transport to protein kinase inhibition (Allan and Ratajczak, 2011). TPR domains are found in several IFT subunits (Taschner et al., 2012). They are involved in the formation of the IFT-B core complex. *Chlamydomonas* IFT88 binds to IFT52 through a region that contains three TPR (Taschner et al., 2014). TPR domains might also be involved in the IFT-cargo interaction. These and other findings illustrate the importance of TPR for IFT protein function. It is, therefore, not surprising, that IFT88

proteins, despite low levels of amino acid conservation between vertebrate and insects species (Fig. 2.1B-D) always have between ten to 15 TPR (Fig. 2.1C). It was suggested that the array of TPRs in *Chlamydomonas* IFT88 could form a superhelix similar to IFT70 (Taschner et al., 2014). The extent of similarity in the actual protein structure of IFT88 proteins from different species has never been explored. The high number of TPR detected across species suggests, however, that IFT88 always maintains an important role in mediating protein-protein-interactions within the IFT-B core complex.

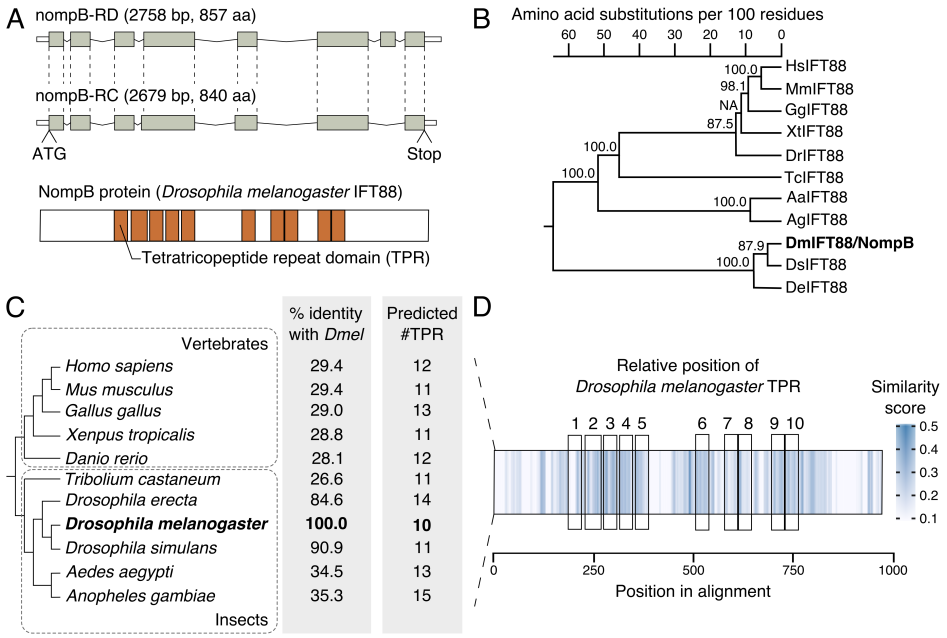

Fig. 2.1: ***Drosophila* IFT88/NompB is poorly conserved in amino acid sequence, but shows signs of structural conservation.** (A) Two nompB isoforms are annotated for *Drosophila melanogaster* in the Ensembl Genome Browser (Yates et al., 2016). They have only small differences in their amino acid sequences (small white boxes – untranslated regions, big gray boxes – coding sequence). The NompB protein contains ten tetratricopeptide repeat domains (TPR, brown boxes, predicted using TPRpred (Karpenahalli et al., 2007)). The TPR domains presumably create interaction surfaces for other proteins (ten TPRs can be predicted for each

isoform) (Allan and Ratajczak, 2011). (B) The IFT88 amino acid sequence was compared between different vertebrate and insect species (Hs – *Homo sapiens*, Mm – *Mus musculus*, Gg – *Gallus gallus*, Xt – *Xenopus tropicalis*, Dr – *Danio rerio*, Tc – *Tribolium castaneum*, Aa – *Aedes aegypti*, Ag – *Anopheles gambiae*, Dm – *Drosophila melanogaster*, Ds – *Drosophila simulans*, De – *Drosophila erecta*). Sequences differences are represented as a tree. Each branching point indicates the number of amino acid substitution per 100 residues required to convert one sequences into another. Support of each branch was calculated using bootstrapping analysis. Values can range from 0 to 100, NA indicates that the support could not be calculated due to the method used to generate the sequence alignment. (C and D) More detailed comparison of IFT88 protein sequences in the sequences compared above. (C) IFT88 sequence properties are ordered according to the phylogenetic relationship of the respective species. The amino acid identity of each sequence compared to *Drosophila melanogaster* is shown in %. The number of predicted TPRs in each species is shown as well. (D) Multiple sequence alignment of the eleven species given above is represented here as a heatmap. To generate the plot a similarity score was calculated using JProfileGrid2 (Roca et al., 2008). Each position in the alignment is shown as a box, which is then colour coded according to the similarity score. The relative positions of the ten TPRs of *Drosophila melanogaster* are indicated with black boxes.

DmIFT88/NompB expression and protein localisation in adult antenna

Both DmIFT88/NompB isoforms can be detected in mRNA isolated from adult antenna (Fig. 2.4B), which suggests that they continue to be important for cilia function in sensory neurons beyond biogenesis. The primers used here were shown to amplify each isoform specifically (tested with cDNA for each isoform) and do not amplify genomic DNA (data not shown). In order to investigate the localization of NompB protein, I obtained flies expressing the RD-isoform fused to GFP under control of a 2.2 kb endogenous promoter fragment (Fig. 2.2B). This construct can rescue the NompB mutant phenotype (Han et al., 2003). Pericentrin-like protein (PLP, a basal body marker) and polyglutamylated tubulin (GT335, a marker for the ciliary axoneme) were used as structural markers here

(schematic presentation in Fig. 2.2B). DmIFT88/NompB was detected strongly at the ciliary base and at the ciliary dilation. Additionally, GFP dots were detected along the axoneme. The strong signal near base and tip (ciliary dilation) represent probably an immobile fraction of the cellular NompB pool. The smaller dots of weaker signal intensity along the axoneme are likely to represent IFT trains. It is not possible, however, to address in fixed material whether those putative trains are in fact motile. I therefore developed methods to look at NompB protein in living tissue.

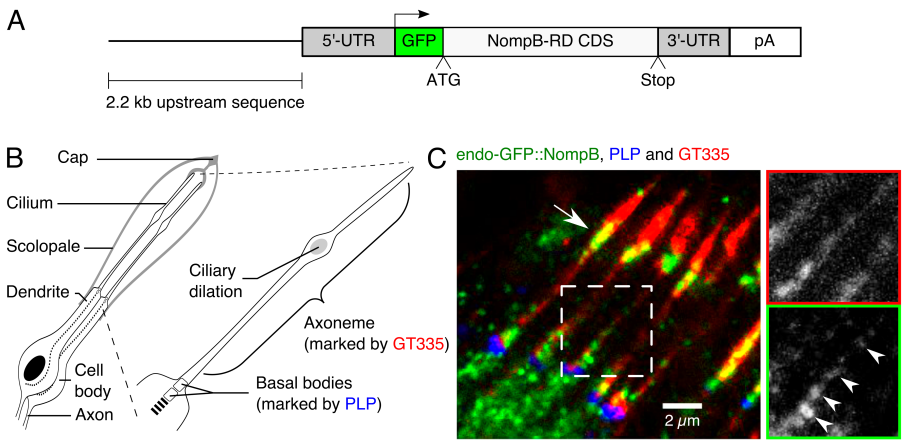

Fig. 2.2: ***Drosophila* IFT88/NompB protein is present in fully formed cilia**. (A) Schematic representation of the transgene used here (from (Han et al., 2003)). A 2.2 kb upstream sequence containing regulatory elements was cloned in front of the cDNA of nompB-RD together with a polyadenylation sequence (pA). The NompB protein was fused to a GFP-tag at the N-terminus. The transgenic flies were a kind gift from Daniel Eberl. (B) Schematic representation of the chordotonal neuron architecture, two neurons form a functional unit with their cilia enclosed by a support cell (scolopale). The markers label the basal bodies (Pericentrin-like protein - PLP) and the axoneme (stained here with an antibody labeling glutamylated tubulin – GT335). (C) Immunoflurescence image showing the localization of the NompB transgene with respect to the two markers. NompB accumulates at the ciliary dilation (arrow). Weaker NompB signals were detected along the axoneme (arrow heads in inset). NompB also accumulates at the ciliary base near the PLP signal.

DmIFT88/NompB expression and protein localisation in adult antenna

Both DmIFT88/NompB isoforms can be detected in mRNA isolated from adult antenna (Fig. 2.4B), which suggests that they continue to be important for cilia function in sensory neurons beyond biogenesis. The primers used here were shown to amplify each isoform specifically (tested with cDNA for each isoform) and do not amplify genomic DNA (data not shown). In order to investigate the localization of NompB protein, I obtained flies expressing the RD-isoform fused to GFP under control of a 2.2 kb endogenous promoter fragment (Fig. 2.2B). This construct can rescue the NompB mutant phenotype (Han et al., 2003). Pericentrin-like protein (PLP, a basal body marker) and polyglutamylated tubulin (GT335, a marker for the ciliary axoneme) were used as structural markers here (schematic presentation in Fig. 2.2B). DmIFT88/NompB was detected strongly at the ciliary base and at the ciliary dilation. Additionally, GFP dots were detected along the axoneme. The strong signal near base and tip (ciliary dilation) represent probably an immobile fraction of the cellular NompB pool. The smaller dots of weaker signal intensity along the axoneme are likely to represent IFT trains. It is not possible, however, to address in fixed material whether those putative trains are in fact motile. I therefore developed methods to look at NompB protein in living tissue.

IFT88 undergoes IFT in chordotonal neurons of L3 larvae

IFT88 has been shown to undergo antegrade and retrograde transport continuously in different species in fully formed cilia (Tab. 2.5) (Trivedi et al., 2012; Wei et al., 2012). Velocity quantifications are only available for mouse and *C. elegans* (Tab. 2.5). The numbers vary between the two species, which might be for two reasons. First, the motor proteins that drive the IFT trains

might have different speeds in different species. Second, differences could also come from the fact that the measurements are made at different temperatures (i.e. mouse cells are usually imaged at 37°C whereas *C. elegans* is imaged at 20°C). Even within the same species there are considerable differences reported in the literature (Tab. 2.1). Velocities might vary between cell type and conditions. The speed at which IFT88 moves in ciliated neurons in *Drosophila* is currently unknown.

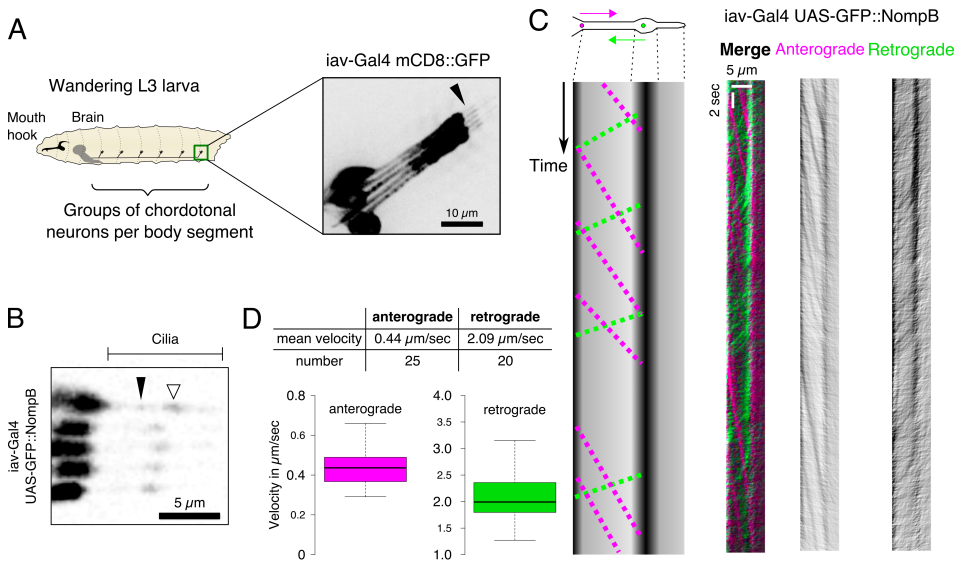

Fig. 2.3: **Description of IFT trains in wandering L3 larvae reveals similarities with IFT in other species**. (A) Schematic representation of a L3 larva showing the segmentally arranged groups of chordotonal neurons (five neurons per group). Membrane-bound GFP (mCD8::GFP) was used to visualize the morphology of one such group of neurons with the cilia marked by an arrowhead. (B) Still from a movie showing GFP-tagged NompB expressed in these neurons. Iav-Gal4 (almost exclusively active in chordotonal neurons) was used to drive the expression of the protein. The length of the cilia is indicated above the image. An empty arrowhead marks the ciliary dilation. An IFT particle can be seen (filled arrowhead). (C) Schematic representation of a cilium with IFT particles traveling in anterograde and retrograde direction. Below, a hypothetical kymograph is shown that would result

from the two particles moving in time along the cilium. An example kymograph with IFT particle tracks colour-coded depending on their direction is shown on the right. The tracks were extracted using the *KymographClear* macro toolset for ImageJ,(Mangeol et al., 2016)). IFT particles seem to be accumulating at the ciliary dilation (vertical line in all kymographs) (D) Quantifications of the speed of the anterograde and retrograde IFT particles and numbers of trains are given in the table (data was obtained from movies from five different larvae each).

The transgenic line generated by the Kernan lab (Han et al., 2003) does not allow for live imaging, due to the weakness of the GFP signal. Therefore, I generated transgenic lines expressing GFP::NompB using inducible promoters (i.e. driven with UAS elements). For that purpose, I cloned the coding sequence of the NompB-RD isoform in frame with an enhanced GFP-tag (at the N-terminus) into a plasmid that allows for P-element insertion. Transgenic flies were generated at BestGene.

In order to visualize IFT, I expressed the transgene using a chordotonal neuron specific driver line (Iav-Gal4). I imaged the chordotonal neurons in wandering L3 larvae. At that developmental stage, the chordotonal neurons are arranged in groups of five neurons on both sides of each body segment (Fig. 2.3A). The flies require the neurons at that developmental stage to detect sound or vibration. Stimulation of these neurons drives the larvae to burrow into the substrate (Zhang et al., 2013). The larvae depend on these neurons being fully functional at this developmental stage to avoid predators (i.e. larvae show escape behaviour in responds to sounds generated by wasps).

Quantifications of the velocity of the GFP::NompB signal (Fig. 2.3D, movie 1 in supplementary CD) reveals that the particles move about five times faster in the retrograde direction (2.09 µm/s) than in the anterograde direction (0.44 µm/s). The signal intensities of the anterograde trains appear stronger than the intensities of the

retrograde trains (Fig. 2.3C). It is not clear from the literature what to expect for the ratio between anterograde and retrograde velocity, as there is much variation (Tab. 2.1). In *Trypanosoma brucei* retrograde transport is faster. Similar to our observation, the signal intensities for retrograde trains are reported to be weaker than for anterograde trains (Buisson et al., 2013). This suggests that retrograde contain fewer subunits than anterograde trains, but compensate with speed and frequency. A similar model could apply to IFT88 in *Drosophila melanogaster* chordotonal neurons.

Tab. 2.5: Overview of IFT88 velocities in mouse and *C. elegans*

Species	**Anterograde velocity**	**Retrograde velocity**	**Reference**
***Mus musculus* (IMCD3 cells)**	0.32 µm/s	0.64 µm/s	(Besschetnova et al., 2010)
***Mus musculus* (IMCD3 cells)**	1.19 µm/s	1.0 µm/s	(Ishikawa et al., 2014)
***Mus musculus* (IMCD3 cells)**	0.68 µm/s	0.35 µm/s	(Ye et al., 2013)
***Mus musculus* (IMCD3 cells)**	0.38 µm/s	0.56 µm/s	(Tran et al., 2008)
***Mus musculus* (MEF)**	1.09 µm/s	1.06 µm/s	(He et al., 2014)
Mus musculus* *(olfactory neurons)	0.23 µm/s	0.14 µm/s	(Williams et al., 2014)
C. elegans	0.71 µm/s (middle segment) 1.31 µm/s (distal segment)	1.22 µm/s	(Wei et al., 2012)

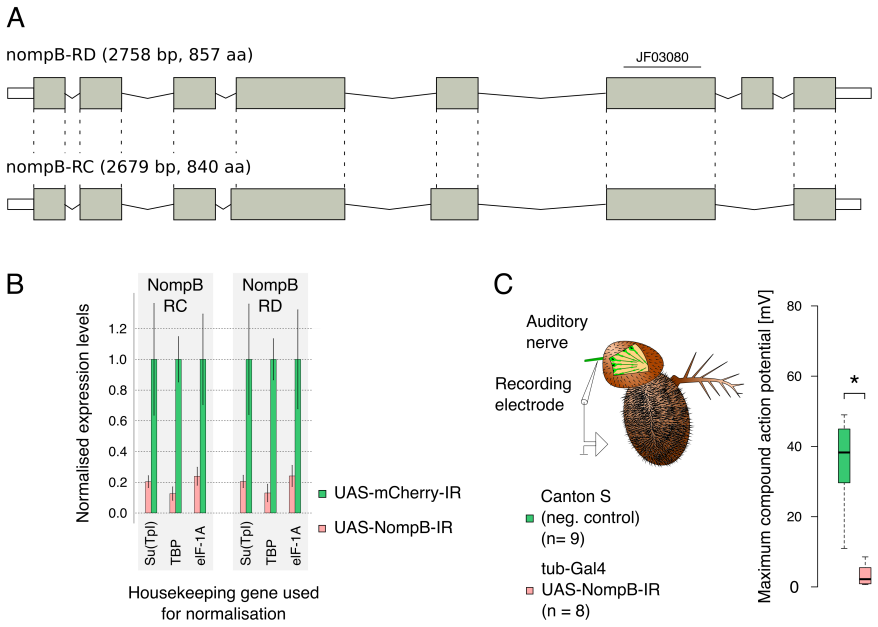

Fig. 2.4: **Validation of NompB inverted repeat (IR) used in this study to downregulate NompB expression**. (A) Schematic representation of the two NompB isoforms encoded in the *Drosophila* genome. The hairpin used here (ID: JF03080) affects both isoforms by targeting a common exon. (B) Real-time PCR quantification of NompB isoform levels. The mRNA was extracted from antennae of flies that either expressed a hairpin against mCherry (neg. control) or against NompB. The hairpin expression was driven using the tubulin promoter (see main text for more detail). The error bars indicate one standard deviation in each direction. The total mRNA was extracted three times per hairpin and measured in triplicates. The data was normalized using three different housekeeping genes (Su(Tpl), TBP and eIF-1A) to account for potential transcription changes in a house keeping gene as a consequence of the knockdown. (C) Maximum compound action potentials were recorded from the auditory nerve of individual antennae representing the combined response of the chordotonal neurons to acoustic stimulation. The response is almost abolished upon knockdown of NompB (data was obtained in collaboration with Martin Göpfert's group in Göttingen, Germany, experiment was conducted by Christian Spalthoff, *p-value = $6.274e^{-05}$ from Welch Two Sample t-test). Flies were tested four to six days after eclosure.

Taken together the results from the live imaging (Fig. 2.3), the DmIFT88/NompB gene expression (Fig. 2.4B) and the stainings of antenna sections (Fig. 2.2), my results indicate that IFT88 has a role in *Drosophila melanogaster* chordotonal cilia beyond ciliogenesis. Subsequently, DmIFT88/NompB protein levels were perturbed in order to address its necessity for cilia maintenance in these cells.

Validation of DmIFT88/NompB hairpin for mRNA knockdown

Since DmIFT88/NompB is absolutely essential for ciliogenesis in *Drosophila melanogaster* sensory neurons (Han et al., 2003), NompB mutants cannot be used to address the role of the protein in cilia maintenance. I, therefore, developed an RNAi-based knockdown strategy. To avoid potential off-target effects, I validated the hairpin extensively.

The hairpin I used for this study comes from the Transgenic RNAi Project (TRiP). It was inserted as one copy on the second chromosome in a specific landing site (Perkins et al., 2015). The hairpin targets an exon common to both NompB isoforms (Fig. 2.4A). To test whether the hairpin can phenocopy the mutant phenotype, I expressed it using a constitutively active promoter (tub-Gal4) that is strongly active in all cells of the fly and all developmental stages. The NompB mRNA levels of both isoforms are significantly reduced (Fig. 2.4B) in total mRNA isolated from antenna of flies expressing the NompB hairpin, as compared to animals that express a hairpin against mCherry (negative control – protein is normally not encoded in the *Drosophila melanogaster* genome). With the help of Christian Spalthoff from the Göpfert lab I could show that the chordotonal neurons from NompB knockdown flies produce much weaker action potentials upon acoustic stimulation compared to control flies (Fig. 2.4C). Additionally, we could show using electron microscopy that the NompB knockdown flies do not form cilia (Fig. 2.5, with the

help of Susana Mendonça). Both findings were expected from the known mutant phenotypes (Han et al., 2003). The ciliary transition zone seems to form independently of IFT88 (Fig. 2.5D), which was not previously reported to this level of detail.

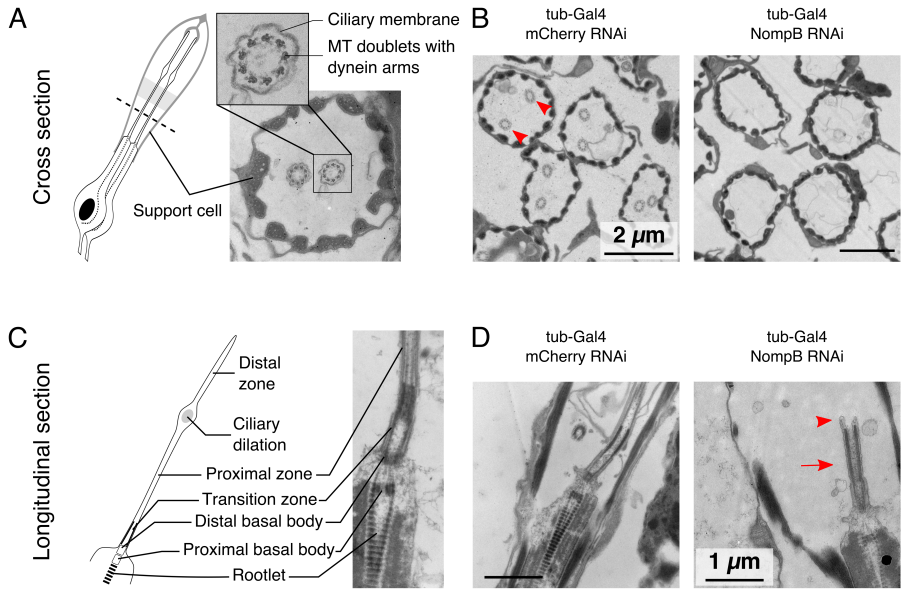

Fig. 2.5: **Ultrastructural analysis of constitutive NompB knockdown indicates that ciliary transition zone is built in an IFT-independent manner in *Drosophila***: (A) A schematic representation of a scolopidium showing two chordotonal neurons with one cilium each. Two cilia are encircled by a support cells (scolopale). A representative electron microscopy (EM) image that highlights the main features of the scolopidium in cross section (section at the level of the dashed line). (B) Representative EM images of tissue from animals expressing a control hairpin (mCherry RNAi) or the hairpin against NompB. Two cilia are seen within each scolopale in the control situation (red arrowheads). No cilia are found in animals when NompB was knocked-down using a tubulin promoter. The phenotype was fully penetrant in all sections observed. (C) Schematic representation and representative EM image of a chordotonal cilium in longitudinal section. The main features are highlighted. (D) Representative images of cross-sections from animals expressing a control hairpin (mCherry RNAi) or the hairpin against NompB. Upon

knockdown, the ciliary transition zone is formed (red arrow), but the axoneme is not extended (red arrowhead). All EM samples were prepared and sectioned by Susana Mendonça.

All phenotypes observed here are in line with the expectations from the NompB mutants. The hairpin seems, hence, suitable to manipulate NompB protein levels. In order for biogenesis to occur normally, however, an inducible system was used to repress hairpin activity during ciliogenesis (McGuire et al., 2003).

Inducible knockdown of DmIFT88/NompB causes gravitaxis defects without obvious structural defects in chordotonal cilia

The primary readout for defects in chordotonal cilia in this study is a simple gravitaxis assay (Fig. 2.6B). However, defects in gravitaxis behavior could stem from defects in various cells of the fly (e.g. peripherial nervous system, central nervous system, muscles). According to the modENCODE gene expression database (Celniker et al., 2009), NompB is weakly expressed in the digestive tissue. However, no phenotype has been associated with these cells in NompB mutant flies. Furthermore, the cells in the digestive tract do not form cilia. It is hence unlikely that NompB has a function there. In order to reduce the chance of observing behavioural changes resulting from continuous knockdown of NompB in cells unrelated to ciliated sensory neurons, I carried out the experiments using a pan-neuronal driver (Chat-Gal4). It is difficult to rule out that DmIFT88/NompB is expressed and required in other cells of the central nervous system, which could give rise to problems in gravitaxis. In stainings of brain sections, however, I never detected a clear signal for NompB using the endo-GFP::NompB transgene (described in Fig. 2.2). Preliminary western blot analysis yielded a clear band of the appropriate size for NompB protein from antenna samples and heads with antennae, but not from head samples

without antennae (data not shown). This assay would not be sensitive enough, however, to detect small cell populations in the brain that might depend on NompB protein for their function. No central nervous system defect was previously described for NompB mutant flies.

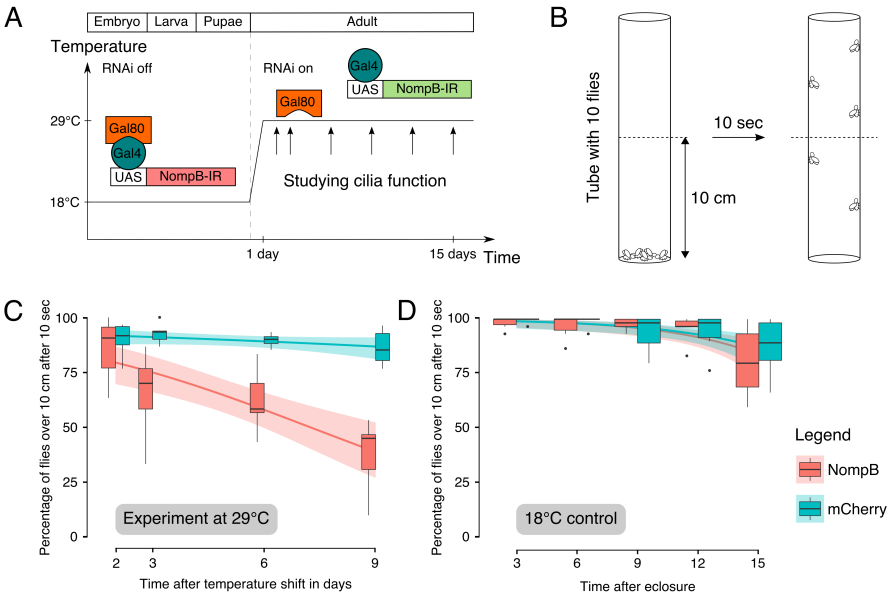

Fig. 2.6: **Inducible knockdown of NompB leads to impaired gravitaxis behaviour**. (A) Experimental approach and time line of the experiment: NompB is knocked-down using a pan-neuronal promoter (Cha-Gal4). The expression of the hairpin is repressed during development through co-expression of a temperature-sensitive version of Gal80. Gal80 prevents interaction of Gal4 protein with polymerase at the UAS element. There is, hence, no activation of transcription of the hairpin at the non-permissive temperature. The animals were reared at the non-permissive temperature (18°C). The expression of the hairpin is induced through temperature shift to the permissive temperature (29°C). The effect on cilia function is approximated by quantification of gravitaxis behaviour of the flies after temperature shift. (B) Schematic representation of the gravitaxis assay used here: Ten flies of the same sex are transferred to a tube. The tube is tapped which causes the flies to fall to the bottom of the tube. The number of flies that climb up to or

above 10 cm within 10 sec is recorded. (C and D) Results from the gravitaxis assay are shown with temperature shift as outlined above (C) or, without temperature shift, to control for the genetic background of the two lines. Each boxplot corresponds to a total of 60 flies measured in sets of ten animals each. The data was fitted using linear regression. The curve fitted to the data is shown as a solid line, and the area around the curve represents the 95 % confidence interval. The two lines are significantly different at 29°C, but no difference can be detected at 18°C.

The Chat-Gal4 driver is active in chordotonal neurons and olfactory neurons in all developmental stages of the fly (Salvaterra and Kitamoto, 2001), but activity is already observed during late stages of ciliogenesis at least in olfactory ciliated neurons (Jana et al., 2011). In order to avoid confounding effects from late ciliogenesis defects, Gal4 activity was repressed through co-expression of a temperature sensitive version of Gal80 (denoted $Gal80^{ts}$) (McGuire et al., 2003). At the non-permissive temperature (18°C) Gal80 binds to Gal4 and prevents it from attracting polymerase to a UAS element in the fly genome (Rodríguez et al., 2011). NompB mRNA will only be reduced through RNAi if flies are kept at the permissive temperature (29°C). Flies were reared at 18°C, shifted to the permissive temperature after eclosure, and then submitted to the gravitaxis assay for up to two weeks after the temperature shift (Fig. 2.6A-B).

I initially established that young flies expressing a hairpin against mCherry (3 days after temperature shift, negative control) take about 10 seconds to climb 10 cm. This speed was used as a reference for all experiments conducted here. I subsequently scored for all time points and genotypes how many flies crossed this height within ten seconds after tapping the cylinder (Fig. 2.6B). NompB RNAi flies develop a significant gravitaxis phenotype within 3 days after the temperature shift when compared with mCherry controls (Fig. 2.6C). In order to test whether the worse performance of the NompB

animals might be a consequence of the genetic background, I performed the assay with flies that never experienced a temperature shift (Fig. 2.6D). At 18°C the two genotypes are indistinguishable in their performance in the assay.

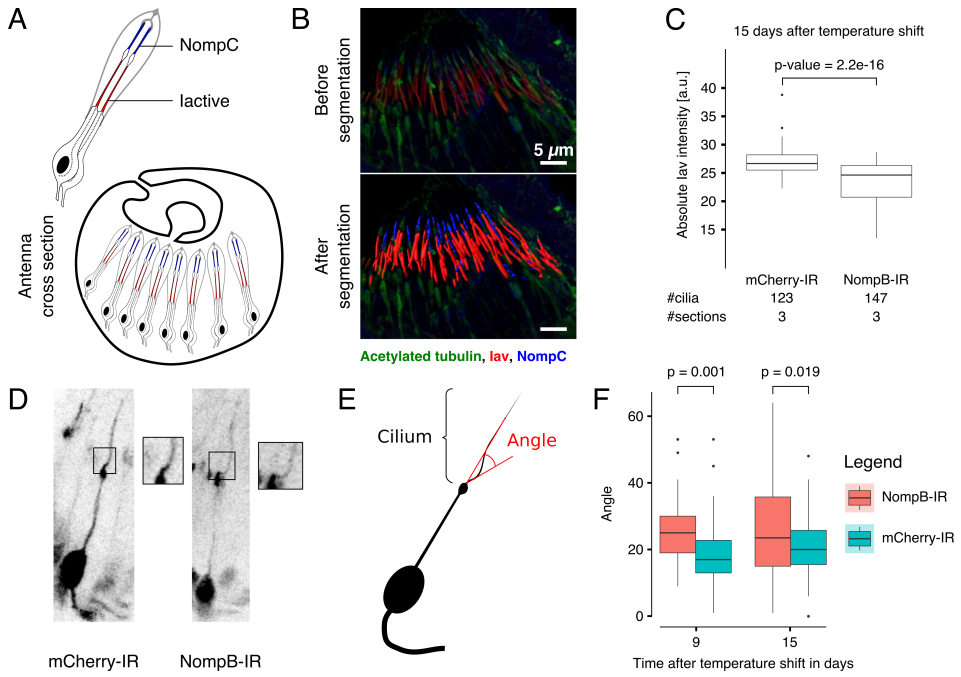

Fig. 2.7: **Long-term consequences of inducible NompB knockdown**. (A) Schematic representation of a scolopidium: Two ion channels that specifically localise to subcompartments of the auditory cilia are shown (NompC in blue and Inactive (Iav) in red). Below, there is a representation of a cross section through the second antenna segment showing the relative distribution of the cilia of several scolopidia. (B) Image stack from an antenna section before (upper image) and after segmentation (lower image) based on fluorophore distribution. Segmentation was performed using the Imaris software. (C) Quantification of pixel intensities within each segment shows slight but significant decrease of Iav intensities at 15 days after induction of knockdown (p-value from Welch Two Sample t-test, data was not normalised between experiments because of the lack of appropriate internal control). (D) Morphological changes at the ciliary base were observed after long-term knockdown of NompB. The cilia seem to project out at a different angle from the dendrite. This suggests bending of the ciliary axoneme. Data was obtained from

antenna whole mounts to avoid artefacts from sectioning. The cuticle was made transparent using FocusClear to allow for imaging of the neuron morphology. The neurons were visualized using co-expression of GFP together with the respective hairpin. (E) Measured angles are plotted here for two different time points. The p-values were calculated using Welch Two Sample t-test. Each box plot corresponds to 50 angles from 5 different antennae.

Inducible knockout of IFT88 in mouse photoreceptors causes the axoneme to disintegrate (Jiang et al., 2015). This and other observations led to the idea that DmIFT88/NompB knockdown could give rise to similar phenotypes in *Drosophila*. However, I never found any evidence for cilia shortening in EM (i.e. empty caps, data not shown). I also did not observe cilia that lacked the ciliary dilation or the distal segment in antenna whole mounts (Fig. 2.7).

Transient receptor potential vanilloid channels (TRPV) are transported by IFT in sensory cilia in *C. elegans* (Qin et al., 2005). There are two TRPV channels (nanchung and inactive) encoded in the *Drosophila melanogaster* genome (Matsuura et al., 2009); both are required for gravity sensation (Sun et al., 2009). I obtained an antibody against inactive (iav) and performed stainings in antenna sections from flies that experience NompB knockdown for 15 days (Fig. 2.7A-B). I quantified iav signal intensities in those samples and observed a significant, albeit small, reduction in NompB knockdown flies when compared with mCherry controls (Fig. 2.7C). Given the small reduction and the late time point, it is hard to make conclusions about its contribution to the gravitaxis phenotype. It is possible, however, that the phenotype is caused by several small changes in several components of the signal transduction machinery of the chordotonal cilia. I also stained for another TRP channel (NompC), but the poor quality of the staining made quantification impossible. NompC has been previously shown, however, to not be required for gravity sensation (Sun et al., 2009).

I could not find evidence for cilia resorption from antenna whole mounts, but I observed morphological changes at the base of the cilium (Fig. 2.7D-F). After continuous knockdown of NompB, cilia appear to have increased curvature as compared to control cilia (Fig. 2.7D). In order to quantify this phenotype, I measured the angle under which cilia project out from the dendrite (Fig. 2.7E). This phenotype was observed at two different time points (9 days and 15 days), but to my knowledge has never been described in the literature before. It is difficult at this point to judge its significance. Bending suggests changes in the mechanical properties of the cilia that might translate to differences in their excitability, which in turn could cause a difference in the ability of the flies to sense gravity.

Discussion and conclusions

I showed here that DmIFT88/NompB continues to be active in fully formed cilia in chordotonal neurons of *Drosophila melanogaster* larvae (Fig. 2.3). DmIFT88/NompB can also be found in cilia of chordotonal neurons in the antennae of adult flies (Fig. 2.2). These findings suggest a role of IFT beyond ciliogenesis in those neurons. Constitutive knockdown of DmIFT88/NompB can replicate the NompB mutant phenotype (Fig. 2.4 and Fig. 2.5). My data suggest that the transition zone in *Drosophila* is formed independently of IFT88 (Fig. 2.5D). Using an inducible knockdown approach, I provided evidence that DmIFT88/NompB has a role in maintaining cilia function (Fig. 2.6). I reported small changes in the concentration of a TRPV channel (Iav) in cilia after 15 days of continuous knockdown. While the cilia were intact, I also found some morphological changes. It is difficult, however, to attribute the gravitaxis phenotype to any one of these changes specifically. It seems likely that these changes have additive effects that translate into the overall phenotype, perhaps in combination with other

changes that were not identified here (e.g. changes in the other TRPV channel Nanchung).

As a next step, it would be important to understand the consequences of DmIFT88/NompB knockdown for the entire IFT complex to interpret the results obtained here. In *Chlamydomonas,* loss of IFT88 leads to loss of IFT57 from the cell, whereas other IFT subunits remain stable (Pazour et al., 2000). IFT88 and IFT57 form part of the interface between the IFT-B1 and IFT-B2 subcomplex (Fig. 1.5) (Mourão et al., 2016). Losing the two proteins together might therefore destabilize the entire IFT-B complex. This could in turn impair more than just the transport of IFT88-specific cargoes to and from cilia; it could affect several IFT cargoes at the same time. Furthermore, in *Trypanosoma* the loss of IFT88 does not change the total levels of IFT81 in the cell, but YFP-labelled IFT81 no longer exhibits ciliary motility in the absence of IFT88 (Fort et al., 2016). Additional experiments are, hence, necessary to address the consequences of DmIFT88/NompB knockdown for other IFT proteins in the Drosophila chordotonal neurons. Otherwise it is impossible to conclude whether the changes described here are directly due to removal of IFT88 from the IFT complex or due to changes in the entire IFT complex.

One way to test whether other IFT proteins are affected in IFT88 depletion would be to visualize them in IFT88 knockdown flies. IFT81, which was monitored by Fort and colleagues in the absence of IFT88 in *Trypanosoma*, is not conserved in Drosophila (Fig. 1.5) (Fort et al., 2016). IFT57 has not been described in *Drosophila* yet, but it is a known interaction partner of IFT88 in other systems and lost from Chlamydomonas IFT88 mutants (Katoh et al., 2016; Pazour et al., 2000; Taschner et al., 2016). It would hence be informative to investigate if IFT57 shows signs of ciliary motility in the absence of IFT88 in the fruit fly. Unfortunately, only very few tools are available

to monitor IFT in *Drosophila.* No antibody against any of the IFT proteins has yet been established and few transgenic fly lines exist. One interesting transgene to study in the absence of IFT88 would be the GFP-fusion protein of DmIFT140/RempA (Lee et al., 2008). DmIFT140/RempA is a member of the IFT-A subcomplex. Investigating its localisation in cilia during DmIFT88/NompB depletion might inform about the effect of loss of IFT88 on the whole IFT complex. Additionally, if IFT88 depletion disables the entire IFT complex in the chordotonal cilia, then the removal of IFT88 should be indistinguishable from the removal of the cilia-specific IFT anterograde motor kinesin-2. Indeed, the mutant phenotypes of IFT88 and kinesin-2 are very similar, suggesting that the two proteins are equally important for IFT function in cilia biogenesis (Han et al., 2003; Sarpal et al., 2003). Removing kinesin in the maintenance assay could be an alternative, albeit indirect, way to estimate the effect of IFT88 depletion for the whole IFT88 complex. If, however, the phenotype for kinesin depletion in the maintenance were to be worse than what I described for DmIFT88/NompB here, it would suggest that the IFT complex remains partially functional in the absence of IFT88 in *Drosophila*.

The electron micrographs obtained from flies with constitutive DmIFT88/NompB knockdown indicate that the ciliary transition zone is built independently of IFT88 (Fig. 2.5). Similar observations were made for kinesin-2 mutants (Sarpal et al., 2003). Given that the transition zone does not seem to require IFT for its assembly, it is unlikely that is maintained by IFT, although not impossible. It would be important, however, to investigate further whether the molecular composition of the transition zone is unchanged in the absence of IFT. Many molecules required for *Drosophila* transition zone assembly are known (e.g. Chibby and Cep290), and tools are available to test this question (Vieillard et al., 2016). Additionally, the

live-imaging experiments (Fig. 2.3) and the stainings of antenna sections (Fig. 2.2) show that there is a stationary NompB pool at the ciliary base and the ciliary dilation. This suggests that NompB is present in excess at both ends of the cilium and is poised for assembly into trains. A model for IFT assembly at the ciliary base was recently proposed for IFT in *Chlamydomonas.* The waiting time at the base might be required to allow for sequential assembly of the subunits (Wingfield et al., 2017). The waiting time at the ciliary tip, on the other hand, is probably required for remodelling of the IFT. We know about several changes in the IFT complex that occur at the ciliary tip (e.g. activation of the dynein motor that is a passive cargo in anterograde trains, train size changes) (Buisson et al., 2013; Toropova et al., 2017). Our understanding about the events that happen at the ciliary tip, however, is very limited.

No binding partner of any of the IFT proteins has been identified in *Drosophila,* and the work presented in this chapter did not allow us to arrive at any conclusions about specific IFT88 or general IFT cargoes. The reduction in Iav protein in cilia upon DmIFT88/NompB knockdown (Fig 2.7) could be related to insufficient replenishment of Iav protein caused by compromised IFT function. The *Drosophila* homologue of Tulp3 (ktub) is required for localisation of Iav to cilia (Park et al., 2013). Mammalian Tulp3 in turn is necessary to localise certain G-protein-coupled receptors to the ciliary membrane in an IFT-A-dependent manner (Mukhopadhyay et al., 2010). If removal of DmIFT88/NompB were to affect the entire IFT complex, it would be expected that ciliary Iav protein levels would decrease as a consequence. Iav is essential for gravitaxis behaviour (Sun et al., 2009), and could, hence, contribute to the gravitaxis defect reported here. It is, however, not clear whether the small reduction in Iav levels that is seen here after 15 days of DmIFT88/NompB knockdown is sufficient to explain the gravitaxis defect (Fig. 2.6). In

order to address this question, it would be necessary to systematically establish a threshold in the ciliary Iav concentration below which cilia function is impaired. At this point it seems more parsimonious, however, to assume that the gravitaxis phenotype found here is due to a combination of several proteins no longer undergoing appropriate trafficking.

Alternatively, it is conceivable that the phenotype is caused through a specific protein cargo of DmIFT88/NompB that is still unknown. From the results presented here, however, it would be expected that this cargo protein is not affecting the compartmentalisation of the cilia (Fig. 2.7). Instead it might be acting specifically in the signalling transduction cascade required for the neurons to generate or amplify an electric signal from environmental stimulation. Rhodopsins were recently found to be involved in hearing in *Drosophila*. Two rhodopsin proteins localise to the cilia in the chordotonal neurons. In the absence of those proteins the fly is deaf, but the ultrastructure of the cilia is not changed (Senthilan et al., 2012). This indicates that rhodopsins are an important part of the signal transduction machinery, but dispensable for cilia compartmentalisation. Rhodopsins are known for their role in phototransduction. How rhodopsins function in the chordotonal neurons is not clear yet, but the authors suggested an evolutionary relationship between the different sensory neurons, involving co-option of the same molecular machinery in the transduction of different physical stimuli (Senthilan et al., 2012).

Supporting the evolutionary connection of different types of sensory neurons, atonal, an important transcription factor in establishing the chordotonal neurons, is also involved in specifying photoreceptor cells (Jarman and Groves, 2013). Gucy2d, a cGMP-generating enzyme, is essential for the function of mammalian photoreceptors (Kuhn, 2016). Patients with mutations in the corresponding gene

develop a retina-specific ciliopathy (den Hollander et al., 2008). The protein requires IFT88 to be transported to the photoreceptor outer segment (Bhowmick et al., 2009). It is not clear at the moment whether a *Drosophila* homologue of Gucy2d exists and what could be the function of the protein in chordotonal neurons. The aim of the following chapter will be to explore if a homologue exist in the fruit fly, if it interacts with DmIFT88/NompB, and if the protein can account at least partially for the gravitaxis phenotypes found here.

Acknowledgements

The endo-GFP::NompB fly strain was generated by the Kernan lab and made accessible to us through Daniel Eberl (Fig. 2.2). Changsoo Kim and Yun Doo Chung kindly donated the anti-sera against Iav and NompC, respectively (Fig. 2.7).

Chapter III – Insights into the transport of the evolutionary conserved guanylyl cyclase CG34357 suggest disease mechanism

Author contribution

If not indicated otherwise, I conducted the experiments myself. Gabriel Martins generated the 3D model of the GFP-positive cells from antenna whole-mount images (Fig. 3.3D). The method to clear the antenna cuticle for whole mount imaging was developed with the help of Ânia Gonçalves from the imaging facility. The protocol to isolate the CG34357 protein from cultured cells was developed in close collaboration with Sihem Zitouni, who also helped in the immunoprecipitation experiments (Fig. 3.4, Fig. 3.5 and Fig. 3.8).

Summary

The protein composition of cilia is distinct from the rest of the cell. Ciliary proteins are delivered to the organelle by a dedicated protein complex called Intraflagellar transport (IFT). The IFT complex is known to be important for cilia formation and maintenance in many species. Few cargoes, however, have been reported until today, and none are known in the *Drosophila melanogaster*. The lack of knowledge about cargoes makes it difficult to predict which properties are maintained by IFT. Here I show that an evolutionary conserved guanylyl cyclase, which binds to DmIFT88/NompB, functions in ciliated sensory neurons in *Drosophila*. Through truncation experiments the binding site was narrowed down to 200 amino acids, and the relevance of these residues was partially addressed in chordotonal neurons. Sequence analysis showed that these 200 amino acids are conserved across several animal species, which suggests that they are important for the function of the full-length protein. Several mutations found in human patients with Leber congenital amaurosis (LCA) were found to be conserved and to localise in this stretch of the guanylyl cyclase protein. This result

suggests that the mutations might affect binding to IFT88, which in suggests a novel disease mechanism for LCA patients.

Introduction

The work in the previous chapter led to the conclusion that DmIFT88/NompB is required for the maintenance of cilia function in chordotonal neurons in *Drosophila* antennae. Depletion of the protein causes a gravity sensation phenotype in the animals. It was not possible, however, to deduce a molecular mechanism explaining that phenotype. Some late cellular changes are described that were seen after prolonged knockdown of NompB. The cilia showed signs of morphological changes, as well as a reduction in the ciliary concentration of the TRPV channel Iav (Fig. 2.7). It is difficult, however, to draw conclusions about the contribution of these cellular phenotypes to the gravitaxis defect that was seen in flies expressing a hairpin against NompB (Fig. 2.6). The gravity sensing phenotype could be either caused by the combined effect of small changes in several proteins due to insufficient transport or due to the loss of one particular DmIFT88/NompB cargo. In the latter case, that specific cargo is not required for maintenance of cilia length or compartmentalisation (Fig. 2.7).

This chapter explores the hypothesis that insufficient delivery of a previously unknown DmIFT88/NompB cargo to the cilia causes impaired function of the chordotonal neurons. A member of the class of particulate guanylyl cyclases, Gucy2d, required for dark adaptation in the mammalian retina (Kuhn, 2016), is transported to the outer segment of photoreceptors through binding to IFT88 (Bhowmick et al., 2009). The outer segment of the photoreceptor is a modified cilium (Khanna, 2015). Guanylyl cyclases generate cGMP, a small signalling molecule involved in several signalling processes (Kuhn, 2016). It has been proposed that cGMP signalling correlates

positively with the ability of different eukaryotic species to form cilia (Johnson and Leroux, 2010). Chapter III of this thesis addresses whether cGMP signalling plays a role in the chordotonal cilia of *Drosophila,* and whether a potential homologue of Gucy2d in the fly has a role in gravity sensation. cGMP signalling has not been implicated in any form of mechanosensation in insects thus far.

Known roles of guanylyl cyclases in sensory cilia

Two groups of guanylyl cyclase exist, soluble and particlulate (membrane-bound). They were initially discovered in cell fractionation experiments from rat lungs. cGMP-generating capacity was detected in the particulate and the cytosolic fraction of the lysates (Chrisman et al., 1975). The small signalling molecule cGMP can modulate many cellular processes through stimulating the activity of cGMP-gated ion channels and cGMP-dependent protein kinases (Kots et al., 2009). A phylogenetic analysis found a positive correlation between the distribution of the cGMP machinery encoded in the genomes of eukaryotic species with the ability to form cilia (Johnson and Leroux, 2010). The human genome harbours six particulate guanylyl cyclases. Three of those are known to localize in the cilia and are involved in olfaction and vision (Kuhn, 2016). *C. elegans* experienced an expansion of the guanylyl cyclase repertoire. Its genome encodes 27 particulate guanylyl cyclases (Johnson and Leroux, 2010), which regulate a wide range of sensory processes very often experimentally linked to ciliated neurons (Maruyama, 2016). The *Drosophila* genome has six particulate guanyly cyclases (Morton, 2004), none of which have been associated to cilia function directly. Two soluble guanlylyl cyclases, however, are expressed in ciliated sensory neurons and modulate gustatory behaviour as well as the response to hypoxia (Vermehren-Schmaedick et al., 2010, 2011).

It should be mentioned here that the nomenclature for the mammalian guanylyl cyclases is confusing. The human gene Gucy2d (also sometimes referred to as GC-1, retGC1 or GC-E) is the homologue of the mouse gene Gucy2e (Kuhn, 2016). The mouse genome also encodes a gene called Gucy2d, which has no functional equivalent in humans. I will use Gucy2d here, and I will use Gucy2e when describing the corresponding gene in mice.
The mouse particulate guanylyl cyclase Gucy2e is transported to the outer segment of the photoreceptors through binding to IFT88 (Bhowmick et al., 2009), and mutations in this gene have been found in patients with the ciliopathy Leber congenital amaurosis (den Hollander et al., 2008). A cGMP-gated ion channel has been shown to be expressed in the chordotonal neurons of the fruit fly (Marx et al., 1999), which makes it likely that cGMP signalling is involved in hearing and gravity sensation in the fly. The fly could thus encode a homologue of Gucy2d, which might be transported by DmIFT88/NompB and play a role in signal transduction in the chordotonal cilia.

Leber congenital amaurosis (LCA) and Gucy2d transport

Leber congenital amaurosis (LCA) is a recessive autosomal disease that affects one in 30,000 people (den Hollander et al., 2008). LCA patients suffer from retinal dystrophy, sometimes associated with other ciliopathy symptoms such as mental retardation or olfactory dysfunction (den Hollander et al., 2008). LCA can also be found in patients diagnosed with other ciliopathies, such as Joubert syndrome related disorders (Waters and Beales, 2011). Several known disease genes involved in LCA are directly involved in ciliogenesis and cilia function (e.g. TULP1, CEP290, RPGRIP1). However, for mutations in other genes associated to the disease (e.g. RD3) it is less clear how they cause LCA (den Hollander et al., 2008). Gucy2d was found

mutated in LCA patients from independent cohorts with frequencies ranging from 5 to 16% (Astuti et al., 2016; Coppieters et al., 2010; Li et al., 2011; Simonelli et al., 2007; Verma et al., 2013; Xu et al., 2016; Zernant et al., 2005) making it one of the most important genes for this disease. Some mutations in Gucy2d impair or abolish the catalytic function of the protein leading to reduced or no production of cGMP (Rozet et al., 2001; Tucker et al., 2004). For other mutations, especially outside of the catalytic domain, it is still unclear how and to what extent they impact protein function and cause disease (for an overview of known missense mutations see Fig. 3.9B and Tab. 3.5).

Gucy2d binds to IFT88 and requires it to be localized to cilia (Bhowmick et al., 2009). Interestingly, another LCA disease gene (LCA5, which encodes Lebercilin) abolishes IFT when mutated (Boldt et al., 2011). These findings suggest that some Gucy2d disease variants impair trafficking and correct localization of Gucy2d. This could be in turn be due to inefficient binding to IFT88. Ectopic expression of mouse Gucy2e full-length protein and protein fragments did not lead to the identification of one particular protein domain required for outer segment targeting (Karan et al., 2011). Gucy2d also binds rhodopsin directly and requires it for transport (Pearring et al., 2015). However, Bhowmick and colleagues did not provide any evidence as to through which domain Gucy2d binds IFT88 (Bhowmick et al., 2009). Taken together, these findings make it difficult to explain the effect of disease Gucy2d mutations on transport in LCA patients. Exploring the conservation of the Gucy2d transport via IFT88 in a very distant species could yield new insights into protein targeting as well as guide new hypotheses regarding disease mechanisms.

Goals

7. Identification of a particulate guanylyl cyclase that could be related to Gucy2d and that is involved in gravitaxis in *Drosophila melanogaster*
8. Provide evidence for molecular interaction of that cyclase with DmIFT88/NompB, if possible establish binding site(s) on the cyclase
9. Analyse the binding site(s) for evolutionary conservation, if possible, derive hypotheses for the implications of the mutations for the interaction of the two proteins, with a focus on outcome for LCA patients

Experimental strategy

Knockdown of DmIFT88/NompB leads to a defect in gravity sensation in *Drosophila melanogaster*. A *Drosophila* homologue of Gucy2d potentially has the following two properties: (1) Reduction of the protein in chordotonal neurons should impair gravitaxis and (2) it should rely on DmIFT88/NompB for its localisation to cilia. I carried out a screen for a gravitaxis phenotype with particulate guanylyl cyclases encoded in the *Drosophila melanogaster* genome. Following amino acid sequence comparison I cloned the most similar protein to Gucy2d (CG34357). In order to address whether the protein localises to chordotonal cilia I generated transgenic flies. Additionally, with the help of Sihem Zitouni, I carried out immunoprecipitation assays to test for binding between NompB and CG34357. We also generated protein fragments and described their localisation in ciliated neurons as well as in cultured cells. Finally, to extend the insights gained here to the human protein Gucy2d, I carried out bioinformatics analyses to investigate protein conservation and generate predictions about the underlying disease mechanism of mutations found in patients with LCA.

Material and methods

Bioinformatic analysis of guanylyl cyclase sequences

Analysis was performed as described in chapter II (for protein sequences used here see Tab. 3.1). The gene model for CG34357 (Fig. 3.2) was taken from the Ensembl Genome Browser (Yates et al., 2016). In addition, the protein structure of CG34357 was predicted using the web browser-based structure prediction tool Phyre2 (Kelley et al., 2015) using the “intensive mode”. Phyre2 executes a PSI-BLAST (Position-Specific Iterated Basic Local Alignment Search Tool) search using the amino acid sequence that is given as input. A PSI-BLAST is more sensitive than a regular BLAST search in detecting homology in distantly related proteins, because its scoring matrix is updated dynamically whenever a hit is found. Features that are particularly conserved in an amino acid sequence for a particular protein or protein family, are thus given more weight than in a regular BLAST search. The program then selects the hits that have a published associated protein crystal structure and uses that information to model similar parts of the input sequence. Additionally, the “intensive mode” includes a step for *ab initio* structure prediction for the parts of the protein that cannot be modelled using available crystal structures. Phyre2 also provides information on the individual amino acid residues that are of putative relevance for a particular protein domain. Domains for CG34357 (Fig. 3.2) were assigned using these predictions. Phyre2 also offers a variety of other features that are not discussed here. The signal peptide in CG34357 and the associated cleavage site were predicted using SignalP (Nielsen, 2017).

Tab. 3.1: Protein sequences used for bioinformatic analysis in this chapter of the thesis. Whenever several isoforms were available for the same gene, the longest protein sequence was chosen.

Name	Species	Accession number
Aa_AAEL007359-PA	*Aedes aegypti*	EAT40967
Ag_AGAP002233-PA	*Anopheles gambiae*	XP_307952
De_GG11511	*Drosophila erecta*	XP_001978835
Dm_CG10738	*Drosophila melanogaster*	NP_729905.2
Dm_CG31183	*Drosophila melanogaster*	NP_001287342.1
Dm_CG3216	*Drosophila melanogaster*	NP_726013
Dm_CG34357	*Drosophila melanogaster*	NP_001189166.1
Dm_Gyc32E	*Drosophila melanogaster*	NP_001097148.1
Dm_Gyc76C	*Drosophila melanogaster*	NP_001163473.1
Dm_Gyc89-Da	*Drosophila melanogaster*	NP_001036718.1
Dm_Gyc89-Db	*Drosophila melanogaster*	NP_650551.1
Dr_retGC2	*Danio rerio*	NP_001103165
Ds_GD19673	*Drosophila simulans*	XP_016033187
Gg_retGC1	*Gallus gallus*	AAC24500
Hs_Gucy2d	*Homo sapiens*	NP_000171
Mm_Gucy2e	*Mus musculus*	NP_032218
Ms_GC-II	*Manduca sexta*	AAN16469
Tc_GC-2	*Tribolium castaneum*	KYB27701
Xt_retGC1	*Xenopus tropicalis*	XP_002942678

Screen for potential Gucy2d homologue using gravitaxis assays

Behavioural assays were executed as described in chapter II. The assay was, however, simplified to test more hairpins and genes at the same time. Hairpins were expressed with Chat-Gal4 directly without tubGal80^{ts}-mediated repression during development (for a list of all fly stocks used here, see Tab. 3.2). Flies were reared at 29°C to intensify potential phenotypes. All flies were measured six days after eclosure. For CG34357, the maintenance assay using tubGal80^{ts} was repeated as described in chapter II.

Tab. 3.2: *Drosophila melanogaster* transgenic lines used in this chapter (BSC – Bloomington Stock Center, VDRC – Vienna Drosophila Resource Center, DGRC – Drosophila Genomics Resource Center)

Name	Genotype	Source
40xUAS-IVS-mCD8::GFP	w[*];; P{y[+t7.7] w[+mC]=40XUAS-IVS-mCD8::GFP}attP2	BSC, #32195
mCherry RNAi	y[1] sc[*] v[1]; P{y[+t7.7] v[+t1.8]=VALIUM20-mCherry}attP2	BSC #35785
CG10738 RNAi 1	y[1] v[1];; P{y[+t7.7] v[+t1.8]=TRiP.HMS01814}attP2	BSC, #38346
CG10738 RNAi 2	y[1] v[1];; P{y[+t7.7] v[+t1.8]=TRiP.HM05067}attP2	BSC, #28580
CG31383 RNAi 1	y[1] v[1];; P{y[+t7.7] v[+t1.8]=TRiP.HM05092}attP2/TM3, Sb[1]	BSC, #28604
CG31383 RNAi 2	y[1] v[1]; P{y[+t7.7] v[+t1.8]=TRiP.HMJ22232}attP40	BSC, #58224
CG3216 RNAi 1	y[1] sc[*] v[1];; P{y[+t7.7] v[+t1.8]=TRiP.HM05270}attP2/TM3, Sb[1]	BSC, #31877
CG3216 RNAi 2	y[1] v[1];; P{y[+t7.7] v[+t1.8]=TRiP.HMC04174}attP2	BSC, #55895
CG34357 GD29276	w1118;; UAS-IR[GD8469]	VDRC, #29276/GD
CG34357 GD8469	w1118; UAS-IR[GD8469]	VDRC #8469/GD
CG34357 HM05010	y[1] v[1];; P{y[+t7.7] v[+t1.8]=TRiP.HM05010}attP2	BSC, #28524
CG34357[NP0270]	y[*] w[*];; P{w[+mW.hs]=GawB}CG34357[NP0270] / TM6, P{w[-]=UAS-lacZ.UW23-1}UW23-1	Kyoto stock center, DGRC #103574
Chat-Gal4	w[*]; Chat-Gal4/CyO	Swadhin Jana
tub-Gal80ts	w[*]; sna[Sco]/CyO; P{w[+mC]=tubP-GAL80[ts]}7	From Florence Janody's lab
Gyc89-Da RNAi	y[1] sc[*] v[1];; P{y[+t7.7] v[+t1.8]=TRiP.HM05246}attP2/TM3, Sb[1]	BSC, #30502
Gyc89-Db RNAi 1	y[1] v[1];; P{y[+t7.7] v[+t1.8]=TRiP.HM05207}attP2	BSC, #29529
Gyc89-Db RNAi 2	y[1] v[1]; P{y[+t7.7]	BSC,

	v[+t1.8]=TRiP.HMJ22088}attP40	#58139
iav-Gal4	w[*];; Iav-Gal4	M. Goepfert lab's
UAS-CG34357-T1::GFP	w[*];; UAS-CG34357-T1::GFP/TM6B	our lab (IGC facility)
UAS-CG34357-T2::GFP	w[*];; UAS-CG34357-T2::GFP	our lab (IGC facility)
UAS-CG34357-T3::GFP	w[*];; UAS-CG34357-T3::GFP	our lab (IGC facility)
UAS-CG34357-T4::GFP	w[*]; UAS-CG34357-T4::GFP	our lab (IGC facility)
UAS-CG34357-T5::GFP	w[*]; UAS-CG34357-T5::GFP/Cyo	our lab (IGC facility)
UAS-CG34357-T6::GFP	w[*]; UAS-CG34357-T6::GFP	our lab (IGC facility)
UAS-CG34357::GFP	w[*]; UAS-CG34357::GFP/CyO	our lab (BestGene)
UAS-CG34357::GFP	w[*];; UAS-CG34357::GFP/TM3	our lab (BestGene)
UAS-CG34357::HA	w[*]; UAS-CG34357::HA/CyO	our lab (BestGene)
UAS-CG34357::HA	w[*];; UAS-CG34357::HA/TM3	our lab (BestGene)

Detection of CG34357 gene expression

In order to detect gene expression of CG34357 in different developmental stages, an enhancer trap line was obtained. This line (CG34357[NP0270]) results from a genome wide insertion screen. The *Saccharomyces cerevisiae* Gal4 was randomly inserted into the *Drosophila melanogaster* genome. Whenever the insertion event happened in or close to the regulatory region of a gene, the Gal4 expression pattern can be used to make inferences about the spatial and temporal activity pattern of the respective gene (Brand and Perrimon, 1993). Flies carrying the enhancer trap insertion were

crossed with flies encoding 40xUAS-IVS-mCD8::GFP. The mCD8::GFP fusion protein is targeted to the membrane of the cells that express it and is used to visualize the morphology of cells. 40 UAS tandem insertions were chosen to increase the signal intensity.

Wandering L3 larvae were mounted and imaged as described for the live-imaging of L3 larvae in chapter II. For imaging adult antenna, the cuticle was cleared and images were acquired as described in chapter II. The second antenna segment was imaged entirely on an SP5 Live Upright microscope (Leica). Confocal Z-stack images were deconvolved using the Huygens v17.4 software (SVI) and 3D reconstructed using the Imaris v6.4 software (Bitplane), which was also used to prepare the movie (movie 2 on accompanying CD).

Tab. 3.3: Details of the antibodies used to obtain the results presented in this chapter

Antibody	Dilution	Species	Source
Primary antibodies			
anti-GFP	1:1000	chicken	Aves
anti-GFP	1:1000	rabbit	Roche
anti-GFP	1:1000	rabbit	Abcam
anti-HA	1:1000	mouse	Biolegend
anti-PLP	1:1000	chicken	Glover lab
GT335	1:500	mouse	Janke lab
anti-NompC	1:200	rabbit	Chung lab
anti-lav	1:500	rat	Kim lab
Secondary antibodies			
anti-chicken FITC	1:500	donkey	Jackson
anti-rat Rhod	1:500	donkey	Jackson
anti-mouse IRDye 680	1:10000	goat	LI-COR
anti-mouse IRDye 800	1:10000	goat	LI-COR
anti-rabbit IRDye 800	1:10000	goat	LI-COR
anti-rabbit Alexa647	1:10000	donkey	Jackson

Cryosectioning and immunolabeling of *Drosophila* antennae

Samples were prepared, stained and imaged as described in chapter II (for antibodies used here see Tab. 3.3).

Cloning of CG34357 and generation of transgenic flies

The CG34357 coding sequence was cloned from mRNA isolated from adult antenna (for isolation procedure and details of cDNA synthesis see chapter II of this thesis). CG34357 could only be amplified from cDNA produced with random hexamer primers (included in the Transcriptor First Strand cDNA Synthesis kit, Roche), which suggests that the transcript is not polyadenylated. Additionally, either CG34357 expression levels agree low and/or the CG34357 gateway primers could have low amplification efficiency due to length and secondary structures (for all primer sequences see Tab. 3.4). In order to overcome this problem, a nested PCR strategy was used. To enhance the chance to amplify the desired target (coding sequence of CG34357-RD, Fig. 3.2A) even further, I reverse-transcribed the mRNA using a primer on the 3'-untranslated region of CG34357 (CG34357_3UTR_rev 2 µM in a 20 µl reaction volume, 1 µg of total mRNA were used as template). Two rounds of PCRs were performed to obtain the CG34357 with the appropriate overhangs for Gateway cloning (Invitrogen). In the first round the CG34357 coding sequence was amplified using primers located on each of the untranslated regions. For the second PCR, 2 µl of unpurified PCR product of the first PCR was used as a template. Primers containing appropriate sequences for gateway cloning were used for the second PCR. The coding sequence was cloned without the stop codon to allow for gene fusion at the C-terminus. Tagging at the N-terminus was not considered, since the protein is predicted to undergo cleavage of the signal peptide (30 amino acids, Fig. 3.2 A). Any N-terminal tag is potentially lost from the functional protein. The

coding sequence was confirmed through sequencing and subcloned into pTWG and pTWH (Drosophila Genomic Resource Center) for C-terminal fusion with GFP- and 3xHA-tag, respectively (for more details see chapter II). Both plasmids can be used to generate transgenic flies through P-element transgenesis. They also contain a mini-white gene for selection of positive transformants. Injection of *Drosophila* embryos and selection process was outsourced (BestGene). All transgenic animals encoding truncated forms of CG34357 were generated at the IGC transgenics facility.

Tab. 3.4: Primers used for the experiments in this chapter, annealing temperatures (T_a) were used as stated here. The OligoCalc tool was used for prediction (Kibbe, 2007). PCR extension times were chosen according to the length of expected product and the properties of the respective polymerase according to the manufacturer.

Name	Purpose	Sequence	T_a
CG34356_5UTR_fwd	Outer primer pair for nested PCR strategy to amplify full-length CG34357 coding sequence	GGCAATGTTGGAA GGCACTG	52°C
CG34357_3UTR_rev	See above	CCCATGTCGTCAG CCATCTAA	
CG34357_gateway_FLfwd	Gateway cloning of full-length CG34357	GGGGACAAGTTTG TACAAAAAAGCAGG CTTCATGAAGTTAA CAACCTGTCAAATT GCTAAAG	53°C
CG34357_gateway_FLrev	Gateway cloning of full-length CG34357	GGGGACCACTTTG TACAAGAAAGCTGG GTCTCTGCTCAGCA GTTGCTCTGCATTA AGGG	53°C
CG34357_trunc_fwd	Gateway cloning of T1-CG34357	GGGGACAAGTTTG TACAAAAAAGCAGG	53°C

		CTTCATGCGTAAGC GTCTCTCCAAGGG	
CG34357_trunc_rev1	Gateway cloning of T2-CG34357	GGGGACCACTTTG TACAAGAAAGCTGG GTCGTTCGCCGTG GTTGTGATG	53°C
CG34357_trunc_rev2	Gateway cloning of T3-CG34357	GGGGACCACTTTG TACAAGAAAGCTGG GTCTCTGGTTCTTG GCGGAAGTC	53°C
CG34357_trunc_rev3	Gateway cloning of T4-CG34357	GGGGACCACTTTG TACAAGAAAGCTGG GTCAAATTCTTCCG GGTCGACGG	53°C
CG34357_trunc_rev4	Gateway cloning of T5-CG34357	GGGGACCACTTTG TACAAGAAAGCTGG GTCAGATTCTCCAA TAGGCGGCG	53°C
CG34357_seq_fwd1	To confirm PCR products through sequencing	TGGCAGGACAATA CGTGACC	--
CG34357_seq_fwd2	To confirm PCR products through sequencing	GGACTGGTCGTTTC GGCTAA	--
CG34357_seq_fwd3	To confirm PCR products through sequencing	TCCTGGCGCATCC ATATGTC	--
CG34357_seq_rev1	To confirm PCR products through sequencing	GAACCCATGCTGA GTGTCCA	--
CG34357_seq_rev2	To confirm PCR products through sequencing	TTTCTCGAGGTCAA GGCACC	--
CG34357_seq_rev3	To confirm PCR products through sequencing	GGTGGAATTGGAG TCCAGGG	--

Cell culture and immunoprecipitation experiments

For co-immunoprecipitation of ectopically expressed proteins, Dmel cells were co-transfected with the corresponding constructs (GFP-CG34357 full-length or fragments (T1-T6) and HA-NompB). Cells were seeded at a density of $3x10^6$ cells/well in 6-well plates (Orange Scientific). Cells were transfected one hour after seeding using Effectene Transfection Reagent (Quiagen) according to manufacturer. Cells were harvested three days after transfection. Cells were resuspended, the suspension was collected and centrifuged and pellets were stored at -80°C, if not processed immediately. Ectopically expressed GFP::CG34357 was immunoprecipitated at 4℃ for 2 hrs from Dmel cell lysates (three wells in total for each condition per experiment) using polyclonal anti-GFP antibodies and protein A or G magnetic Dynabeads (Thermo Fisher Scientific). 2 µg anti-GFP antibodies were added to protein-A or -G magnetic beads and incubated for 30 min at room temperature. Cells were homogenized in lysis buffer: 50 mM Tris-HCl pH 8, 250 mM NaCl, 1 mM DTT, 2% NP-40, 0.5% of SDS, 0.5% sodium-deoxycholate, 1× protease inhibitor, 5yg/ml Leupeptin and 15yg/ml Aprotinin, 0.1% Digitonin at 4℃ for 30 min. Then, benzonase was added to the lysate (final concentration 0.25 units/µl) and incubated for another 15 min. After centrifugation at 13,500 g for 20 min at 4ºC, the pre-cleared supernatants were incubated with the coupled beads with antibodies. After several washes with lysis buffer, bead pellets were boiled in SDS sample buffer, separated by 4-15 % gradient SDS-PAGE and transferred onto LI-COR nitrocellulose membranes for Odyssey. GFP-CG and HA-NompB were visualized with anti-GFP or anti-HA antibodies. Secondary LI-COR antibodies IRDye 680RD over IRDye 800 (Li-COR) were used as a second step.

Results

CG34357 is a potential homologue for mouse Gucy2e

The *Drosophila* genome encodes six particulate guanylyl cyclases (Morton, 2004), none of which has been previously associated with cilia function nor mechanosensation or gravitaxis. I performed a PSI-Blast search (Altschul et al., 1997) against the *Drosophila melanogaster* genome using the protein sequence of Gucy2e. I retrieved all six *Drosophila* guanylyl cyclase (Fig. 3.1).

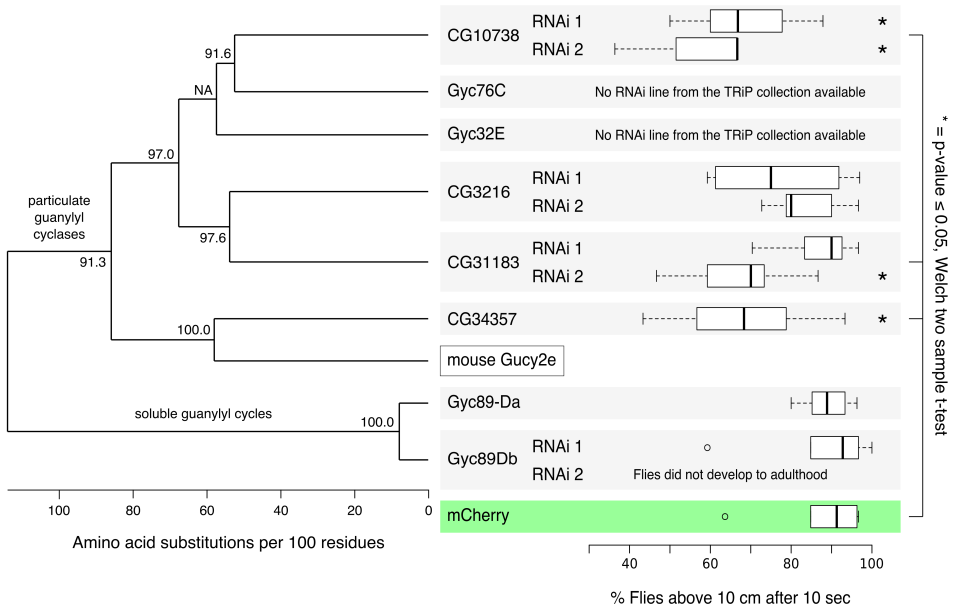

Fig. 3.1: **CG34357 is a potential homologue of mouse Gucy2d**. A PSI-BLAST search was performed against the fly genome using the mouse Gucy2d protein sequence. All the six particulate guanylyl cyclases encoded in the *Drosophila* genome were found (Morton, 2004). The similarity of the proteins to each other is shown on the left side. The tree shows the minimum number of amino acid changes necessary to convert one sequence into another as a measure of sequence similarity. Support for each branch was calculated using a bootstrapping analysis. Values can range from 0 to 100, NA indicates that support could not be calculated

due to the method used to generate the sequence alignment. Two soluble guanylyl cyclases were included as outgroups. A behavioural screen was conducted to determine if any of the enzymes could be involved in gravity sensing. A simple gravitaxis assay was used as described before. Results are shown on the right side. The genes were knocked down using RNAi with a hairpin against mCherry as a negative control. The RNAi was driven using the pan-neuronal driver Chat-Gal4, and the flies were raised at 29°C to increase the potential phenotype. Only fly lines from the TRiP (Transgenic RNAi Project) library were considered here (see Methods). When possible, two RNAi lines were used against the same gene. Each boxplot corresponds to 60 flies measured in groups of ten flies each. Significance was calculated as indicated on the figure.

Any cyclase that functions in chordotonal cilia should give rise to a gravitaxis phenotype upon knockdown. The candidate proteins were depleted using RNAi driven by a pan-neuronal driver (Chat-Gal4), and the gravitaxis behaviour of the animals was assessed. I included two soluble guanylyl cyclases in the assay as well, because they are expressed in several ciliated sensory neurons in the fruit fly (Vermehren-Schmaedick et al., 2011). Different *Drosophila* RNAi libraries are available. The GD library of the Vienna *Drosophila* Resource Center (VDRC) was generated through P-element transgenesis and might generate false-positive results due to the random insertion site of the transgene. The KK library available from VDRC was generated through site-directed insertion, but has been associated with dominant-negative phenotypes associated to the specific insertion site (Green et al., 2014). Transgenic animals from the TRiP library were used in the screen (Transgenic RNAi Project). Transgenes in those animals were integrated into defined landing sites (Perkins et al., 2015). In the assay carried out here, four fly lines exhibited a gravitaxis phenotype upon knockdown (Fig. 3.1).
CG34357, one of the genes that seems to be involved in gravitaxis, is the gene most similar to mouse Gucy2e, which makes it an interesting candidate to investigate in more detail. CG34357 is

predicted to have all the features of a typical particulate guanylyl cyclase (i.e. signal peptide, transmembrane domain, kinase homology domain, dimerization domain and cyclase domain, see Fig. 3.2A and C). CG34357 was found in a proteomics data set specifically enriched for membrane proteins from the head of adult flies (Aradska et al., 2015), indicating that it is inserted into membranes. Three transcripts are expressed from the CG34357 gene locus (Fig. 3.2A). Two of those only differ in the length of the 3'-untranslated region (CG34357-RD and RC). The third transcript results from alternative splicing leading to a truncated protein that only contains the extracellular part of the protein.

The functional significance of the smallest transcript is unclear (Fig. 3.2A). In some particulate guanylyl cyclase, the extracellular domain responds to stimulation through ligands. CG34357-RB might be excreted from the cell and act as a sponge for potential ligands. The mammalian Gucy2d protein, however, does not have an extracellular ligand (Kuhn, 2016). Alternatively, the extracellular part could be required for the interaction with extracellular matrix proteins. CG34357-RB could function as a negative regulator for such an interaction. The protein resulting from the smallest transcript should not be able to bind to DmIFT88, which most likely requires the intracellular domain of the protein. Additionally, since it lacks a cyclase domain, it can also not produce cGMP. I, hence, decided to disregard it within the frame of the work presented here.

I validated the phenotype found for CG34357 with two additional hairpins from a different collection (Fig. 3.2). The hairpin from the TRiP library targets all three transcripts (Fig.3.2A, HM05010). The additional two RNAi lines come from the GD library (Dietzl et al., 2007) and target the two larger transcripts specifically. Only one of those yielded a significant reduction in the gravity response of the corresponding flies (Fig. 3.2B). Since the knockdown with two out of

three RNAi lines resulted in a behavioural phenotype, I decided to analyse CG34357 further.

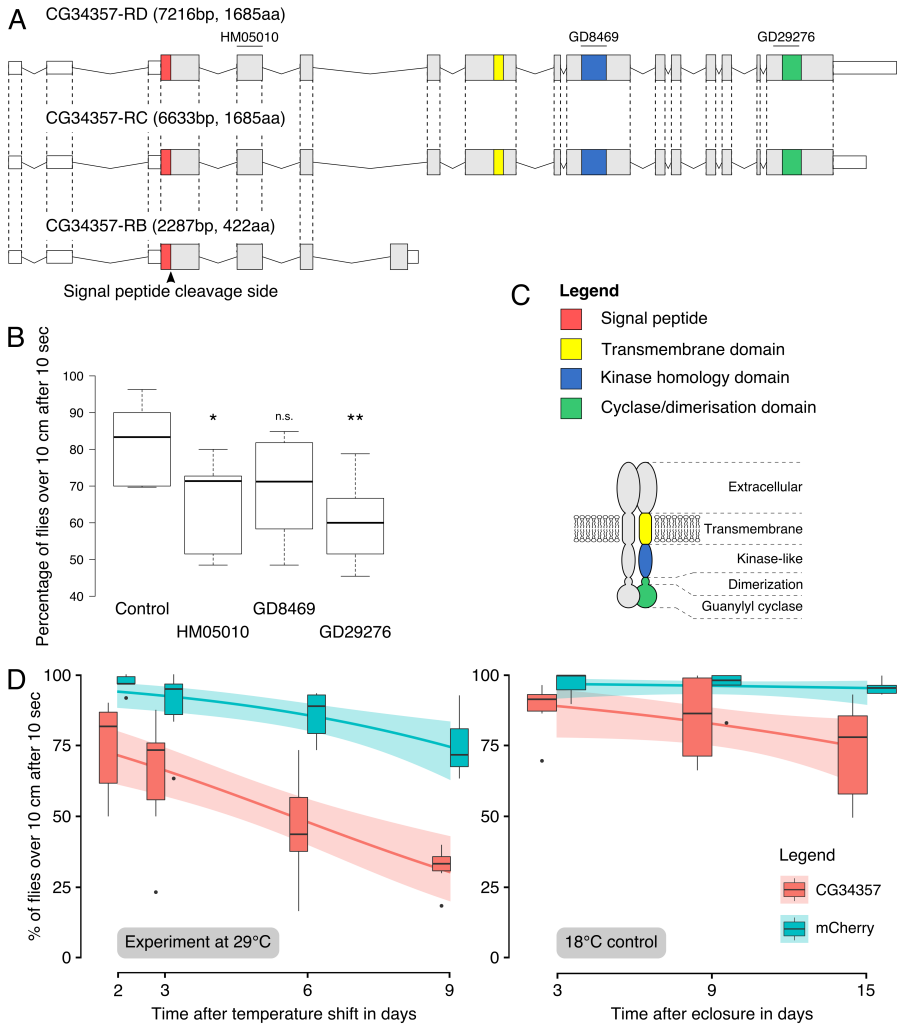

Fig. 3.2: **Validation of the gravitaxis phenotype in CG34357 knockdown**. (A) Three transcripts are annotated for the CG34357 gene in the Ensembl Genome Browser (Yates et al., 2016). Isoform RC and RD lead to the same protein and only vary in the length of the 3'-UTR. Isoform RB results from one alternative splice event leading to a drastically shorter amino acid sequence containing only extracellular parts of the protein. The different functional domains are colour-coded (for legend see C). The exons targeted by the hairpins used in B are indicated in the scheme.

Gene model was not drawn to scale for better visualisation. (B) A gravitaxis assay was used to determine the role of CG34357 in gravity sensing. A RNAi line against mCherry was used as a negative control. The RNAi lines against CG34357 come from two different collections. HM05010 (used also in Fig. 3.1) comes from the TRiP (Transgenic RNAi Project) library. GD8469 and GD29276 come from the GD collection from the Vienna stock center. HM05010 targets all isoforms; the two GD lines only target the two larger isoforms. The RNAi was driven using the pan-neuronal driver Chat-Gal4 and the flies were raised at 29°C to increase the potential phenotype. Significance was determined using the Welch two sample t-test (*p-value < 0.05, **p-value < 0.01). (C) Protein model was drawn analogously to vertebrate particulate guanylyl cyclase (Kuhn, 2016), and functional domains were indicated using the same colours as in A. The signal peptide is not shown in the protein model, because it should be cleaved off according to signal peptide prediction (Nielsen, 2017). (D) Results from the gravitaxis assay are shown with temperature shift (to permissive temperature for knockdown) or without temperature shift to control for the genetic background of the two lines (knockdown not induced, see also Fig. 2.6). Each boxplot corresponds to a total of 60 flies measured in sets of ten animals each. The data was fitted using linear regression. The curve fitted to the data is shown as a solid line, and the area around the curve represents the 95 % confidence interval. The two lines are significantly different at 29°C, but no difference can be detected at 18°C.

CG34357 is expressed in chordotonal neurons

CG34357 is involved in gravitaxis (Fig. 3.1 and Fig. 3.2), but the promoter used in this assay (Chat-Gal4) drives hairpin expression pan-neuronally (i.e. it is also active in neurons such as the ones in the central nervous system). Consequently, a gravitaxis phenotype associated with the depletion of any guanylyl cyclase could also come from impaired cGMP signalling in the central nervous system. It is therefore important to understand if the gene is actually expressed in chordotonal neurons. Gene expression in *Drosophila melanogaster* can be visualized through the use of enhancer trap lines (Brand and Perrimon, 1993). These transgenic flies encode the yeast protein Gal4 in their genomes, randomly integrated through the use of transposable elements. If the Gal4 gene is inserted in the

proximity of an enhancer, its expression pattern can be used to report the activity of the enhancer. Gal4 can in turn be used to drive visual markers such as GFP to report in which cells the corresponding gene is active (Fig. 3.3B).

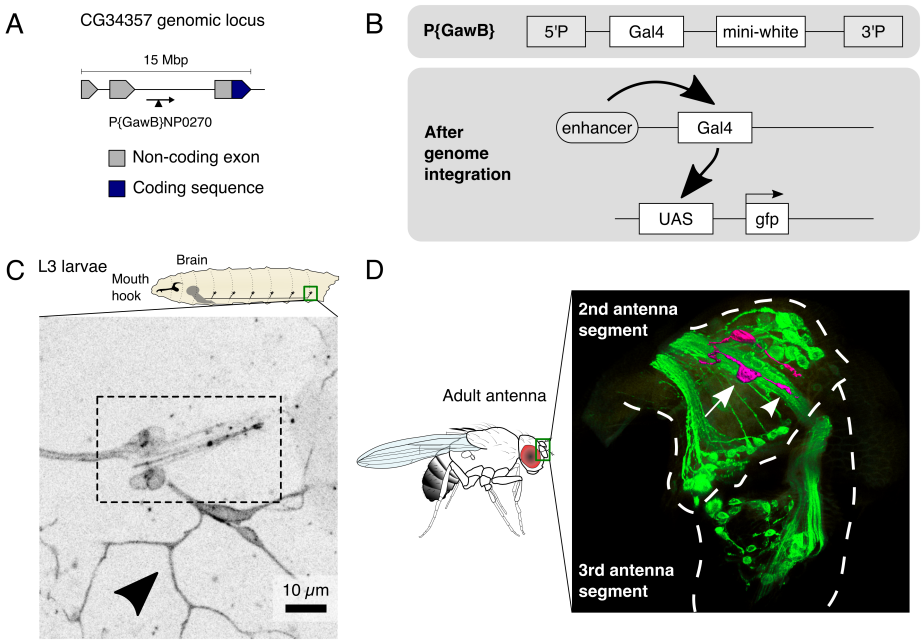

Fig. 3.3: **CG34357 is expressed in chordotonal neurons at two different developmental stages**. (A) A P-element insertion line (NP0270) was used to determine the expression of the CG34357 gene. The P-element contains a Gal4 gene and was inserted randomly after exon 2 of the CG34357 gene. (B) The upper box contains a schematic representation of the P{GawB} element. Two P-element arms flank a Gal4 gene and a mini-white gene. The mini-white gene is only required to screen for flies carrying the P-element insertion. The lower box shows schematically how gene expression pattern can be determined. The same enhancers that activate CG34357 presumably also activate the Gal4 gene. Gal4 protein is made in the corresponding cells and can be used to drive the expression of reporter genes such as GFP (adapted after (Brand and Perrimon, 1993)). (C) Using the reporter line NP02070 to drive mCD8::GFP gene expression, the CG34357 gene can be detected in chordotonal neurons in L3 larvae (dashed box). Other neurons in the peripheral nervous system are also GFP-positive (arrow head,

probably class I dendritic arborization neurons). (D) Gene expression of the CG34357 gene can also be detected in the antennae of adult flies. Antenna cuticle was made transparent prior to imaging using the FocusClear reagent. Antenna whole mounts were imaged, and the image stack was converted into a 3D model (video of the model is available on the CD accompanying the thesis). The outline of the second and third antenna segment was drawn using the autofluorescence of the cuticle. Two neurons in the second antenna segment were highlighted in magenta to show that they possess the typical morphology of chordotonal neurons. The cell body (arrow) and the dendrite (arrow head) are indicated on the image.

One such line exists for CG34357 (NP0270, see Fig. 3.3A for insertion of enhancer trap) and is publically available through the Kyoto stock center. The strain is reported to express Gal4 in the peripheral nervous system (Hayashi et al., 2002). I used a membrane-bound version of GFP (mCD8::GFP) to visualize the morphology of the cells expressing the CG34357 gene. I found that the enhancer is active in chordotonal neurons in different stages (Fig. 3.3C and D).

The expression reported here is for L3 larvae in chordotonal neurons (Fig. 3.3C, dashed box), but expression is not restricted to ciliated sensory neurons. Non-ciliated class I dendritic arborization neurons also express CG34357 (Fig. 3.3C, arrow head). It is interesting that ciliated and non-ciliated neurons produce CG34357, but it is possible that the cells express different isoforms (Fig. 3.2A).

CG34357 is also expressed in chordotonal neurons in adult flies (Fig. 3.3D). In order to estimate the number of cells in the antenna where the enhancer is active, I imaged whole antenna after clearing the cuticle. With the help of Gabriel Martins from the IGC imagining facility, I generated a 3D representation of such an image stack. We highlighted two neurons in magenta (Fig. 3.3D, for a rotating movie of the 3D model refer to movie 2 on the CD accompanying this thesis).

The strength of the GFP signal varies between different cells, which could be related to the different functions of chordotonal neurons. The fly has about ~480 neurons per second antenna segment, which can be functionally subdivided according to their responsiveness to different stimuli such as gravity sensing, hearing and wind detection (Kamikouchi et al., 2009; Yorozu et al., 2009). The GFP signal is detected in significantly less neurons. It is possible that not all subgroups use CG34357 for signal transduction. Alternatively, the enhancer trap line might only recapitulate part of the actual expression pattern of the gene. *In situ* hybridisation experiments could help to clarify the issue.

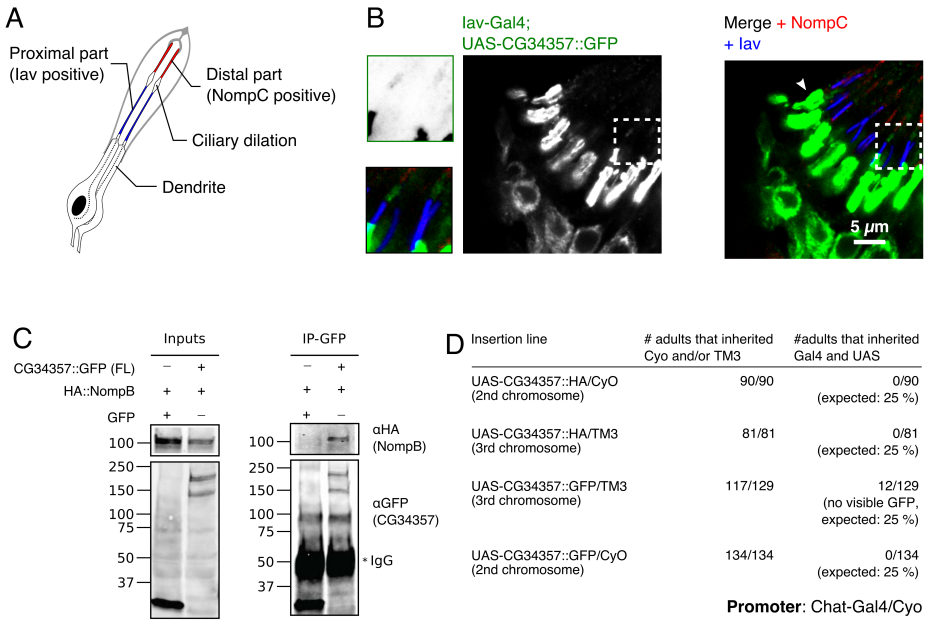

Fig. 3.4: **CG34357 localizes to the dendrite and the cilium of chordotonal neurons and binds DmIFT88/NompB in cultured cells**. (A) Schematic representation of two chordotonal neurons forming one unit showing the localisation of the two transient receptor potential channels Iav and NompC. They mark distinct segments of the chordotonal cilium adjacent to the dendrite of the neurons. (B) CG34357 protein was expressed in the chordotonal neurons using iav-Gal (driver

specific for chordotonal neurons). The protein strongly accumulates at the dendrite of the neurons (white arrow head in merge image). Insets (dashed boxes) show that the GFP signal can also be detected in the ciliary dilation adjacent to the Iav protein signal, indicating that CG34357 localises to the cilia. (C) CG34357 protein was fused to GFP at the C-terminus and co-expressed with NompB N-terminally labeled with a 3xHA-tag. CG34357 expression always leads to the formation of three distinct bands. Co-expression of CG34357 and NompB reduces overall NompB levels. GFP serves as a negative control in this experiment. NompB can be detected upon precipitation of CG34357. Co-immunoprecipitation experiments were performed with the help of Sihem Zitouni to determine binding of the two proteins. (D) Pan-neuronal expression of CG34357 using Chat-Gal4 leads to developmental lethality. The parental strains used here are each heterozygous and carry the respective insertions over a balancer chromosome (TM3 or CyO). Only 25 % of the offspring should hence inherit both Gal4 and the UAS insertions. The actual frequencies of offspring with and without balancer chromosomes are indicated in the table here. The lethality is independent of the chromosome in which the P-element was inserted and the tag that was used to label CG34357.

CG34357 shows specific localisation in chordotonal neurons

The expression pattern of CG34357 in ciliated sensory neurons suggests that one of the gene products has a function in these cells. Additionally, the gravitaxis defect upon RNAi-mediated knockdown points towards CG34357 being required for gravitaxis. Taken together, these findings indicate that CG34357 could be the functional equivalent of Gucy2d. From the known properties of Gucy2d it is expected that CG34357 localizes to the cilia of chordotonal neurons and binds DmIFT88/NompB. In order to test localization of the protein I cloned the coding sequence and generated transgenic flies for overexpression experiments. It should be mentioned here that the cDNA was amplified from mRNA isolated from antennae, which lends additional credibility to the expression pattern observed in the sensory neurons (Fig. 3.3). The protein was always tagged at the C-terminus to avoid compromising the signal peptide (Fig. 3.2A).

Initial attempts to ectopically express the protein pan-neuronally using Chat-Gal4 failed. The flies died in development (Fig. 3.4D). I obtained the same results with different transgenic fly lines and tags for the CG34357 protein. The lethality is, hence, neither due to a particular insertion site nor a particular tag. Consequently, overexpression of CG34357 in the developing nervous system is fatal for the animals. The overexpression experiments were conducted using a chordotonal specific promoter (iav-Gal4).

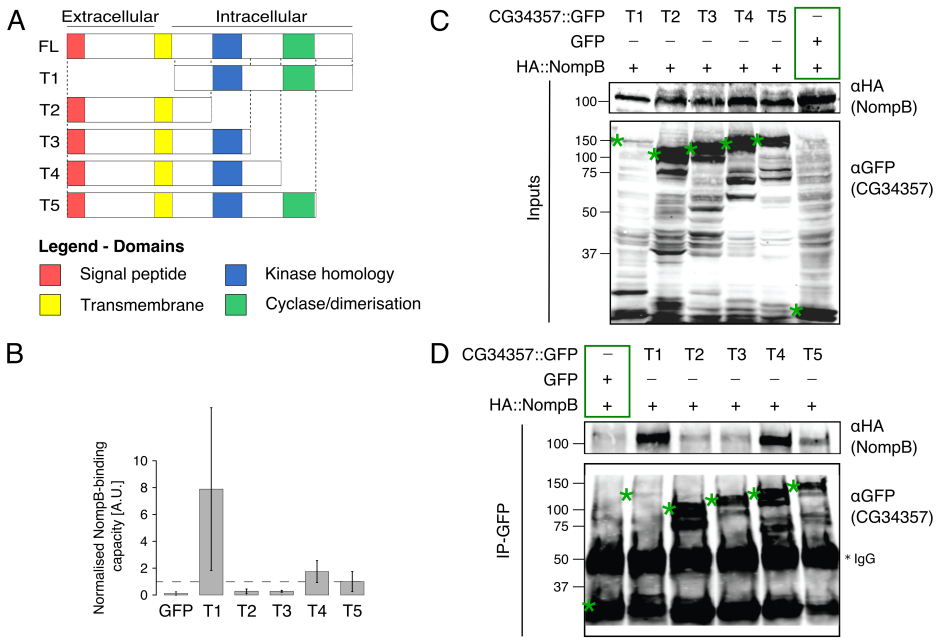

Fig. 3.5: **Determining NompB-binding domain on CG34357**. (A) Overview of the five truncations generated to determine the NompB-binding site on CG34357. For an overview summarizing all experiments with the CG34357 protein fragments refer to Fig. 3.7. (B) Quantification of the NompB-binding capacity of the five fragments used here. For normalization, the NompB signal intensity after co-immunoprecipitation was divided by the amount of NompB and CG34357 in the respective inputs. Each bar contains normalized intensity values for at least three experiments. The large error bar for T1 results from weak expression levels of T1 as seen in D. (C) Inputs from the transfection experiments. Co-transfection with GFP

(green box) was used as negative control. Bands of expected molecular weight are marked with green asterisks. Note that T1 is always expressed at very low levels when compared to the other fragments. (D) Representative result from a co-immunoprecipitation experiment. T1 is detected very weakly even after immunoprecipitation using a GFP antibody (negative control). T1, T4 and T5 precipitate NompB.

In the chordotonal neurons the GFP-tagged CG34357 strongly localizes to the dendrite of the neurons and can also be weakly detected in the cilia (Fig. 3.4B). The localization data was confirmed using a HA-tag (data not shown).

CG34357 binds NompB in cultured cells

The ability of CG34357 to bind to DmIFT88/NompB was tested in cultured cells with the help of Sihem Zitouni. For the immunoprecipitation experiments we co-expressed GFP-tagged CG34357 together with HA-tagged NompB. Expression of CG34357 always yields three bands (Fig. 3.4C). I can only speculate about the identity of those bands. Gucy2d purified from bovine photoreceptors was found to be highly phosphorylated and possess autophosphorylation capacity (Aparicio and Applebury, 1996). The upper two bands found in our western blot experiments could hence be the phosphorylated and the unphosphorylated form of the protein. Other posttranslational modifications such as glycosylation were also reported for some guanylyl cyclases (Kuhn, 2016). It would require purification of the bands followed by mass spectrometry to identify their exact identity. Investigating the protein modifications in *Drosophila* might be rewarding, because it would allow me to conclude which other aspects of the physiology of the particulate guanylyl cyclases can be modelled in the fly.

When we precipitated GFP-tagged CG34357 using a GFP antibody, we could detect HA-tagged DmIFT88/NompB co-precipitating with it.

GFP alone, however does not bind NompB (Fig. 3.4C). We validated the result with swapped tags using a HA-antibody to precipitate CG34357 (data not shown). The results show that the two proteins interact in cultured cells.

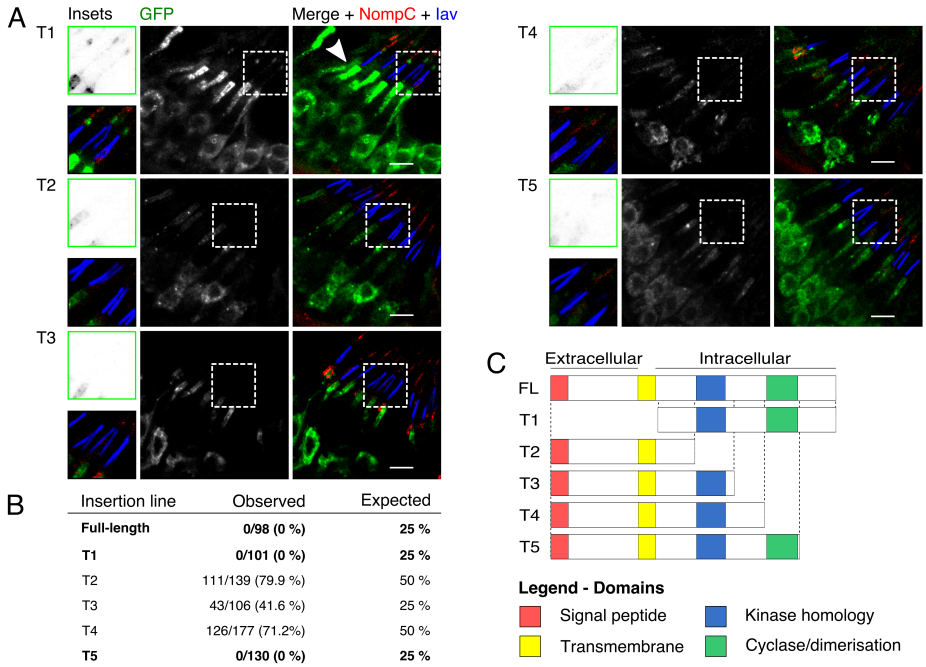

Insertion line	Observed	Expected
Full-length	**0/98 (0 %)**	**25 %**
T1	**0/101 (0 %)**	**25 %**
T2	111/139 (79.9 %)	50 %
T3	43/106 (41.6 %)	25 %
T4	126/177 (71.2%)	50 %
T5	**0/130 (0 %)**	**25 %**

Fig. 3.6: **Localisation of CG34357 fragments in chordotonal neurons**. (A) Expression of the five CG34357 fragments was driven using the chordotonal neuron specific iav-Gal4 line. Proximal and distal cilia segments are marked with Iav and NompC, respectively. Representative insets are given for each image (dashed boxes). Only fragment T1 accumulates at the dendrite (white arrow head in merge image) and can be seen clearly inside the cilia. (B) Expression of the five fragments was driven using the pan-neuronal driver Chat-Gal4. The parental driver line is only heterozygous viable. Some parental UAS insertion lines were homozygous, some heterozygous. Since the Gal4 and the UAS-element need to be inherited together for gene expression, the offspring should be observed at 50 % or 25 % frequency, respectively. Observed frequencies are shown as well. Lethality correlates with the cyclase domain being present in the

fragments (fragments highlighted in bold). (C) Overview of the five truncations used for the experiments.

NompB-binding domain on CG34357 is involved in localisation of the cyclase

In the description of the interaction of mouse IFT88 and Gucy2e it was not shown whether the protein interaction is dependent on a particular domain in the cyclase (Bhowmick et al., 2009). Ectopic expression of the mouse protein in the *Xenopus* retina did not yield a particular domain responsible for targeting to the photoreceptor outer segment (Karan et al., 2011). Additionally, the mouse Gucy2e was also found to depend on rhodopsin for transport (Pearring et al., 2015), but rhodopsin itself localizes to the photoreceptor outer segment independently of IFT (Jiang et al., 2015). IFT88 can target Gucy2e to cilia even in IMCD3 cells (mouse kidney cell line), when the cyclase is ectopically expressed in those cells (Bhowmick et al., 2009). This localisation is independent of rhodopsin, because rhodopsin was not found in the proteome of cilia isolated from IMCD3 cells (Ishikawa et al., 2012). This suggests that IFT88 is sufficient for ciliary targeting of the cyclase. Taken together these findings indicate that the cyclase can be transported to cilia potentially in two independent ways: (1) Through binding to IFT88 as well as (2) through binding to rhodopsin. In order to understand the significance of these two modes of transportation, it is important to be able to uncouple them experimentally. For that it is necessary to know how IFT88 and the cyclase bind to each other. Understanding the interaction between the cyclase and DmIFT88/NompB could guide hypotheses in other species as well.

I generated several protein fragments of CG34357 (Fig. 3.5A). One fragment (T1) only contains the intracellular part of the protein. Since NompB is a cytoplasmic protein, this fragment is expected to bind to

NompB. Additionally, I generated four fragments (T2-5) containing the extracellular part of the protein to maintain membrane localisation of the fragments. The association with cellular membranes might constrain the ability of the fragments to interact with other proteins. The fragments were designed to be successively longer, each containing one more domain of the previous one (Fig. 3.5A).

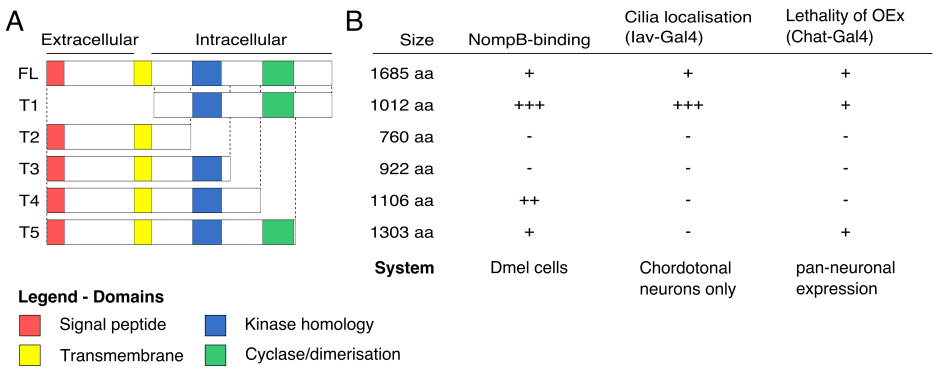

B

	Size	NompB-binding	Cilia localisation (Iav-Gal4)	Lethality of OEx (Chat-Gal4)
FL	1685 aa	+	+	+
T1	1012 aa	+++	+++	+
T2	760 aa	-	-	-
T3	922 aa	-	-	-
T4	1106 aa	++	-	-
T5	1303 aa	+	-	+
System		Dmel cells	Chordotonal neurons only	pan-neuronal expression

Fig. 3.7: **Overview of the results obtained with the CG34357 fragments**. (A) Five fragments were generated. Four presumably membrane-bound fragments (T2-5) and one cytoplasmic fragment (T1). Predicted domains are annotated in the scheme. (B) Overview of the results obtained with the fragments and the systems in which the experiments were conducted. The full-length protein as well as T1, T4 and T5 are able to bind DmIFT88/NompB. Note: Dmel cells do not express other members of the IFT complex. This shows that the binding does not depend on the whole IFT complex. Pan-neuronal expression of the CG34357 full-length protein (FL) and fragments leads to developmental lethality only for those constructs that contain the cyclase domain.

GFP alone cannot co-precipitate NompB. We could, however, observe strong binding between T1 and full-length NompB (Fig. 3.5B, D). Out of the four membrane-bound fragments only T4 and T5 co-precipitated NompB. Of note, the total protein levels between the different fragments (T1 to T5) varied strongly. We

therefore quantified the levels of NompB detected after immunoprecipitation relative to the amount of the CG34357 fragments in the input (Fig. 3.5B). NompB binds most strongly to T1. It is difficult, however, to compare the strength of binding between T1 and the other four fragments, because it is not membrane-bound. The three fragments (T1, T4 and T5) that show significantly stronger binding when compared to the background band observed in the GFP control share one protein domain that is not present in T2 and

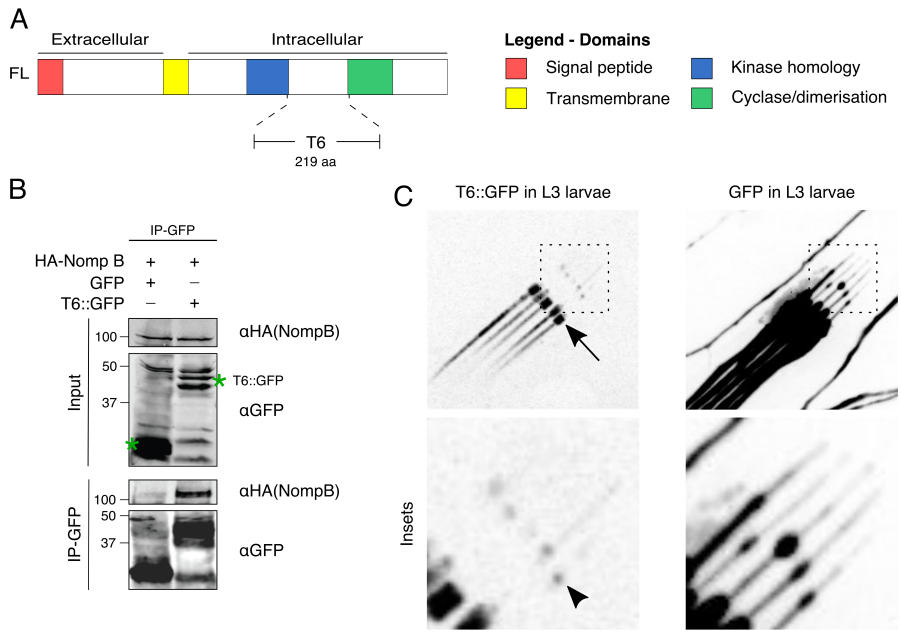

T3.

Fig. 3.8: **A small CG34357 fragment is sufficient to bind DmIFT88/NompB and accumulate at the ciliary base**. (A) A small CG34357 fragment was generated to test whether the NompB binding domain (denoted as T6) predicted from previous co-immunoprecipitation experiment (Fig. 3.5) is sufficient to bind NompB and target to the cilium. (B) Co-immunoprecipitation experiment conducted in Dmel cells shows that T6 can bind NompB protein. Two potential T6 bands are observed in the inputs. In the immunoprecipitation blot, two different GFP antibodies were used for precipitation and for probing the membrane, respectively, to avoid IgG signal as

seen on previous blots (compare for example 3.5.D). Green asterisks indicate specific bands of expected size. (C) T6::GFP was driven with iav-Gal4 in chordotonal neurons of L3 larvae. The protein clearly accumulates at the ciliary base of the neurons but can also be detected inside the cilia. Cilia are shown in magnification below the original image. The ciliary dilation is indicated with a black arrowhead in magnifications. In comparison, no preferential localization can be seen for GFP alone.

I generated transgenic animals for an overexpression experiment to relate the differential ability of the five fragments to bind NompB to their localisation in ciliate neurons. Only T1 can be detected in chordotonal cilia (Fig. 3.6A). This indicates that the ability to bind NompB is not sufficient to target the CG34357 fragments to cilia. Otherwise T4 and T5 should also be detectable in the cilia. The experiments demonstrate, however, that the ciliary localization of the full-length protein (Fig. 3.4B) is not due to passive diffusion. If diffusion would explain the localisation of the full-length protein in the cilia, it would be expected that T2-5 also localise in the cilia. Perhaps additional protein-protein interactions are required to permit ciliary localisation of the protein. The localisation pattern of the full-length protein and the fragments suggest that the C-terminus (only shared by the full-length protein and T1, Fig. 3.7) is also involved in ciliary localisation. It would be interesting to test the role of rhodopsin (also expressed in chordotonal neurons) in this system. One approach could be to study the localisation of the fragments in rhodopsin mutants flies that form cilia (Senthilan et al., 2012).

Lethality caused by CG34357 overexpression is caused by the cyclase domain

Overexpression of the full-length protein causes lethality, perhaps due to excessive amounts of cGMP in the developing nervous system (Fig. 3.4C). To support this idea I overexpressed the five

fragments pan-neuronally (using Chat-Gal4) and quantified lethality. In the case of overexpression of the full-length protein, T1 and T5, no animals developed to adulthood (Fig. 3.6B). These findings strongly suggest that lethality is associated to the cyclase domain. Excess levels of cGMP can cause cell death in neurons (Montoliu et al., 2001). In *C. elegans* the particulate guanylyl cyclase GCY-8 controls the morphology of ciliated sensory neurons through cGMP levels (Singhvi et al., 2016). I have not formally demonstrated that CG34357 indeed produces cGMP, but it is the most likely explanation for the results presented here. The activity of CG34357 that leads to lethality, however, does not seem to depend on cilary targeting. This is based on the observation that pan-neuronal expression causes developmental lethality (Fig. 3.4D and 3.6 B), whereas expressing specifically in chordotonal neurons does not (Fig. 3.4B). It is most likely necessary to regulate the activity of particulate guanylyl cyclase closely. I postulate that the ciliated neurons have additional regulatory mechanisms to constrain the cyclase activity (perhaps through localisation) that allow them to cope with excess protein. Further experiments, however, are required to demonstrate this.

Sequence comparison reveals strong conservation of the CG34357 DmIFT88/NompB-binding domain with potential disease relevance

The mechanisms in regulating the localization and activity of CG34357 might be shared between species and hence rely on amino acid sequence conservation. I compared the sequences of guanylyl cyclases from different species to address to what extent the IFT88-binding side might be conserved. This could provide further insights into the mechanism how the protein is targeted to cilia. Analysis of the amino acid sequence of different vertebrate

Gucy2d homologues showed that the protein is poorly conserved. Only 51% of the amino acid residues are the same between humans and mice (Fig. 3.9A). When comparing between humans and fruit flies, sequence identity drops to 30%. To obtain some hints about important residues for protein function, I compiled a table with missense mutations found in patients with LCA (Tab. 3.5). There is no particular hotspot for mutations in the human protein (Fig. 3.9B). Several of the mutations in the intracellular part of the protein, however, are conserved in *Drosophila* (highlighted in bold, Fig. 3.9B), suggesting that they are of vital importance for the protein function even across large evolutionary distances.

To obtain a more detailed understanding of the sequence conservation between different species, I generated a multiple sequence alignment comparing the protein sequences from the vertebrate species discussed above (Fig. 3.9A). I included six insect species to avoid a bias towards vertebrates in the analysis. For better visualization a score was calculated for each position in the alignment based on amino acid similarity using JProfileGrid2 (Roca et al., 2008). The scores are displayed as a heatmap with colour intensity indicating similarity per position in the alignment (Fig. 3.10). The analysis reveals strong conservation in the kinase homology domain, the cyclase domain and the segment linking the two (Fig. 3.10). The conservation in the two catalytic domains is not surprising, as it most likely relates to preservation of cyclase activity as well as the autoregulatory kinase activity (as found for bovine Gucy2d (Aparicio and Applebury, 1996)). There is, however, also strong conservation in the protein part linking the two domains. This stretch of the protein (hereafter donated as T6, Fig. 3.8A) is shared only between the full-length protein and the fragments that can bind DmIFT88/NompB (Fig. 3.7). When comparing the T6 fragment directly to the human protein, sequence identity increases strongly

(from 30% for the entire sequence to 50% when considering just the T6 fragment).

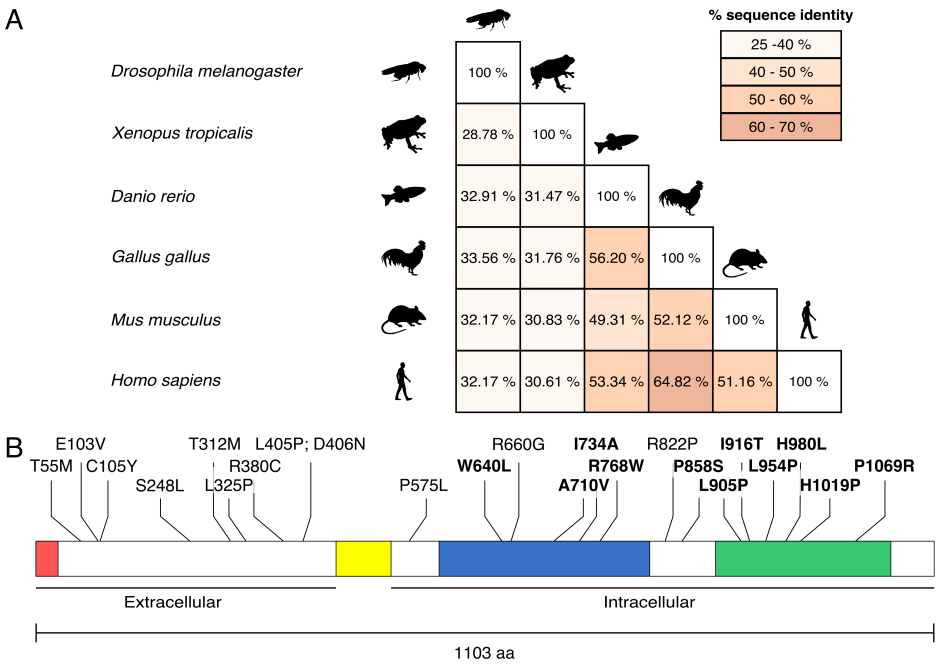

Fig. 3.9: Cross species comparison of Gucy2d homologues and overview of known mutations in human Gucy2d in patients from Leber congenital amaurosis (LCA). (A) Matrix shows pair-wise comparison of different Gucy2d homologues between different vertebrate species and *Drosophila melanogaster*. Numbers indicate percentages of identical residues in pair-wise alignments. Even within vertebrate species the sequence similarity is rather low. (B) Known sites mutated in patients with LCA. Residues highlighted in bold are conserved in *Drosophila melanogaster*. There is no clear hotspot region for mutations in humans (for more details on mutations refer to Tab. 3.5).

I predicted the protein structure of CG34357 using Phyre2 (see method sections for details) (Kelley et al., 2015) and highlighted functional domains as well as conserved residues found to be mutated in LCA patients (Fig. 3.10). Several missense mutations lie within the cyclase domain and most likely reduce the ability of the protein to generate cGMP, which is likely to be the underlying cause

for the disease. This was indeed shown for L954P (Tucker et al., 2004). One missense mutation was reported in the kinase homology domain, but no functional analysis was performed (Tab. 3.5). Four mutations fall into the protein segment corresponding to T6 (Fig. 3.10). Except for P858S, none of these has been studied functionally until now. P858S causes reduced cyclase activity (Tucker et al., 2004). The ability of T6 to bind DmIFT88/NompB and the strong sequence conservation make it tempting to speculate that any of those four mutations can compromise binding to IFT88 and in turn reduce localization to the photoreceptor outer segment. Due to time constraints, however, I was unable to address this hypothesis so far experimentally.

Tab. 3.5: Missense mutations reported in patients with Leber congenital amaurosis

Mutation	Functional significance	Reference
c.2129C>T (p.A710V)	Conserved residue in the kinase homology domain, might impact autoregulation of the protein	(Gradstein et al., 2016)
c.743C>T (p.S248L)	No mechanism proposed	(Safieh et al., 2016)
c.2714T>C (p.L905P)	Disrupts an alpha-helix in the cyclase domain	(Hosono et al., 2015)
p.P575L p.H1019P p.P1069R	All three mutations render the cyclase domain less active or inactive altogether	(Zägel and Koch, 2014)
p.I916T	No mechanism proposed	(de Castro-Miró et al., 2014)
c.1138C>T (p.Arg380Cys)	Found in healthy individuals as well, potential modifier mutation (rendering an individual more susceptible to additional mutations in other genes)	(Jinda et al., 2014)

c.164C>T (p.T55M) c.935C>T (p.T312M) c.2302C>T (p.R768W) c.2200A>G;c.2201T>C] (p.I734A) c.1919G>A (p.W640L) c.1214T>C;c.1216G>A (p. L405P;D406N) c.308A>T (p.E103V) c.1979G>A (p.R660G)	No mechanism proposed	(Li et al., 2011)
p.R768W p.R822P p.H980L	All three mutant proteins show no cyclase activity	(Jacobson et al., 2013)
p.C105Y p.L325P p.P858S p.L954P	C105Y and L325P show normal basal activity, but weakened response to stimulation; P858S and L954P also show low activity, but also exert dominant negative effect on wild type allele	(Tucker et al., 2004)

Discussion and conclusions

The work presented here suggests strongly that CG34357 is the *Drosophila melanogaster* homologue of human Gucyd2d or a functional equivalent. The gene is expressed in ciliated sensory neurons (Fig. 3.3) and knockdown of the protein causes defects in cilia function (Fig. 3.1 and 3.2). The protein localizes to cilia in sensory neurons and binds to DmIFT88/NompB (Fig. 3.4). A truncation experiment suggested that a region in the protein of about 200 amino acids is required for binding to DmIFT88/NompB (Fig. 3.5). Results regarding localisation from ectopic expression in the fly are less clear. Not all fragments that bind NompB in cultured cells are also targeted to cilia (Fig. 3.6). Additional experiments are required to further explain the underlying mechanisms for localizing

the protein to cilia. Sufficiency experiments, however, demonstrated that those 200 amino acids are enough to bind NompB. Ectopic expression in chordotonal neurons suggests that they contain information to target the peptide to the ciliary base as well as the cilium (Fig 3.7). Bioinformatic analysis of this fragment revealed evolutionary conservation that might be of relevance for LCA patients with certain mutations in Gucy2d (Fig. 3.10).

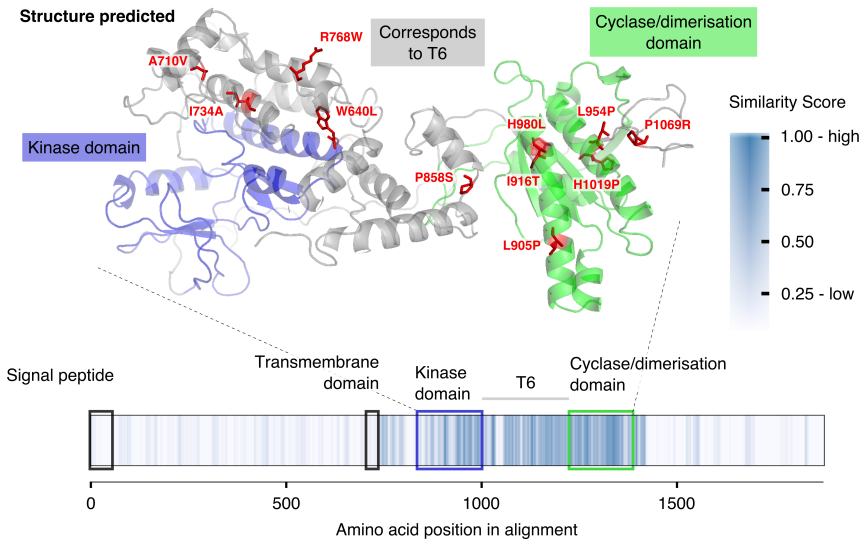

Fig. 3.10: **Detailed sequence comparison between various (potential) Gucy2d homologues reveals conserved stretch that might be related to transport**. Top: Predicted protein structure corresponding to the stretch in the intracellular part of CG34357 that includes the kinase homology domain (blue), the T6 fragment (grey) and the cyclase domain (green). Superimposed are conserved residues that are known to cause Leber congenital amaurosis in humans when mutated (red). Bottom: Heatmap representation of a multiple protein alignment for the six species shown in Fig. 3.9 plus additional six insects species to avoid a vertebrate bias in the alignment. The two domains related to the protein function are strongly conserved, but the part corresponding to the T6 fragment is conserved as well. Given the results concerning DmIFT88/NompB binding to T6, this pattern in sequence conservation might suggest a conserved role in protein transport.

It remains to be seen, however, if the ciliary localization in fact depends on DmIFT88/NompB. The two fragments T4 and T5 are able to bind DmIFT88/NompB in cultured cells (Fig. 3.5B-D). This is, however, not sufficient to target the fragments to cilia when ectopically expressed in chordotonal neurons (Fig. 3.6A). Only the T1 fragment and the full-length protein were found to localise to cilia (Fig. 3.4B and 3.6A). Both have the ~380 amino acids from the C-terminus of the protein in common (Fig. 3.7), that are missing in all other fragments. It is possible that an additional protein-binding event through the C-terminus is required to target the protein to the cilia. One candidate for such an interaction could be rhodopsin. Rhodopsin is required to target Gucy2e to the outer segment of photoreceptors in the mouse retina (Pearring et al., 2015). Furthermore, rhodopsins were found to localise in cilia in the chordotonal neurons and to be required for their function (Senthilan et al., 2012).

There are several ways to address the issues raised above experimentally. In order to test whether DmIFT88/NompB is also required for targeting of CG34357 to the chordotonal cilia, it is important to study the localisation of the protein in chordotonal cilia depleted of NompB after cilia formation. Alternatively, one could generate transgenic animals expressing truncated CG34357 where the 200 amino acids corresponding to T6 have been deleted (Fig. 3.8). The role of the C-terminus could be studied by fusing the last 380 amino acids of the full-length protein to T4. If those are essential in targeting the protein to cilia, fusing the 380 amino acids to T4 should permit the resulting fragment to localise to cilia. The role of rhodopsin could be studied by expressing the fragments in rhodopsin mutant flies that form cilia (Senthilan et al., 2012). If rhodopsin were important in this system for the localisation of

CG34357 to cilia, it would be expected that T1 and the full-length protein could not localise properly in rhodopsin mutants.

It is formally possible that the binding of CG34357 to DmIFT88/NompB depends on other IFT complex members. The interaction surface to bind the cyclase might require heterodimer formation of two different IFT subunits. This is unlikely, however, because almost none of the IFT proteins should be present in *Drosophila* cultured cells judging from publically available gene expression data. DmIFT70 is the only member of the IFT-B complex that is expressed at a very low level in Drosophila cultured cells (S2R+) according to the modENCODE database (Celniker et al., 2009). This suggests that the interaction of the DmIFT88/NompB and CG34357 is most likely direct.

If CG34357 in fact depends on DmIFT88/NompB for its ciliary localisation, depletion of the IFT protein should result in less cGMP in the cilia. This might concern basal cGMP levels as well as cGMP levels after stimulation of the sensory neurons. The role of cGMP in chordotonal neurons is not clear, however. We also do not know which are the molecules that respond to cGMP in this system. One potential candidate is a cyclic-nucleotide gated ion channel that was found to be expressed in the antennae of *Drosophila* (Marx et al., 1999). This channel, however, was never functionally characterized in chordotonal neurons, and its role in gravitaxis is unclear. It is also difficult to measure cGMP levels *in vivo*. Antibodies against cGMP exist and have been used in immunofluorescence microscopy (Michalakis et al., 2013), but they are, however, not particularly sensitive and not suitable for detection of cGMP reduction below normal levels (Stylianos Michalakis, personal communication). One role for cGMP in this system might be in modulating the response of the neurons. Neuronal stimulation leads to calcium influx into the neurons, and the intracellular calcium concentration is frequently

used to measure neuronal activity (Tian et al., 2009). It is known since the 1970ies that calcium levels stimulate cGMP production (Kots et al., 2009). In the case of Gucy2d there is a specific activating protein that responds to intracellular calcium levels (Kuhn, 2016). It is therefore possible that CG34357 has a role in modulating neuronal activity in response to calcium as oppose to being part of the initial signalling transduction cascade. Physiological studies of these neurons would be required to test the role of cGMP in the system. Genetically encoded fluorescent calcium sensors can be used to report the activity of the neurons (Tian et al., 2009). It would be interesting to see how the activity of these neurons changes when incubated with non-hydrolyzable cGMP analogs (e.g. 8-bromo-cGMP) or in the overexpression of enzymes that break down cGMP (e.g. PDE6).

The expression data obtained with the CG34357 enhancer trap line from adult antenna (Fig. 3.3D) indicates that the gene is not active in all chordotonal neurons in the second antenna segment. There are two possible explanations for this observation. Either the enhancer trap line does not fully recapitulate the activity of the gene or only a fraction of the neurons rely on the cyclase for their function. The neurons in the second antenna segment fall into five distinct groups that respond distinctly to different stimuli (e.g. gravity, wind, sound) (Kamikouchi et al., 2009; Yorozu et al., 2009; Zhang et al., 2013). It would be interesting to co-label the different subgroups to interpret the expression pattern together with the function of the corresponding neurons. The appropriate tools for these experiments need to be Gal4 independent (because the CG34357 enhancer trap line produces Gal4) and were not available in the lab when the experiment was conducted.

CG34357 expression can also be seen in some sensory neurons in the third antenna segment (Fig. 3.3D). These neurons also form cilia

and express DmIFT88/NompB (Kuzhandaivel et al., 2014). I have not addressed the maintenance role of NompB in those neurons, and it is not known whether CG34357 has a role in olfaction. cGMP signalling, however, is involved in chemosensation in the fly (Vermehren-Schmaedick et al., 2010, 2011). It is hence tempting to speculate that CG34357 has a more general role in signal transduction in sensory cilia. This role might also apply in the case of non-ciliated sensory neurons, which would explain why CG34357 is also expressed in class I dendritic arborization neurons (Fig. 3.3C). This could have to do with a more general role of the enzyme in modulating neuronal activity (as postulated above) as opposed to a specific role of the cyclase in the transduction of one particular environmental stimulus.

It is difficult to explain the lethality caused by pan-neuronal expression of the cyclase without knowing which cells specifically cannot cope with the enzyme. It is known, however, that excessive amount of cGMP can cause cell death in neurons (Montoliu et al., 2001), which could be for example due to inappropriate excitation of neurons. Ciliated sensory neurons might have a mechanism to regulate activity of the cyclase through localisation. To address this hypothesis one could overexpress CG34357 in the larval brain and monitor cell death in the tissue. If the protein causes cell death in some neurons, but not in others, it would be interesting to see if the protein shows different localisation patterns in the two groups of neurons.

The predictions made here regarding the sequence conservation of CG34357 and human Gucy2d remain unexplored. If the human protein binds IFT88 through the equivalent residues that have been found relevant for *Drosophila* then these residues might be of interest for human disease. Several conserved mutations have been found in LCA patients (Fig. 3.9B), but it is not yet clear how they

impact protein function (Tab. 3.5). My work predicts that some of these mutations impact binding of the cyclase to IFT88. LCA might arise in those patients due to insufficient delivery of the protein to the photoreceptor outer segment. It should be possible to test this prediction through mutation of the relevant residues in human Gucy2d and ectopic expression in ciliated cells in culture. Bhowmick and colleagues showed that mouse Gucy2e can be targeted to cilia in kidney cells in culture through binding to IFT88 (Bhowmick et al., 2009). A similar experimental setting should be sufficient to address the localization issue. A reduced localization of any of these mutant proteins to cilia would support the disease mechanism as outlined here. If one were to demonstrate that certain mutations reduce targeting of Gucy2d to the photoreceptor outer segment by affecting binding to IFT88, it would be important to include this in the characterisation of novel disease mutations. I am not certain, however, if this insight would lead to novel therapy options. No pharmaceutical interventions for LCA exist and the only therapy option that is under development is gene replacement therapy (Weleber et al., 2013).

Chapter IV – Final discussion

Cilia play very important roles in the development and physiology of many eukaryotic species. They are also very versatile as they execute different functions ranging from motility to sensing. They also show structural differences in different species, suggesting that they were frequently adapted in the course of evolution. Despite the many discoveries that were made in ciliogenesis, little is known about the maintenance of this organelle. Cilia depend for their biogenesis on the activity of a dedicated transport system called intraflagellar transport (IFT) (Eguether et al., 2014; Jiang et al., 2015; Kozminski et al., 1995; Pazour et al., 2002). IFT is a protein complex comprised of 22 subunits. One complex member, called IFT88, is required for IFT-mediated ciliogenesis in all species investigated so far. It was also found that IFT88 is essential for cilia maintenance in different systems, suggesting that maintenance may use the same machinery as biogenesis (Fort et al., 2016; Jiang et al., 2015; Pazour et al., 2002). Recent findings from Fort and colleagues show that it is not always obvious how IFT contributes to the maintenance of the ciliary properties (Fort et al., 2016). My work aims to further understand the role of IFT in cilia maintenance. I will summarize my findings here briefly, followed by a discussion of the implications of my work and the future directions that should be followed.

In the frame of this thesis I provided evidence that the fly homologue of IFT88 (DmIFT88/NompB) is highly divergent from IFT88 in other species but retains structural signatures (Fig. 2.1). DmIFT88/NompB is present in fully formed cilia (Fig. 2.2) and is continuously motile in cilia, which is suggestive of active transport (Fig. 2.3). The DmIFT88/NompB gene is continuously expressed, and constitutive knockdown with RNAi recapitulates the mutant phenotype (Fig. 2.4 and 2.5 (Han et al., 2003)). Additionally, the electron microscopy data suggests that the transition zone forms even in the absence of DmIFT88/NompB (Fig. 2.5). Depletion of the protein after

ciliogenesis in ciliated sensory neurons leads to behavioural phenotypes in the fly (Fig. 2.6). This suggests that translation of novel DmIFT88/NompB protein is required to maintain the function of the cilium in those cells. I described molecular and morphological changes on the level of the cilia upon DmIFT88/NompB depletion (Fig. 2.7). I could not, however, attribute those phenotypes to one distinct molecular mechanism. It was proposed in the mouse retina that the guanylyl cyclase GC-E (Gucy2d in humans) is transported to the photoreceptor outer segment by IFT88. GC-E is a cGMP-generating enzyme essential for photoreceptor function (Kuhn, 2016). In an effort to identify a DmIFT88/NompB cargo, I screened candidate genes for a fly homologue of GC-E with a role in cilia-related sensing. I identified one candidate (Fig. 3.1 and 3.2) and demonstrated that this previously undescribed gene CG34357 is expressed in ciliated neurons (Fig. 3.3). The protein can localise to cilia as well as bind DmIFT88/NompB in cultured cells (Fig. 3.4). Through truncation experiments I identified a binding side for NompB on CG34357 (Fig. 3.5). Not all CG34357 fragments that contain the NompB-binding site, however, localise to cilia (Fig. 3.6). This suggests that binding to NompB is not sufficient to target the protein to cilia. Nonetheless, the sequence of 200 amino acid residues, which binds to NompB in cultured cells, localises to cilia (Fig. 3.8). This indicates that the full-length protein is under more complex regulation. Sequence comparisons showed that the NompB-binding side on CG34357 is evolutionary conserved. Gucy2d is frequently found mutated in human patients with a retina-specific ciliopathy called Leber congenital amaurosis (LCA). Some of the mutations are in the conserved IFT88-binding site and could hence affect trafficking of the protein in the retina (Fig. 3.9 and 3.10). Many aspects of the regulation of the localisation of CG34357 are, however, still unknown. Next I will discuss my data on NompB trafficking in the

light of the current literature before arguing for its role in the transport of CG34357.

Regulation of IFT waiting time and remodelling

The work carried out here suggests that some features of anterograde and retrograde IFT trains (multiple arrays of the IFT complex) are shared between *Drosophila, Chlamydomonas* and *Trypanosoma*. It was shown in both *Chlamydomonas* as well as *Trypanosoma* that retrograde trains are smaller than anterograde trains, but retrograde trains are more frequent (Buisson et al., 2013; Wingfield et al., 2017). The data from GFP-labelled DmIFT88/NompB suggests similar behaviour for the IFT trains in *Drosophila* (Fig. 2.3). Additionally, there are stationary pools of DmIFT88/NompB molecules visible at the base and the tip of the cilium, which most likely relate to regulation of the IFT proteins. In *Trypanosoma* as well as *Chlamydomonas,* IFT trains disassemble at the ciliary tip and base and are recycled and reassembled into new trains after a certain waiting time (Buisson et al., 2013; Wingfield et al., 2017). Furthermore, IFT trains move progressively and without pausing or changing direction from the ciliary base to the tip and back (Buisson et al., 2013; Prevo et al., 2015; Stepanek and Pigino, 2016; Ye et al., 2013). Recently, it was proposed in *Chlamydomonas* that anterograde trains move along B-tubules and retrograde trains move along A-tubules to avoid collision (Stepanek and Pigino, 2016). Additionally, since trains never seem to switch direction in the middle of the axoneme, there cannot be a “tug-of-war” between kinesin and dynein within the same train. Several remodelling events thus have to occur before a new IFT train (irrespective of the direction) can travel along the ciliary axoneme. Dynein is a cargo of the anterograde IFT complex, but somehow competition with kinesin has to be prevented within a train. Recent work suggests that dynein is

transported in an inactive form (Toropova et al., 2017). At the ciliary tip, however, dynein has to be activated in order to pull retrograde trains. Kinesin, on the other hand, has to be regulated in the opposite way. The motor needs to be inactivated at the ciliary tip to avoid competition with dynein in retrograde trains. The Lechtreck lab showed in *Chlamydomonas* that kinesins are almost never a cargo of retrograde IFT (Wingfield et al., 2017). This and other observations led to the proposal that kinesin is inactivated at the ciliary tip and passively diffuses back to the ciliary base. Diffusion rate could hence be a way to regulate cilia length by limiting the number of kinesin molecules available at the ciliary base (Chien et al., 2017). In *Drosophila* antennae chordotonal cilia vary in length. If the *Chlamydomonas* model of kinesin inactivation and passive diffusion applies to *Drosophila*, longer cilia should have more kinesin available at the ciliary base to compensate for the length of the cilium. Alternatively, less anterograde trains should be visible in longer cilia, because the diffusion would limit the amount of kinesin available to assemble anterograde trains at the ciliary base. *Drosophila* could hence be a good system to test generality of the models on IFT regulation developed in *Chlamydomonas*. This is, of course, under the assumption that all chordotonal cilia in the antenna have similar requirements for IFT. Beyond IFT dynamics, however, we still have very limited knowledge about the molecular events through which IFT contributes to ciliary maintenance. Additionally, it is not clear if IFT has similar or distinct roles in ciliogenesis versus maintenance.

Does IFT have different roles in ciliogenesis and cilia maintenance?

The results from the work on flagella maintenance in *Trypanosoma* (Fort et al., 2016) and my work here could be interpreted in the way

that IFT has different relevance for the cilium during biogenesis and maintenance. In both systems, in the absence of IFT no cilium is formed, whereas during maintenance, the axonemal structure does not show obvious defects. In *Trypanosoma,* tyrosinated tubulin (a marker for newly assembled microtubules) is absent from old flagella. This suggests that there is little to no tubulin turnover in *Trypanosoma* flagella (Sherwin et al., 1987). This is different to what is reported in *Chlamydomonas* where continuous tubulin turnover at the ciliary tip is required to maintain the cilium stable (Marshall and Rosenbaum, 2001). In *Drosophila* it is not clear whether tubulin turns over at the ciliary tip. The *Drosophila* cilium, however, might not need IFT88 for tubulin turnover as it was suggested that tubulin is transported by the anterograde IFT motor kinesin directly (Girotra et al., 2017). If tubulin transport does not require IFT88 then it is not clear why *Drosophila* cannot extend the ciliary axoneme in the absence of IFT88. The most parsimonious explanation seems to be that kinesin can only transport tubulin during ciliogenesis when IFT88 is present. Perhaps kinesin requires IFT88 to assemble into an active motor. After biogenesis is completed, similar to what Fort and colleagues suggested (Fort et al., 2016), the microtubules in *Drosophila* cilia might not undergo tubulin turnover anymore and are intrinsically stable. One way to address the issue would be to conduct fluorescence recovery after photobleaching (FRAP) experiments with GFP-labelled tubulin in the chordotonal cilia. It seems necessary to understand the dynamic properties of different cilia when comparing IFT in different species because the demands for transport might vary between species and also between ciliogenesis versus maintenance.

The observation that IFT is not required for maintenance of cilia structure and compartmentalisation in *Trypanosoma* and *Drosophila* was unexpected. In *Trypanosoma*, however, it was observed that

without IFT the flagella beat frequency is drastically reduced. This could not be explained by the loss of dynein arms, which bring about the motility in cilia and flagella (Fort et al., 2016). IFT88 must hence be required to maintain the activity of the dynein arms. Perhaps in *Trypanosoma* IFT88 is involved in transport of a signalling molecule that induces or coordinates flagella beating. Dynein arms are also required in chordotonal cilia in *Drosophila*, although it is not clear what kind of movement these cilia execute (Karak et al., 2015). From the *Trypanosoma* results it is not expected that dynein arms are maintained by IFT in *Drosophila.* The gravitaxis phenotype found here (Fig. 2.6) would thus not be caused by the loss of the motility apparatus, but instead by the loss of the signalling machinery coordinating cilia movement. This issue needs to be clarified, however, using electron microscopy.

Maintaining IFT transport should be energetically costly for the cells. It does not seem to be required, however, to maintain ciliary structure in *Trypanosoma* and *Drosophila*. This raises the question what other purposes IFT might have in a fully formed cilium. Several models have been put forward about the regulation of ciliary length in *Chlamydomonas*. One proposal is that the amount of tubulin loaded onto the IFT trains regulates the length of the cilium (Pan and Snell, 2014). Primary cilia can also shorten their length dynamically in responds to stimulation (Rich and Clark, 2012), which could be due to an increase in tubulin export from the cilium through IFT. Cilia length in turn was implicated in the regulation of the signalling capacity in some cilia (Lopes et al., 2010; Thompson et al., 2016). The results presented here, however, show that IFT has no role in length regulation in chordotonal cilia. This is probably because chordotonal cilia are held by a cap structure at the ciliary tip, which makes it quite unlikely that the cilia can change length in adaptation to changing stimuli. It is possible to imagine, however, that other

ciliary properties could be altered in chordotonal cilia in an adaptive process. Auditory chordotonal cilia usually respond best to a sound at a frequency around 160 Hz (Todi et al., 2004). Perhaps IFT could adapt the mechanical properties of the cells to change the best frequency according to environment. Although there is currently no evidence for plasticity in the system, it is certainly a feature that is worth exploring. In *Trypanosoma* it was shown that flagella beating adapts to the viscosity of the medium (Heddergott et al., 2012). IFT has not been implicated in this process, but it would be another interesting model to explore the role of IFT in cilia plasticity.

In order to understand the potential of IFT in regulating various different properties, it is important to know which cargos are transported by IFT and what other factors might determine their ciliary localisation. Next, I will discuss my results on ciliary transport of the evolutionarily conserved guanylyl cyclase CG34357.

A refined transport model for Gucy2d/CG34357 transport

Gucy2d (also GC-E) is a particulate guanlylyl cyclase required for cGMP production in the outer segment of human photoreceptors. Mutations in Gucy2d can lead to the retina-specific ciliopathy Leber congenital amaurosis (LCA) (den Hollander et al., 2008). The enzyme was shown to bind to IFT88 and to use IFT for transport to cilia (Bhowmick et al., 2009). IFT88, however, does not seem to be sufficient for transport of GC-E in mice, because in rhodopsin mutants, GC-E is lost from the photoreceptor outer segment (Pearring et al., 2015).

In the work presented here, I provided evidence that CG34357 is the *Drosophila* homologue of Gucy2d. Depletion of the protein from chordotonal neurons gives rise to a gravity sensing phenotype (Fig. 3.1 and 3.2). The protein localises to cilia (Fig. 3.4), and it binds

to DmIFT88/NompB in cultured cells. I identified a 200 amino acid binding site for DmIFT88/NompB on CG34357 (Fig. 3.8). Truncation experiments, however, suggest that binding to IFT88 is not sufficient to transport CG34357 to the cilia (Fig. 3.7). Interestingly, rhodopsin was found to be expressed in chordotonal neurons and to localise to cilia in *Drosophila* (Senthilan et al., 2012). It is therefore important to study the localisation of CG34357 in the absence of either DmIFT88/NompB or rhodopsin.

Analysis of a gene expression reporter of CG34357 suggests that the gene is also active in olfactory neurons, which are ciliated and express DmIFT88/NompB as well. Additionally, the gene is found active in non-ciliated sensory neurons (Fig. 3.3), but the localisation of the protein was not studied in those neurons here. Rhodopsins were also found in the transcriptome of olfactory sensory neurons in *Drosophila* (Shiao et al., 2013), but rhodopsins were never implicated in olfaction. My results, however, suggest that CG34357 might also localise to olfactory cilia in a similar fashion as in chordotonal cilia. How CG34357 localises in non-ciliated sensory neurons is not clear. Investigating the protein in different cell types might contribute to a more generalized understanding about the transport mechanism required for localisation of CG34357.

Sequence comparisons of Gucy2d/CG34357 between different species suggest that the DmIFT88/NompB-binding site is evolutionarily conserved. Mutations found in human patients with LCA might compromise binding to IFT88 and explain the disease phenotype through inefficient transport of the guanylyl cyclase (Fig. 3.10). The transport mechanism of the mutant protein is still open to investigation, but might be complicated by different layers of regulation. It is also not clear how the cyclase functions in chordotonal cilia. In the following I will speculate about possible mechanisms through which the protein might modulate cilia activity.

Role of CG34357 in chordotonal cilia function

Auditory chordotonal neurons are incredibly sensitive sound-receivers that can even detect vibrations near Brownian motion (Göpfert et al., 2005). This has been attributed to the ability of the neurons to adjust their mechanical properties according to the frequency at which they are stimulated (Albert and Göpfert, 2015). CG34357 could contribute to signal amplification in two ways. It could modify the mechanical properties of the cilium, or it could open additional ion channels in response to low-level stimulation. The mechanical properties of the chordotonal cilium are largely generated by the dynein arms (Karak et al., 2015). In the unicellular ciliate *Paramecium* a cGMP-dependent kinase was shown to phosphorylate ciliary dynein (Wyatt, 2015). Such a phosphorylation event could affect ciliary motility. In the chordotonal neurons CG34357 might adjust dynein arm activity in order to modulate the mechanical properties of the cilia. No cGMP-dependent kinase, however, was ever described in chordotonal cilia. Alternatively, CG34357 activity could open additional ion channels in response to an initial calcium influx. Calcium is known to regulate the activity of Gucy2d (Kuhn, 2016). Small initial increases in ciliary calcium levels might thus be amplified through opening of additional ion channels in a positive feedback loop. A cGMP-gated ion channel was found to be expressed in chordotonal neurons, but never further investigated in those cells (Marx et al., 1999).

The expression pattern of CG34357 in different ciliated cells (Fig. 3.3) makes it more likely, however, that CG34357 is involved in amplification or modulation of neuronal activity in general as opposed to amplifying ciliary signalling specifically in chordotonal cilia. In order to address this issue, it is important to identify the

molecules that respond to CG34357 activity in the different cells and characterize their mechanism of action.

The work presented here is the first example of an IFT cargo in *Drosophila*. Future efforts should extend the number of IFT cargoes in the fly more systematically to obtain a more complete picture of the functions that IFT executes in *Drosophila* cilia. A detailed analysis of IFT in the fruit fly might also yield novel insights into IFT in other species and in disease mechanisms. Additionally, research on the cilium as a confined compartment could lead to the development of broader theories about the role of structural and functional maintenance and turnover, as I discuss next.

Implications of findings for maintenance and turnover in general

When Keith Porter described ciliary microtubules in his Harvey lecture in 1956, he surely had a static picture of the ciliary cytoskeleton in mind (Satir, 2005). Tubulin dynamics in flagella were only visualized about 40 years later (Marshall and Rosenbaum, 2001). Today, owing to modern live imaging and proteomics techniques it is more and more appreciated how dynamic cellular compartments are. The giant muscle protein titin that organizes sarcomere structure was shown to undergo turnover and even components of the nuclear pore complex are replaced with time (da Silva Lopes et al., 2011; Toyama et al., 2013). Many aspects of cellular turnover are, however, still unclear. Turnover in a structure might be necessary for different reasons. Dynamicity in a structure might be required to replace building blocks to change properties of the overall structures. In muscle fibres for example myosin is replaced by different isoforms in response to stimulation in order to change the contractile properties of the muscle (Wisdom et al., 2015). This adaption through remodelling is hard to envision in static

structures. In a dynamic structure, however, this can be achieved without having to disassemble the entire structure. In the case of the muscle fibre this would mean that remodelling could take place while the muscle is continuously able to contract. Turnover of proteins is also important to remove functionally compromised molecules. In neurons it is established that turnover via protein transport is necessary to prevent accumulation of damaged proteins at the synapse. A lack of sufficient turnover results in neurodegeneration. Neuronal transport processes can even scale with neuronal activity (Sheehan et al., 2016).

Transport to and within specific cellular compartments is a vital aspect of the turnover of their components. Active transport becomes particularly important when protein synthesis and degradation are spatially separated from the place where the proteins execute their functions (e.g. in cilia or neuronal synapses). Understanding transport in cilia might hence help to develop models for other cellular compartments as well. The work from the Bastin lab (Fort et al., 2016) and my work presented here suggest that maintenance of structure and function might not be regulated in the same way or at least not on the same time scale. Function perhaps needs to be regulated faster than remodelling of the structure might allow. Many IFT cargos (at least during ciliary maintenance) should hence be modifiers of ciliary activity rather then structural elements. If that is the case then this should be reflected in the turnover of different ciliary components (i.e. structural versus functional components). It should be possible to perform pulse-chase experiments similar to what was done in mice followed by mass-spec analysis (Toyama et al., 2013) to obtain a more global picture of protein turnover in antennae. Ciliary proteins with high turnover are more likely to require IFT, which might also yield novel IFT cargos.

Final remarks

Robert Bloodgood said we entered the “Golden Age of Primary Cilia” (Bloodgood, 2009) and according to Peter Satir the transition was marked by the discovery of IFT (Satir, 2017). We have a solid understanding of the composition of the IFT complex, how it is assembled and how it moves along the cilium. Still, little is known about what functions it executes and when. The complex might also be regulated differently in biogenesis versus maintenance. Maintenance of a structure probably depends less on addition of building blocks than biogenesis. Perhaps the opposite is true for removal of building blocks. Furthermore, not all building blocks of a structure might require turnover at steady state. It is hence expected that transport needs to account for different requirements in maintenance as compared to biogenesis. This should also be reflected in the activity of the respective transport systems such as IFT. Through the use of modern technology we hopefully can extend the list of IFT cargos in the future and obtain deeper insights into the role and composition of IFT in cilia maintenance and plasticity. Studying IFT will hopefully also guide findings regarding plasticity and maintenance (and their limitations) of other cellular structures.

References

Afzelius, B.A., 1976. A human syndrome caused by immotile cilia. Science 193, 317–319.

Akhmanova, A., Steinmetz, M.O., 2015. Control of microtubule organization and dynamics: two ends in the limelight. Nat. Rev. Mol. Cell Biol. 16, 711–726.

Al Jord, A., Lemaître, A.-I., Delgehyr, N., Faucourt, M., Spassky, N., Meunier, A., 2014. Centriole amplification by mother and daughter centrioles differs in multiciliated cells. Nature 516, 104–107.

Albert, J.T., Göpfert, M.C., 2015. Hearing in Drosophila. Curr. Opin. Neurobiol. 34, 79–85.

Albert, J.T., Nadrowski, B., Kamikouchi, A., Gopfert, M.C., 2006. Mechanical tracing of protein function in the Drosophila ear. Protoc. Exch.

Allan, R.K., Ratajczak, T., 2011. Versatile TPR domains accommodate different modes of target protein recognition and function. Cell Stress Chaperones 16, 353–367.

Altschul, S.F., Madden, T.L., Schäffer, A.A., Zhang, J., Zhang, Z., Miller, W., Lipman, D.J., 1997. Gapped BLAST and PSI-BLAST: a new generation of protein database search programs. Nucleic Acids Res. 25, 3389–3402.

Andersen, J.S., Wilkinson, C.J., Mayor, T., Mortensen, P., Nigg, E.A., Mann, M., 2003. Proteomic characterization of the human centrosome by protein correlation profiling. Nature 426, 570–574.

Aparicio, J.G., Applebury, M.L., 1996. The photoreceptor guanylate cyclase is an autophosphorylating protein kinase. J. Biol. Chem. 271, 27083–27089.

Aradska, J., Bulat, T., Sialana, F.J., Birner-Gruenberger, R., Erich, B., Lubec, G., 2015. Gel-free mass spectrometry analysis of Drosophila melanogaster heads. Proteomics 15, 3356–3360.

Astuti, G.D.N., Bertelsen, M., Preising, M.N., Ajmal, M., Lorenz, B., Faradz, S.M.H., Qamar, R., Collin, R.W.J., Rosenberg, T., Cremers, F.P.M., 2016. Comprehensive genotyping reveals RPE65 as the most frequently mutated gene in Leber congenital amaurosis in Denmark. Eur. J. Hum. Genet. EJHG 24, 1071–1079.

Avasthi, P., Marshall, W.F., 2012. Stages of ciliogenesis and regulation of ciliary length. Differ. Res. Biol. Divers. 83, S30-42.

Avidor-Reiss, T., Ha, A., Basiri, M.L., 2017. Transition Zone Migration: A Mechanism for Cytoplasmic Ciliogenesis and Postaxonemal Centriole Elongation. Cold Spring Harb. Perspect. Biol.

Avidor-Reiss, T., Maer, A.M., Koundakjian, E., Polyanovsky, A., Keil, T., Subramaniam, S., Zuker, C.S., 2004. Decoding cilia function: defining specialized genes required for compartmentalized cilia biogenesis. Cell 117, 527–539.

Azimzadeh, J., Wong, M.L., Downhour, D.M., Sánchez Alvarado, A., Marshall, W.F., 2012. Centrosome loss in the evolution of planarians. Science 335, 461–463.

Baehr, W., 2014. Membrane Protein Transport in Photoreceptors: The Function of PDEδ. Invest. Ophthalmol. Vis. Sci. 55, 8653–8666.

Baehr, W., Karan, S., Maeda, T., Luo, D.-G., Li, S., Bronson, J.D., Watt, C.B., Yau, K.-W., Frederick, J.M., Palczewski, K., 2007. The function of guanylate cyclase 1 and guanylate cyclase 2 in rod and cone photoreceptors. J. Biol. Chem. 282, 8837–8847

Balestra, F.R., Strnad, P., Flückiger, I., Gönczy, P., 2013. Discovering regulators of centriole biogenesis through

siRNA-based functional genomics in human cells. Dev. Cell 25, 555–571.

Balmer, S., Dussert, A., Collu, G.M., Benitez, E., Iomini, C., Mlodzik, M., 2015. Components of Intraflagellar Transport complex A (IFT-A) function independently of the cilium to regulate canonical Wnt signaling in Drosophila. Dev. Cell 34, 705–718.

Bangs, F., Anderson, K.V., 2017. Primary Cilia and Mammalian Hedgehog Signaling. Cold Spring Harb. Perspect. Biol. 9.

Basiri, M.L., Ha, A., Chadha, A., Clark, N.M., Polyanovsky, A., Cook, B., Avidor-Reiss, T., 2014. A migrating ciliary gate compartmentalizes the site of axoneme assembly in Drosophila spermatids. Curr. Biol. CB 24, 2622–2631.

Bayless, B.A., Giddings, T.H., Jr, Winey, M., Pearson, C.G., 2012. Bld10/Cep135 stabilizes basal bodies to resist cilia-generated forces. Mol. Biol. Cell 23, 4820–4832.

Bazzi, H., Anderson, K.V., 2014. Acentriolar mitosis activates a p53-dependent apoptosis pathway in the mouse embryo. Proc. Natl. Acad. Sci. U. S. A. 111, E1491–E1500.

Bechstedt, S., Albert, J.T., Kreil, D.P., Müller-Reichert, T., Göpfert, M.C., Howard, J., 2010. A doublecortin containing microtubule-associated protein is implicated in mechanotransduction in Drosophila sensory cilia. Nat. Commun. 1, 1–11.

Besharse, J.C., Hollyfield, J.G., 1979. Turnover of mouse photoreceptor outer segments in constant light and darkness. Invest. Ophthalmol. Vis. Sci. 18, 1019–1024.

Besschetnova, T.Y., Kolpakova-Hart, E., Guan, Y., Zhou, J., Olsen, B.R., Shah, J.V., 2010. Identification of signaling pathways

regulating primary cilium length and flow-mediated adaptation. Curr. Biol. CB 20, 182–187.

Bhogaraju, S., Cajanek, L., Fort, C., Blisnick, T., Weber, K., Taschner, M., Mizuno, N., Lamla, S., Bastin, P., Nigg, E.A., Lorentzen, E., 2013. Molecular basis of tubulin transport within the cilium by IFT74 and IFT81. Science 341, 1009–1012.

Bhowmick, R., Li, M., Sun, J., Baker, S.A., Insinna, C., Besharse, J.C., 2009. Photoreceptor IFT complexes containing chaperones, guanylyl cyclase 1 and rhodopsin. Traffic Cph. Den. 10, 648–663.

Bloodgood, R.A., 2009. From central to rudimentary to primary: the history of an underappreciated organelle whose time has come. The primary cilium. Methods Cell Biol. 94, 3–52.

Bloodgood, R.A., 1977. Motility occurring in association with the surface of the Chlamydomonas flagellum. J. Cell Biol. 75, 983–989.

Boekhoff-Falk, G., Eberl, D.F., 2014. The Drosophila auditory system. Wiley Interdiscip. Rev. Dev. Biol. 3, 179–191.

Boldt, K., Mans, D.A., Won, J., van Reeuwijk, J., Vogt, A., Kinkl, N., Letteboer, S.J.F., Hicks, W.L., Hurd, R.E., Naggert, J.K., Texier, Y., den Hollander, A.I., Koenekoop, R.K., Bennett, J., Cremers, F.P.M., Gloeckner, C.J., Nishina, P.M., Roepman, R., Ueffing, M., 2011. Disruption of intraflagellar protein transport in photoreceptor cilia causes Leber congenital amaurosis in humans and mice. J. Clin. Invest. 121, 2169–2180.

Borrego-Pinto, J., Somogyi, K., Karreman, M.A., König, J., Müller-Reichert, T., Bettencourt-Dias, M., Gönczy, P., Schwab, Y., Lénárt, P., 2016. Distinct mechanisms eliminate mother and

daughter centrioles in meiosis of starfish oocytes. J. Cell Biol. 212, 815–827.

Bosch Grau, M., Masson, C., Gadadhar, S., Rocha, C., Tort, O., Marques Sousa, P., Vacher, S., Bieche, I., Janke, C., 2017. Alterations in the balance of tubulin glycylation and glutamylation in photoreceptors leads to retinal degeneration. J. Cell Sci. 130, 938–949.

Boveri, T., 2008. Concerning the origin of malignant tumours by Theodor Boveri. Translated and annotated by Henry Harris. J. Cell Sci. 121 Suppl 1, 1–84. doi:10.1242/jcs.025742

Brancati, F., Dallapiccola, B., Valente, E.M., 2010. Joubert Syndrome and related disorders. Orphanet J. Rare Dis. 5, 20.

Brand, A.H., Perrimon, N., 1993. Targeted gene expression as a means of altering cell fates and generating dominant phenotypes. Dev. Camb. Engl. 118, 401–415.

Braun, D.A., Hildebrandt, F., 2017. Ciliopathies. Cold Spring Harb. Perspect. Biol. 9.

Buisson, J., Chenouard, N., Lagache, T., Blisnick, T., Olivo-Marin, J.-C., Bastin, P., 2013. Intraflagellar transport proteins cycle between the flagellum and its base. J. Cell Sci. 126, 327–338.

Busskamp, V., Krol, J., Nelidova, D., Daum, J., Szikra, T., Tsuda, B., Jüttner, J., Farrow, K., Scherf, B.G., Alvarez, C.P.P., Genoud, C., Sothilingam, V., Tanimoto, N., Stadler, M., Seeliger, M., Stoffel, M., Filipowicz, W., Roska, B., 2014. miRNAs 182 and 183 Are Necessary to Maintain Adult Cone Photoreceptor Outer Segments and Visual Function. Neuron 83, 586–600.

Carvalho-Santos, Z., Azimzadeh, J., Pereira-Leal, J.B., Bettencourt-Dias, M., 2011. Evolution: Tracing the origins of centrioles, cilia, and flagella. J. Cell Biol. 194, 165–175.

Celniker, S.E., Dillon, L.A.L., Gerstein, M.B., Gunsalus, K.C., Henikoff, S., Karpen, G.H., Kellis, M., Lai, E.C., Lieb, J.D., MacAlpine, D.M., Micklem, G., Piano, F., Snyder, M., Stein, L., White, K.P., Waterston, R.H., modENCODE Consortium, 2009. Unlocking the secrets of the genome. Nature 459, 927–930.

Chen, C.-T., Hehnly, H., Yu, Q., Farkas, D., Zheng, G., Redick, S.D., Hung, H.-F., Samtani, R., Jurczyk, A., Akbarian, S., Wise, C., Jackson, A., Bober, M., Guo, Y., Lo, C., Doxsey, S., 2014. A unique set of centrosome proteins requires Pericentrin for spindle-pole localization and spindle orientation. Curr. Biol. CB 24, 2327–2334.

Chien, A., Shih, S.M., Bower, R., Tritschler, D., Porter, M.E., Yildiz, A., 2017. Dynamics of the IFT machinery at the ciliary tip. eLife 6.

Choksi, S.P., Lauter, G., Swoboda, P., Roy, S., 2014. Switching on cilia: transcriptional networks regulating ciliogenesis. Dev. Camb. Engl. 141, 1427–1441.

Chrisman, T.D., Garbers, D.L., Parks, M.A., Hardman, J.G., 1975. Characterization of particulate and soluble guanylate cyclases from rat lung. J. Biol. Chem. 250, 374–381.

Christensen, S.T., Morthorst, S.K., Mogensen, J.B., Pedersen, L.B., 2017. Primary Cilia and Coordination of Receptor Tyrosine Kinase (RTK) and Transforming Growth Factor β (TGF-β) Signaling. Cold Spring Harb. Perspect. Biol. 9.

Christensen, S.T., Pedersen, L.B., Schneider, L., Satir, P., 2007. Sensory cilia and integration of signal transduction in human health and disease. Traffic Cph. Den. 8, 97–109.

Clare, D.K., Magescas, J., Piolot, T., Dumoux, M., Vesque, C., Pichard, E., Dang, T., Duvauchelle, B., Poirier, F., Delacour,

D., 2014. Basal foot MTOC organizes pillar MTs required for coordination of beating cilia. Nat. Commun. 5, ncomms5888.

Cole, D.G., Diener, D.R., Himelblau, A.L., Beech, P.L., Fuster, J.C., Rosenbaum, J.L., 1998. Chlamydomonas kinesin-II-dependent intraflagellar transport (IFT): IFT particles contain proteins required for ciliary assembly in Caenorhabditis elegans sensory neurons. J. Cell Biol. 141, 993–1008.

Coppieters, F., Casteels, I., Meire, F., De Jaegere, S., Hooghe, S., van Regemorter, N., Van Esch, H., Matuleviciene, A., Nunes, L., Meersschaut, V., Walraedt, S., Standaert, L., Coucke, P., Hoeben, H., Kroes, H.Y., Vande Walle, J., de Ravel, T., Leroy, B.P., De Baere, E., 2010. Genetic screening of LCA in Belgium: predominance of CEP290 and identification of potential modifier alleles in AHI1 of CEP290-related phenotypes. Hum. Mutat. 31, E1709-1766.

da Silva Lopes, K., Pietas, A., Radke, M.H., Gotthardt, M., 2011. Titin visualization in real time reveals an unexpected level of mobility within and between sarcomeres. J. Cell Biol. 193, 785–798.

Davenport, J.R., Watts, A.J., Roper, V.C., Croyle, M.J., van Groen, T., Wyss, J.M., Nagy, T.R., Kesterson, R.A., Yoder, B.K., 2007. Disruption of intraflagellar transport in adult mice leads to obesity and slow-onset cystic kidney disease. Curr. Biol. CB 17, 1586–1594.

de Castro-Miró, M., Pomares, E., Lorés-Motta, L., Tonda, R., Dopazo, J., Marfany, G., Gonzàlez-Duarte, R., 2014. Combined genetic and high-throughput strategies for molecular diagnosis of inherited retinal dystrophies. PloS One 9, e88410.

Delaval, B., Bright, A., Lawson, N.D., Doxsey, S., 2011. The cilia protein IFT88 is required for spindle orientation in mitosis. Nat. Cell Biol. 13, 461–468.

Delgehyr, N., Sillibourne, J., Bornens, M., 2005. Microtubule nucleation and anchoring at the centrosome are independent processes linked by ninein function. J. Cell Sci. 118, 1565–1575.

Dell, K.R., Vale, R.D., 2004. A tribute to Shinya Inoue and innovation in light microscopy. J. Cell Biol. 165, 21–25.

Delling, M., Indzhykulian, A.A., Liu, X., Li, Y., Xie, T., Corey, D.P., Clapham, D.E., 2016. Primary cilia are not calcium-responsive mechanosensors. Nature 531, 656–660.

den Hollander, A.I., Roepman, R., Koenekoop, R.K., Cremers, F.P.M., 2008. Leber congenital amaurosis: genes, proteins and disease mechanisms. Prog. Retin. Eye Res. 27, 391–419.

Dietzl, G., Chen, D., Schnorrer, F., Su, K.-C., Barinova, Y., Fellner, M., Gasser, B., Kinsey, K., Oppel, S., Scheiblauer, S., Couto, A., Marra, V., Keleman, K., Dickson, B.J., 2007. A genome-wide transgenic RNAi library for conditional gene inactivation in Drosophila. Nature 448, 151–156.

Dobbelaere, J., Josué, F., Suijkerbuijk, S., Baum, B., Tapon, N., Raff, J., 2008. A genome-wide RNAi screen to dissect centriole duplication and centrosome maturation in Drosophila. PLoS Biol. 6, e224.

Dobell, C., Leeuwenhoek, A. van, 1932. Antony van Leeuwenhoek and his “Little animals”; being some account of the father of protozoology and bacteriology and his multifarious discoveries in these disciplines; New York, Harcourt, Brace and company.

Dubruille, R., Laurençon, A., Vandaele, C., Shishido, E., Coulon-Bublex, M., Swoboda, P., Couble, P., Kernan, M., Durand, B., 2002. Drosophila regulatory factor X is necessary for ciliated sensory neuron differentiation. Dev. Camb. Engl. 129, 5487–5498.

Dutcher, S.K., 2003. Long-lost relatives reappear: identification of new members of the tubulin superfamily. Curr. Opin. Microbiol. 6, 634–640.

Edgar, R.C., 2004. MUSCLE: multiple sequence alignment with high accuracy and high throughput. Nucleic Acids Res. 32, 1792–1797.

Eguether, T., San Agustin, J.T., Keady, B.T., Jonassen, J.A., Liang, Y., Francis, R., Tobita, K., Johnson, C.A., Abdelhamed, Z.A., Lo, C.W., Pazour, G.J., 2014. IFT27 links the BBSome to IFT for maintenance of the ciliary signaling compartment. Dev. Cell 31, 279–290.

Eriksson, J.E., Dechat, T., Grin, B., Helfand, B., Mendez, M., Pallari, H.-M., Goldman, R.D., 2009. Introducing intermediate filaments: from discovery to disease. J. Clin. Invest. 119, 1763–1771.

Falk, S., Bugeon, S., Ninkovic, J., Pilz, G.-A., Postiglione, M.P., Cremer, H., Knoblich, J.A., Götz, M., 2017. Time-Specific Effects of Spindle Positioning on Embryonic Progenitor Pool Composition and Adult Neural Stem Cell Seeding. Neuron 93, 777–791.e3.

Fan, Z.-C., Behal, R.H., Geimer, S., Wang, Z., Williamson, S.M., Zhang, H., Cole, D.G., Qin, H., 2010. Chlamydomonas IFT70/CrDYF-1 is a core component of IFT particle complex B and is required for flagellar assembly. Mol. Biol. Cell 21, 2696–2706.

Farina, F., Gaillard, J., Guérin, C., Couté, Y., Sillibourne, J., Blanchoin, L., Théry, M., 2016. The centrosome is an actin-organizing centre. Nat. Cell Biol. 18, 65–75.

Fletcher, D.A., Mullins, R.D., 2010. Cell mechanics and the cytoskeleton. Nature 463, 485–492. doi:10.1038/nature08908

Fong, C.S., Mazo, G., Das, T., Goodman, J., Kim, M., O'Rourke, B.P., Izquierdo, D., Tsou, M.-F.B., 2016. 53BP1 and USP28 mediate p53-dependent cell cycle arrest in response to centrosome loss and prolonged mitosis. eLife 5.

Fort, C., Bonnefoy, S., Kohl, L., Bastin, P., 2016. Intraflagellar transport is required for the maintenance of the trypanosome flagellum composition but not its length. J. Cell Sci. 129, 3026–3041.

Fu, W., Asp, P., Canter, B., Dynlacht, B.D., 2014. Primary cilia control hedgehog signaling during muscle differentiation and are deregulated in rhabdomyosarcoma. Proc. Natl. Acad. Sci. U. S. A. 111, 9151–9156.

Gabriel, E., Ramani, A., Karow, U., Gottardo, M., Natarajan, K., Gooi, L.M., Goranci-Buzhala, G., Krut, O., Peters, F., Nikolic, M., Kuivanen, S., Korhonen, E., Smura, T., Vapalahti, O., Papantonis, A., Schmidt-Chanasit, J., Riparbelli, M., Callaini, G., Krönke, M., Utermöhlen, O., Gopalakrishnan, J., 2017. Recent Zika Virus Isolates Induce Premature Differentiation of Neural Progenitors in Human Brain Organoids. Cell Stem Cell 20, 397–406.e5.

Gadadhar, S., Bodakuntla, S., Natarajan, K., Janke, C., 2017. The tubulin code at a glance. J. Cell Sci. 130, 1347–1353.

Ganem, N.J., Godinho, S.A., Pellman, D., 2009. A mechanism linking extra centrosomes to chromosomal instability. Nature 460, 278–282.

Garcia, G., Reiter, J.F., 2016. A primer on the mouse basal body. Cilia 5, 17.

Girotra, M., Srivastava, S., Kulkarni, A., Barbora, A., Bobra, K., Ghosal, D., Devan, P., Aher, A., Jain, A., Panda, D., Ray, K., 2017. The C-terminal tails of heterotrimeric kinesin-2 motor subunits directly bind to α-tubulin1: Possible implications for cilia-specific tubulin entry. Traffic Cph. Den. 18, 123–133.

Godinho, S.A., 2014. Centrosome amplification and cancer: Branching out. Mol. Cell. Oncol. 2, e993252.

Godinho, S.A., Picone, R., Burute, M., Dagher, R., Su, Y., Leung, C.T., Polyak, K., Brugge, J.S., Théry, M., Pellman, D., 2014. Oncogene-like induction of cellular invasion from centrosome amplification. Nature 510, 167–171.

Gönczy, P., Echeverri, C., Oegema, K., Coulson, A., Jones, S.J., Copley, R.R., Duperon, J., Oegema, J., Brehm, M., Cassin, E., Hannak, E., Kirkham, M., Pichler, S., Flohrs, K., Goessen, A., Leidel, S., Alleaume, A.M., Martin, C., Ozlü, N., Bork, P., Hyman, A.A., 2000. Functional genomic analysis of cell division in C. elegans using RNAi of genes on chromosome III. Nature 408, 331–336.

Gong, Z., Son, W., Chung, Y.D., Kim, J., Shin, D.W., McClung, C.A., Lee, Y., Lee, H.W., Chang, D.-J., Kaang, B.-K., Cho, H., Oh, U., Hirsh, J., Kernan, M.J., Kim, C., 2004a. Two interdependent TRPV channel subunits, inactive and Nanchung, mediate hearing in Drosophila. J. Neurosci. Off. J. Soc. Neurosci. 24, 9059–9066.

Gong, Z., Son, W., Chung, Y.D., Kim, J., Shin, D.W., McClung, C.A., Lee, Y., Lee, H.W., Chang, D.-J., Kaang, B.-K., Cho, H., Oh, U., Hirsh, J., Kernan, M.J., Kim, C., 2004b. Two interdependent TRPV channel subunits, inactive and

Nanchung, mediate hearing in Drosophila. J. Neurosci. Off. J. Soc. Neurosci. 24, 9059–9066.

Göpfert, M.C., Humphris, A.D.L., Albert, J.T., Robert, D., Hendrich, O., 2005. Power gain exhibited by motile mechanosensory neurons in Drosophila ears. Proc. Natl. Acad. Sci. U. S. A. 102, 325–330.

Goshima, G., Wollman, R., Goodwin, S.S., Zhang, N., Scholey, J.M., Vale, R.D., Stuurman, N., 2007. Genes required for mitotic spindle assembly in Drosophila S2 cells. Science 316, 417–421.

Goto, H., Inaba, H., Inagaki, M., 2017. Mechanisms of ciliogenesis suppression in dividing cells. Cell. Mol. Life Sci. CMLS 74, 881–890.

Gottardo, M., Callaini, G., Riparbelli, M.G., 2015. The Drosophila centriole – conversion of doublets into triplets within the stem cell niche. J Cell Sci 128, 2437–2442.

Gradilone, S.A., Radtke, B.N., Bogert, P.S., Huang, B.Q., Gajdos, G.B., LaRusso, N.F., 2013. HDAC6 inhibition restores ciliary expression and decreases tumor growth. Cancer Res. 73, 2259–2270.

Gradstein, L., Zolotushko, J., Sergeev, Y.V., Lavy, I., Narkis, G., Perez, Y., Guigui, S., Sharon, D., Banin, E., Walter, E., Lifshitz, T., Birk, O.S., 2016. Novel GUCY2D mutation causes phenotypic variability of Leber congenital amaurosis in a large kindred. BMC Med. Genet. 17, 52.

Green, E.W., Fedele, G., Giorgini, F., Kyriacou, C.P., 2014. A Drosophila RNAi collection is subject to dominant phenotypic effects. Nat. Methods 11, 222–223.

Grotewiel, M.S., Martin, I., Bhandari, P., Cook-Wiens, E., 2005. Functional senescence in Drosophila melanogaster. Ageing Res. Rev. 4, 372–397.

Guichard, P., Hachet, V., Majubu, N., Neves, A., Demurtas, D., Olieric, N., Fluckiger, I., Yamada, A., Kihara, K., Nishida, Y., Moriya, S., Steinmetz, M.O., Hongoh, Y., Gönczy, P., 2013. Native architecture of the centriole proximal region reveals features underlying its 9-fold radial symmetry. Curr. Biol. CB 23, 1620–1628.

Hall, J.L., Luck, D.J., 1995. Basal body-associated DNA: in situ studies in Chlamydomonas reinhardtii. Proc. Natl. Acad. Sci. U. S. A. 92, 5129–5133.

Hall, J.L., Ramanis, Z., Luck, D.J., 1989. Basal body/centriolar DNA: molecular genetic studies in Chlamydomonas. Cell 59, 121–132.

Han, Y.-G., Kim, H.J., Dlugosz, A.A., Ellison, D.W., Gilbertson, R.J., Alvarez-Buylla, A., 2009. Dual and opposing roles of primary cilia in medulloblastoma development. Nat. Med. 15, 1062–

Han, Y.-G., Kwok, B.H., Kernan, M.J., 2003. Intraflagellar transport is required in Drosophila to differentiate sensory cilia but not sperm. Curr. Biol. CB 13, 1679–1686.

Hancock, W.O., 2015. Aging Gracefully: A New Model of Microtubule Growth and Catastrophe. Biophys. J. 109, 2449–2451.

Harris, J.A., Liu, Y., Yang, P., Kner, P., Lechtreck, K.F., 2016. Single-particle imaging reveals intraflagellar transport-independent transport and accumulation of EB1 in Chlamydomonas flagella. Mol. Biol. Cell 27, 295–307.

Harris, J.R., 2015. Transmission electron microscopy in molecular structural biology: A historical survey. Arch. Biochem. Biophys. 581, 3–18.

Hayashi, S., Ito, K., Sado, Y., Taniguchi, M., Akimoto, A., Takeuchi, H., Aigaki, T., Matsuzaki, F., Nakagoshi, H., Tanimura, T., Ueda, R., Uemura, T., Yoshihara, M., Goto, S., 2002. GETDB, a database compiling expression patterns and

molecular locations of a collection of Gal4 enhancer traps. Genes. N. Y. N 2000 34, 58–61.

He, M., Subramanian, R., Bangs, F., Omelchenko, T., Liem, K.F., Kapoor, T.M., Anderson, K.V., 2014. The kinesin-4 protein Kif7 regulates mammalian Hedgehog signalling by organizing the cilium tip compartment. Nat. Cell Biol. 16, 663–672.

Heddergott, N., Krüger, T., Babu, S.B., Wei, A., Stellamanns, E., Uppaluri, S., Pfohl, T., Stark, H., Engstler, M., 2012. Trypanosome Motion Represents an Adaptation to the Crowded Environment of the Vertebrate Bloodstream. PLoS Pathog. 8.

Herrmann, H., Strelkov, S.V., 2011. History and phylogeny of intermediate filaments: Now in insects. BMC Biol. 9, 16.

Hirono, M., 2014. Cartwheel assembly. Phil Trans R Soc B 369, 20130458.

Hodges, M.E., Scheumann, N., Wickstead, B., Langdale, J.A., Gull, K., 2010. Reconstructing the evolutionary history of the centriole from protein components. J. Cell Sci. 123, 1407–1413.

Hosono, K., Harada, Y., Kurata, K., Hikoya, A., Sato, M., Minoshima, S., Hotta, Y., 2015. Novel GUCY2D Gene Mutations in Japanese Male Twins with Leber Congenital Amaurosis. J. Ophthalmol. 2015, 693468.

Housden, B.E., Muhar, M., Gemberling, M., Gersbach, C.A., Stainier, D.Y.R., Seydoux, G., Mohr, S.E., Zuber, J., Perrimon, N., 2017. Loss-of-function genetic tools for animal models: cross-species and cross-platform differences. Nat. Rev. Genet. 18, 24–40.

Howe, K., FitzHarris, G., 2013. A non-canonical mode of microtubule organization operates throughout pre-implantation development in mouse. Cell Cycle 12, 1616–1624.

Hsu, K.-S., Chuang, J.-Z., Sung, C.-H., 2017. The Biology of Ciliary Dynamics. Cold Spring Harb. Perspect. Biol. 9.

Hu, Q., Milenkovic, L., Jin, H., Scott, M.P., Nachury, M.V., Spiliotis, E.T., Nelson, W.J., 2010. A septin diffusion barrier at the base of the primary cilium maintains ciliary membrane protein distribution. Science 329, 436–439.

Huang, B., Rifkin, M.R., Luck, D.J., 1977. Temperature-sensitive mutations affecting flagellar assembly and function in Chlamydomonas reinhardtii. J. Cell Biol. 72, 67–85.

Huang, P., Schier, A.F., 2009. Dampened Hedgehog signaling but normal Wnt signaling in zebrafish without cilia. Dev. Camb. Engl. 136, 3089–3098.

Huangfu, D., Liu, A., Rakeman, A.S., Murcia, N.S., Niswander, L., Anderson, K.V., 2003. Hedgehog signalling in the mouse requires intraflagellar transport proteins. Nature 426, 83–87.

Huber, F., Boire, A., López, M.P., Koenderink, G.H., 2015. Cytoskeletal crosstalk: when three different personalities team up. Curr. Opin. Cell Biol. 32, 39–47.

Inagaki, H.K., Kamikouchi, A., Ito, K., 2010. Methods for quantifying simple gravity sensing in Drosophila melanogaster. Nat. Protoc. 5, 20–25.

Iomini, C., Li, L., Esparza, J.M., Dutcher, S.K., 2009. Retrograde Intraflagellar Transport Mutants Identify Complex A Proteins With Multiple Genetic Interactions in Chlamydomonas reinhardtii. Genetics 183, 885–896.

Ishikawa, H., Ide, T., Yagi, T., Jiang, X., Hirono, M., Sasaki, H., Yanagisawa, H., Wemmer, K.A., Stainier, D.Y., Qin, H., Kamiya, R., Marshall, W.F., 2014. TTC26/DYF13 is an intraflagellar transport protein required for transport of motility-related proteins into flagella. eLife 3, e01566.

Ishikawa, H., Thompson, J., Yates, J.R., 3rd, Marshall, W.F., 2012. Proteomic analysis of mammalian primary cilia. Curr. Biol. CB 22, 414–419.

Izquierdo, D., Wang, W.-J., Uryu, K., Tsou, M.-F.B., 2014. Stabilization of Cartwheel-less Centrioles for Duplication Requires CEP295-Mediated Centriole-to-Centrosome Conversion. Cell Rep. 8, 957–965.

Jacobson, S.G., Cideciyan, A.V., Peshenko, I.V., Sumaroka, A., Olshevskaya, E.V., Cao, L., Schwartz, S.B., Roman, A.J., Olivares, M.B., Sadigh, S., Yau, K.-W., Heon, E., Stone, E.M., Dizhoor, A.M., 2013. Determining consequences of retinal membrane guanylyl cyclase (RetGC1) deficiency in human Leber congenital amaurosis en route to therapy: residual cone-photoreceptor vision correlates with biochemical properties of the mutants. Hum. Mol. Genet. 22, 168–183.

Jakobsen, L., Vanselow, K., Skogs, M., Toyoda, Y., Lundberg, E., Poser, I., Falkenby, L.G., Bennetzen, M., Westendorf, J., Nigg, E.A., Uhlen, M., Hyman, A.A., Andersen, J.S., 2011. Novel asymmetrically localizing components of human centrosomes identified by complementary proteomics methods. EMBO J. 30, 1520–1535.

Jana, S.C., Girotra, M., Ray, K., 2011. Heterotrimeric kinesin-II is necessary and sufficient to promote different stepwise assembly of morphologically distinct bipartite cilia in Drosophila antenna. Mol. Biol. Cell 22, 769–781.

Jana, S.C., Mendonça, S., Werner, S., Bettencourt-Dias, M., 2016. Methods to Study Centrosomes and Cilia in Drosophila. Methods Mol. Biol. Clifton NJ 1454, 215–236.

Jarman, A.P., Groves, A.K., 2013. The role of Atonal transcription factors in the development of mechanosensitive cells. Semin. Cell Dev. Biol. 24, 438–447.

Jékely, G., Arendt, D., 2006. Evolution of intraflagellar transport from coated vesicles and autogenous origin of the eukaryotic cilium. BioEssays News Rev. Mol. Cell. Dev. Biol. 28, 191–198.

Jenett, A., Rubin, G.M., Ngo, T.-T.B., Shepherd, D., Murphy, C., Dionne, H., Pfeiffer, B.D., Cavallaro, A., Hall, D., Jeter, J., Iyer, N., Fetter, D., Hausenfluck, J.H., Peng, H., Trautman, E.T., Svirskas, R., Myers, E.W., Iwinski, Z.R., Aso, Y., DePasquale, G.M., Enos, A., Hulamm, P., Lam, S.C.B., Li, H.-H., Laverty, T.R., Long, F., Qu, L., Murphy, S.D., Rokicki, K., Safford, T., Shaw, K., Simpson, J.H., Sowell, A., Tae, S., Yu, Y., Zugates, C.T., 2012. A GAL4-Driver Line Resource for Drosophila Neurobiology. Cell Rep. 2, 991–1001.

Jensen, V.L., Carter, S., Sanders, A.A.W.M., Li, C., Kennedy, J., Timbers, T.A., Cai, J., Scheidel, N., Kennedy, B.N., Morin, R.D., Leroux, M.R., Blacque, O.E., 2016. Whole-Organism Developmental Expression Profiling Identifies RAB-28 as a Novel Ciliary GTPase Associated with the BBSome and Intraflagellar Transport. PLoS Genet. 12, e1006469.

Jiang, L., Wei, Y., Ronquillo, C.C., Marc, R.E., Yoder, B.K., Frederick, J.M., Baehr, W., 2015. Heterotrimeric kinesin-2 (KIF3) mediates transition zone and axoneme formation of mouse photoreceptors. J. Biol. Chem. 290, 12765–12778.

Jinda, W., Taylor, T.D., Suzuki, Y., Thongnoppakhun, W., Limwongse, C., Lertrit, P., Suriyaphol, P., Trinavarat, A., Atchaneeyasakul, L., 2014. Whole exome sequencing in Thai patients with retinitis pigmentosa reveals novel mutations in six genes. Invest. Ophthalmol. Vis. Sci. 55, 2259–2268.

Johnson, J.-L.F., Leroux, M.R., 2010. cAMP and cGMP signaling: sensory systems with prokaryotic roots adopted by eukaryotic cilia. Trends Cell Biol. 20, 435–444.

Kalra, H., Drummen, G.P.C., Mathivanan, S., 2016. Focus on Extracellular Vesicles: Introducing the Next Small Big Thing. Int. J. Mol. Sci. 17.

Kamath, R.S., Fraser, A.G., Dong, Y., Poulin, G., Durbin, R., Gotta, M., Kanapin, A., Le Bot, N., Moreno, S., Sohrmann, M., Welchman, D.P., Zipperlen, P., Ahringer, J., 2003. Systematic functional analysis of the Caenorhabditis elegans genome using RNAi. Nature 421, 231–237.

Kamikouchi, A., Inagaki, H.K., Effertz, T., Hendrich, O., Fiala, A., Göpfert, M.C., Ito, K., 2009. The neural basis of Drosophila gravity-sensing and hearing. Nature 458, 165–171.

Karak, S., Jacobs, J.S., Kittelmann, M., Spalthoff, C., Katana, R., Sivan-Loukianova, E., Schon, M.A., Kernan, M.J., Eberl, D.F., Göpfert, M.C., 2015. Diverse Roles of Axonemal Dyneins in *Drosophila* Auditory Neuron Function and Mechanical Amplification in Hearing. Sci. Rep. 5, srep17085.

Karan, S., Tam, B.M., Moritz, O.L., Baehr, W., 2011. Targeting of mouse guanylate cyclase 1 (Gucy2e) to Xenopus laevis rod outer segments. Vision Res. 51, 2304–2311.

Karpenahalli, M.R., Lupas, A.N., Söding, J., 2007. TPRpred: a tool for prediction of TPR-, PPR- and SEL1-like repeats from protein sequences. BMC Bioinformatics 8, 2.

Karsenti, E., 2008. Self-organization in cell biology: a brief history. Nat. Rev. Mol. Cell Biol. 9, 255–262.

Katoh, Y., Terada, M., Nishijima, Y., Takei, R., Nozaki, S., Hamada, H., Nakayama, K., 2016. Overall Architecture of the Intraflagellar Transport (IFT)-B Complex Containing

Cluap1/IFT38 as an Essential Component of the IFT-B Peripheral Subcomplex. J. Biol. Chem. 291, 10962–10975.

Keil, T.A., 2012. Sensory cilia in arthropods. Arthropod Struct. Dev. 41, 515–534.

Kelley, L.A., Mezulis, S., Yates, C.M., Wass, M.N., Sternberg, M.J.E., 2015. The Phyre2 web portal for protein modeling, prediction and analysis. Nat. Protoc. 10, 845–858.

Kernan, M.J., 2007. Mechanotransduction and auditory transduction in Drosophila. Pflugers Arch. 454, 703–720.

Khanna, H., 2015. Photoreceptor Sensory Cilium: Traversing the Ciliary Gate. Cells 4, 674–686.

Khanna, H., Davis, E.E., Murga-Zamalloa, C.A., Estrada-Cuzcano, A., Lopez, I., den Hollander, A.I., Zonneveld, M.N., Othman, M.I., Waseem, N., Chakarova, C.F., Maubaret, C., Diaz-Font, A., MacDonald, I., Muzny, D.M., Wheeler, D.A., Morgan, M., Lewis, L.R., Logan, C.V., Tan, P.L., Beer, M.A., Inglehearn, C.F., Lewis, R.A., Jacobson, S.G., Bergmann, C., Beales, P.L., Attié-Bitach, T., Johnson, C.A., Otto, E.A., Bhattacharya, S.S., Hildebrandt, F., Gibbs, R.A., Koenekoop, R.K., Swaroop, A., Katsanis, N., 2009. A common allele in RPGRIP1L is a modifier of retinal degeneration in ciliopathies. Nat. Genet. 41, 739–745.

Kibbe, W.A., 2007. OligoCalc: an online oligonucleotide properties calculator. Nucleic Acids Res. 35, W43–W46.

Kim, J., Lee, J.E., Heynen-Genel, S., Suyama, E., Ono, K., Lee, K., Ideker, T., Aza-Blanc, P., Gleeson, J.G., 2010. Functional genomic screen for modulators of ciliogenesis and cilium length. Nature 464, 1048–1051.

Kim, S., Lee, K., Choi, J.-H., Ringstad, N., Dynlacht, B.D., 2015. Nek2 activation of Kif24 ensures cilium disassembly during the cell cycle. Nat. Commun. 6, 8087.

Kitagawa, D., Vakonakis, I., Olieric, N., Hilbert, M., Keller, D., Olieric, V., Bortfeld, M., Erat, M.C., Flückiger, I., Gönczy, P., Steinmetz, M.O., 2011. Structural basis of the 9-fold symmetry of centrioles. Cell 144, 364–375.

Koefoed, K., Veland, I.R., Pedersen, L.B., Larsen, L.A., Christensen, S.T., 2014. Cilia and coordination of signaling networks during heart development. Organogenesis 10, 108–125.

Kolesová, H., Čapek, M., Radochová, B., Janáček, J., Sedmera, D., 2016. Comparison of different tissue clearing methods and 3D imaging techniques for visualization of GFP-expressing mouse embryos and embryonic hearts. Histochem. Cell Biol. 146, 141–152.

Kong, D., Loncarek, J., 2015. Correlative light and electron microscopy analysis of the centrosome: A step-by-step protocol. Methods Cell Biol. 129, 1–18.

Kots, A.Y., Martin, E., Sharina, I.G., Murad, F., 2009. A short history of cGMP, guanylyl cyclases, and cGMP-dependent protein kinases. Handb. Exp. Pharmacol. 1–14.

Kozminski, K.G., 2012. Intraflagellar transport—the “new motility” 20 years later. Mol. Biol. Cell 23, 751–753.

Kozminski, K.G., Beech, P.L., Rosenbaum, J.L., 1995. The Chlamydomonas kinesin-like protein FLA10 is involved in motility associated with the flagellar membrane. J. Cell Biol. 131, 1517–1527.

Kozminski, K.G., Johnson, K.A., Forscher, P., Rosenbaum, J.L., 1993. A motility in the eukaryotic flagellum unrelated to flagellar beating. Proc. Natl. Acad. Sci. U. S. A. 90, 5519–5523.

Kuhn, M., 2016. Molecular Physiology of Membrane Guanylyl Cyclase Receptors. Physiol. Rev. 96, 751–804.

Kültz, D., 2005. Molecular and evolutionary basis of the cellular stress response. Annu. Rev. Physiol. 67, 225–257.

Kuzhandaivel, A., Schultz, S.W., Alkhori, L., Alenius, M., 2014. Cilia-mediated hedgehog signaling in Drosophila. Cell Rep. 7, 672–680.

Labour, M.-N., Riffault, M., Christensen, S.T., Hoey, D.A., 2016. TGFβ1 – induced recruitment of human bone mesenchymal stem cells is mediated by the primary cilium in a SMAD3-dependent manner. Sci. Rep. 6, srep35542.

Lambrus, B.G., Daggubati, V., Uetake, Y., Scott, P.M., Clutario, K.M., Sluder, G., Holland, A.J., 2016. A USP28-53BP1-p53-p21 signaling axis arrests growth after centrosome loss or prolonged mitosis. J. Cell Biol. 214, 143–153.

Lattao, R., Kovács, L., Glover, D.M., 2017. The Centrioles, Centrosomes, Basal Bodies, and Cilia of Drosophila melanogaster. Genetics 206, 33–53.

Lawo, S., Hasegan, M., Gupta, G.D., Pelletier, L., 2012. Subdiffraction imaging of centrosomes reveals higher-order organizational features of pericentriolar material. Nat. Cell Biol. 14, 1148–1158.

Le Guen, T., Ragu, S., Guirouilh-Barbat, J., Lopez, B.S., 2014. Role of the double-strand break repair pathway in the maintenance of genomic stability. Mol. Cell. Oncol. 2.

Lee, E., Sivan-Loukianova, E., Eberl, D.F., Kernan, M.J., 2008. An IFT-A protein is required to delimit functionally distinct zones in mechanosensory cilia. Curr. Biol. CB 18, 1899–1906.

Lee, J., Moon, S., Cha, Y., Chung, Y.D., 2010. Drosophila TRPN(=NOMPC) channel localizes to the distal end of mechanosensory cilia. PloS One 5, e11012.

Lehman, J.M., Michaud, E.J., Schoeb, T.R., Aydin-Son, Y., Miller, M., Yoder, B.K., 2008. The Oak Ridge Polycystic Kidney

mouse: Modeling ciliopathies of mice and men. Dev. Dyn. 237, 1960–1971.

Levine, M.S., Bakker, B., Boeckx, B., Moyett, J., Lu, J., Vitre, B., Spierings, D.C., Lansdorp, P.M., Cleveland, D.W., Lambrechts, D., Foijer, F., Holland, A.J., 2017. Centrosome Amplification Is Sufficient to Promote Spontaneous Tumorigenesis in Mammals. Dev. Cell 40, 313–322.e5.

Li, L., Xiao, X., Li, S., Jia, X., Wang, P., Guo, X., Jiao, X., Zhang, Q., Hejtmancik, J.F., 2011. Detection of variants in 15 genes in 87 unrelated Chinese patients with Leber congenital amaurosis. PloS One 6, e19458.

Li, S., Fernandez, J.-J., Marshall, W.F., Agard, D.A., 2012. Three-dimensional structure of basal body triplet revealed by electron cryo-tomography. EMBO J. 31, 552–562.

Liu, C.Y., Fraser, S.E., Koos, D.S., 2009. Grueneberg ganglion olfactory subsystem employs a cGMP signaling pathway. J. Comp. Neurol. 516, 36–48.

Lopes, C.A.M., Jana, S.C., Cunha-Ferreira, I., Zitouni, S., Bento, I., Duarte, P., Gilberto, S., Freixo, F., Guerrero, A., Francia, M., Lince-Faria, M., Carneiro, J., Bettencourt-Dias, M., 2015. PLK4 trans-Autoactivation Controls Centriole Biogenesis in Space. Dev. Cell 35, 222–235.

Lopes, S.S., Lourenço, R., Pacheco, L., Moreno, N., Kreiling, J., Saúde, L., 2010. Notch signalling regulates left-right asymmetry through ciliary length control. Development 137, 3625–3632.

Lucker, B.F., Behal, R.H., Qin, H., Siron, L.C., Taggart, W.D., Rosenbaum, J.L., Cole, D.G., 2005. Characterization of the intraflagellar transport complex B core: direct interaction of the IFT81 and IFT74/72 subunits. J. Biol. Chem. 280, 27688–27696.

Lukinavičius, G., Lavogina, D., Orpinell, M., Umezawa, K., Reymond, L., Garin, N., Gönczy, P., Johnsson, K., 2013. Selective chemical crosslinking reveals a Cep57-Cep63-Cep152 centrosomal complex. Curr. Biol. CB 23, 265–270.

Lynch, E.M., Hicks, D.R., Shepherd, M., Endrizzi, J.A., Maker, A., Hansen, J.M., Barry, R.M., Gitai, Z., Baldwin, E.P., Kollman, J.M., 2017. Human CTP synthase filament structure reveals the active enzyme conformation. Nat. Struct. Mol. Biol. 24, 507–514.

Mangeol, P., Prevo, B., Peterman, E.J.G., 2016. KymographClear and KymographDirect: two tools for the automated quantitative analysis of molecular and cellular dynamics using kymographs. Mol. Biol. Cell 27, 1948–1957.

Margulis, L., Chapman, M., Guerrero, R., Hall, J., 2006. The last eukaryotic common ancestor (LECA): acquisition of cytoskeletal motility from aerotolerant spirochetes in the Proterozoic Eon. Proc. Natl. Acad. Sci. U. S. A. 103, 13080–13085.

Marshall, W.F., 2009. Centriole Evolution. Curr. Opin. Cell Biol. 21, 14–19.

Marshall, W.F., Qin, H., Rodrigo Brenni, M., Rosenbaum, J.L., 2005. Flagellar length control system: testing a simple model based on intraflagellar transport and turnover. Mol. Biol. Cell 16, 270–278.

Marshall, W.F., Rosenbaum, J.L., 2001. Intraflagellar transport balances continuous turnover of outer doublet microtubules: implications for flagellar length control. J. Cell Biol. 155, 405–414.

Maruyama, I.N., 2016. Receptor Guanylyl Cyclases in Sensory Processing. Front. Endocrinol. 7, 173.

Marx, T., Gisselmann, G., Störtkuhl, K.F., Hovemann, B.T., Hatt, H., 1999. Molecular cloning of a putative voltage- and cyclic nucleotide-gated ion channel present in the antennae and eyes of Drosophila melanogaster. Invertebr. Neurosci. IN 4, 55–63.

Masters, B.R., 2009. History of the Electron Microscope in Cell Biology, in: John Wiley & Sons, Ltd (Ed.), Encyclopedia of Life Sciences. John Wiley & Sons, Ltd, Chichester, UK.

Matsuura, H., Sokabe, T., Kohno, K., Tominaga, M., Kadowaki, T., 2009. Evolutionary conservation and changes in insect TRP channels. BMC Evol. Biol. 9, 228.

Mazzarello, P., 1999. A unifying concept: the history of cell theory. Nat. Cell Biol. 1, E13-15.

McGuire, S.E., Le, P.T., Osborn, A.J., Matsumoto, K., Davis, R.L., 2003. Spatiotemporal rescue of memory dysfunction in Drosophila. Science 302, 1765–1768.

McIntosh, J.R., Hays, T., 2016. A Brief History of Research on Mitotic Mechanisms. Biology 5.

Meitinger, F., Anzola, J.V., Kaulich, M., Richardson, A., Stender, J.D., Benner, C., Glass, C.K., Dowdy, S.F., Desai, A., Shiau, A.K., Oegema, K., 2016. 53BP1 and USP28 mediate p53 activation and G1 arrest after centrosome loss or extended mitotic duration. J. Cell Biol. 214, 155–166.

Meunier, A., Spassky, N., 2016. Centriole continuity: out with the new, in with the old. Curr. Opin. Cell Biol. 38, 60–67.

Meyer, M.R., Angele, A., Kremmer, E., Kaupp, U.B., Müller, F., 2000. A cGMP-signaling pathway in a subset of olfactory sensory neurons. Proc. Natl. Acad. Sci. U. S. A. 97, 10595–10600.

Michalakis, S., Xu, J., Biel, M., Ding, X.-Q., 2013. Detection of cGMP in the degenerating retina. Methods Mol. Biol. Clifton NJ 1020, 235–245.

Mick, D.U., Rodrigues, R.B., Leib, R.D., Adams, C.M., Chien, A.S., Gygi, S.P., Nachury, M.V., 2015. Proteomics of Primary Cilia by Proximity Labeling. Dev. Cell 35, 497–512.

Milenkovic, L., Weiss, L.E., Yoon, J., Roth, T.L., Su, Y.S., Sahl, S.J., Scott, M.P., Moerner, W.E., 2015. Single-molecule imaging of Hedgehog pathway protein Smoothened in primary cilia reveals binding events regulated by Patched1. Proc. Natl. Acad. Sci. U. S. A. 112, 8320–8325.

Mishra, M., 2015. A quick method to investigate the Drosophila Johnston's organ by confocal microscopy. J. Microsc. Ultrastruct. 3, 1–7.

Miyamoto, T., Hosoba, K., Ochiai, H., Royba, E., Izumi, H., Sakuma, T., Yamamoto, T., Dynlacht, B.D., Matsuura, S., 2015. The Microtubule-Depolymerizing Activity of a Mitotic Kinesin Protein KIF2A Drives Primary Cilia Disassembly Coupled with Cell Proliferation. Cell Rep.

Mohan, S., Timbers, T.A., Kennedy, J., Blacque, O.E., Leroux, M.R., 2013. Striated rootlet and nonfilamentous forms of rootletin maintain ciliary function. Curr. Biol. CB 23, 2016–2022.

Montoliu, C., Llansola, M., Monfort, P., Corbalan, R., Fernandez-Marticorena, I., Hernandez-Viadel, M.L., Felipo, V., 2001. Role of nitric oxide and cyclic GMP in glutamate-induced neuronal death. Neurotox. Res. 3, 179–188.

Morton, D.B., 2004. Invertebrates yield a plethora of atypical guanylyl cyclases. Mol. Neurobiol. 29, 97–116.

Mostowy, S., Cossart, P., 2012. Septins: the fourth component of the cytoskeleton. Nat. Rev. Mol. Cell Biol. 13, 183–194.

Mourão, A., Christensen, S.T., Lorentzen, E., 2016. The intraflagellar transport machinery in ciliary signaling. Curr. Opin. Struct. Biol. 41, 98–108.

Mukhopadhyay, S., Wen, X., Chih, B., Nelson, C.D., Lane, W.S., Scales, S.J., Jackson, P.K., 2010. TULP3 bridges the IFT-A complex and membrane phosphoinositides to promote trafficking of G protein-coupled receptors into primary cilia. Genes Dev. 24, 2180–2193.

Muroyama, A., Lechler, T., 2017. Microtubule organization, dynamics and functions in differentiated cells. Dev. Camb. Engl. 144, 3012–3021.

Nachury, M.V., Loktev, A.V., Zhang, Q., Westlake, C.J., Peränen, J., Merdes, A., Slusarski, D.C., Scheller, R.H., Bazan, J.F., Sheffield, V.C., Jackson, P.K., 2007. A core complex of BBS proteins cooperates with the GTPase Rab8 to promote ciliary membrane biogenesis. Cell 129, 1201–1213.

Nakazawa, Y., Hiraki, M., Kamiya, R., Hirono, M., 2007. SAS-6 is a cartwheel protein that establishes the 9-fold symmetry of the centriole. Curr. Biol. CB 17, 2169–2174.

Nano, M., Basto, R., 2016. The Janus soul of centrosomes: a paradoxical role in disease? Chromosome Res. Int. J. Mol. Supramol. Evol. Asp. Chromosome Biol. 24, 127–144.

Newton, F.G., zur Lage, P.I., Karak, S., Moore, D.J., Göpfert, M.C., Jarman, A.P., 2012. Forkhead transcription factor Fd3F cooperates with Rfx to regulate a gene expression program for mechanosensory cilia specialization. Dev. Cell 22, 1221–1233.

Nielsen, H., 2017. Predicting Secretory Proteins with SignalP. Methods Mol. Biol. Clifton NJ 1611, 59–73.

Nowogrodzki, A., 2017. How to build a human cell atlas. Nature 547, 24–26.

Nüsslein-Volhard, C., Wieschaus, E., 1980. Mutations affecting segment number and polarity in Drosophila. Nature 287, 795–801.

O'Hagan, R., Piasecki, B.P., Silva, M., Phirke, P., Nguyen, K.C.Q., Hall, D.H., Swoboda, P., Barr, M.M., 2011. The tubulin deglutamylase CCPP-1 regulates the function and stability of sensory cilia in C. elegans. Curr. Biol. CB 21, 1685–1694.

Pan, J., Snell, W.J., 2014. Organelle Size: A Cilium Length Signal Regulates IFT Cargo Loading. Curr. Biol. 24, R75–R78.

Parisi, M., Glass, I., 2017. Joubert Syndrome, in: Adam, M.P., Ardinger, H.H., Pagon, R.A., Wallace, S.E., Bean, L.J., Mefford, H.C., Stephens, K., Amemiya, A., Ledbetter, N. (Eds.), GeneReviews(®). University of Washington, Seattle, Seattle (WA).

Park, J., Lee, J., Shim, J., Han, W., Lee, J., Bae, Y.C., Chung, Y.D., Kim, C.H., Moon, S.J., 2013. dTULP, the Drosophila melanogaster Homolog of Tubby, Regulates Transient Receptor Potential Channel Localization in Cilia. PLoS Genet. 9.

Pazour, G.J., Agrin, N., Leszyk, J., Witman, G.B., 2005. Proteomic analysis of a eukaryotic cilium. J. Cell Biol. 170, 103–113.

Pazour, G.J., Baker, S.A., Deane, J.A., Cole, D.G., Dickert, B.L., Rosenbaum, J.L., Witman, G.B., Besharse, J.C., 2002. The intraflagellar transport protein, IFT88, is essential for vertebrate photoreceptor assembly and maintenance. J. Cell Biol. 157, 103–113.

Pazour, G.J., Dickert, B.L., Vucica, Y., Seeley, E.S., Rosenbaum, J.L., Witman, G.B., Cole, D.G., 2000. Chlamydomonas IFT88 and its mouse homologue, polycystic kidney disease gene tg737, are required for assembly of cilia and flagella. J. Cell Biol. 151, 709–718.

Pazour, G.J., Wilkerson, C.G., Witman, G.B., 1998. A dynein light chain is essential for the retrograde particle movement of intraflagellar transport (IFT). J. Cell Biol. 141, 979–992.

Pearring, J.N., Spencer, W.J., Lieu, E.C., Arshavsky, V.Y., 2015. Guanylate cyclase 1 relies on rhodopsin for intracellular stability and ciliary trafficking. eLife 4.

Pearson, C.G., Osborn, D.P.S., Giddings, T.H., Beales, P.L., Winey, M., 2009. Basal body stability and ciliogenesis requires the conserved component Poc1. J. Cell Biol. 187, 905–920.

Perkins, L.A., Holderbaum, L., Tao, R., Hu, Y., Sopko, R., McCall, K., Yang-Zhou, D., Flockhart, I., Binari, R., Shim, H.-S., Miller, A., Housden, A., Foos, M., Randkelv, S., Kelley, C., Namgyal, P., Villalta, C., Liu, L.-P., Jiang, X., Huan-Huan, Q., Wang, X., Fujiyama, A., Toyoda, A., Ayers, K., Blum, A., Czech, B., Neumuller, R., Yan, D., Cavallaro, A., Hibbard, K., Hall, D., Cooley, L., Hannon, G.J., Lehmann, R., Parks, A., Mohr, S.E., Ueda, R., Kondo, S., Ni, J.-Q., Perrimon, N., 2015. The Transgenic RNAi Project at Harvard Medical School: Resources and Validation. Genetics 201, 843–852.

Pimenta-Marques, A., Bento, I., Lopes, C. a. M., Duarte, P., Jana, S.C., Bettencourt-Dias, M., 2016. A mechanism for the elimination of the female gamete centrosome in Drosophila melanogaster. Science 353, aaf4866.

Pollard, T.D., 2003. The cytoskeleton, cellular motility and the reductionist agenda. Nature 422, 741–745.

Praetorius, H.A., 2015. The primary cilium as sensor of fluid flow: new building blocks to the model. A review in the theme: cell signaling: proteins, pathways and mechanisms. Am. J. Physiol. Cell Physiol. 308, C198-208.

Praetorius, H.A., Spring, K.R., 2001. Bending the MDCK cell primary cilium increases intracellular calcium. J. Membr. Biol. 184, 71–79.

Prevo, B., Mangeol, P., Oswald, F., Scholey, J.M., Peterman, E.J.G., 2015. Functional differentiation of cooperating kinesin-2

motors orchestrates cargo import and transport in C. elegans cilia. Nat. Cell Biol. 17, 1536–1545.

Pugacheva, E.N., Jablonski, S.A., Hartman, T.R., Henske, E.P., Golemis, E.A., 2007. HEF1-dependent Aurora A activation induces disassembly of the primary cilium. Cell 129, 1351–1363.

Qin, H., Burnette, D.T., Bae, Y.-K., Forscher, P., Barr, M.M., Rosenbaum, J.L., 2005. Intraflagellar Transport Is Required for the Vectorial Movement of TRPV Channels in the Ciliary Membrane. Curr. Biol. 15, 1695–1699.

Qin, H., Rosenbaum, J.L., Barr, M.M., 2001. An autosomal recessive polycystic kidney disease gene homolog is involved in intraflagellar transport in C. elegans ciliated sensory neurons. Curr. Biol. CB 11, 457–461.

Reiter, J.F., Blacque, O.E., Leroux, M.R., 2012. The base of the cilium: roles for transition fibres and the transition zone in ciliary formation, maintenance and compartmentalization. EMBO Rep. 13, 608–618.

Reiter, J.F., Leroux, M.R., 2017. Genes and molecular pathways underpinning ciliopathies. Nat. Rev. Mol. Cell Biol. 18, 533–547.

Revenu, C., Athman, R., Robine, S., Louvard, D., 2004. The co-workers of actin filaments: from cell structures to signals. Nat. Rev. Mol. Cell Biol. 5, 635–646. doi:10.1038/nrm1437

Rich, D.R., Clark, A.L., 2012. Chondrocyte primary cilia shorten in response to osmotic challenge and are sites for endocytosis. Osteoarthritis Cartilage 20, 923–930.

Riparbelli, M.G., Colozza, G., Callaini, G., 2009. Procentriole elongation and recruitment of pericentriolar material are downregulated in cyst cells as they enter quiescence. J. Cell Sci. 122, 3613–3618.

Roca, A.I., Almada, A.E., Abajian, A.C., 2008. ProfileGrids as a new visual representation of large multiple sequence alignments: a case study of the RecA protein family. BMC Bioinformatics 9, 554.

Rodríguez, A. del V., Didiano, D., Desplan, C., 2011. Power tools for gene expression and clonal analysis in Drosophila. Nat. Methods 9, 47–55.

Rout, M.P., Field, M.C., 2017. The Evolution of Organellar Coat Complexes and Organization of the Eukaryotic Cell. Annu. Rev. Biochem. 86, 637–657.

Rozet, J.M., Perrault, I., Gerber, S., Hanein, S., Barbet, F., Ducroq, D., Souied, E., Munnich, A., Kaplan, J., 2001. Complete abolition of the retinal-specific guanylyl cyclase (retGC-1) catalytic ability consistently leads to leber congenital amaurosis (LCA). Invest. Ophthalmol. Vis. Sci. 42, 1190–1192.

Safieh, L.A., Al-Otaibi, H.M., Lewis, R.A., Kozak, I., 2016. Novel Mutations in Two Saudi Patients with Congenital Retinal Dystrophy. Middle East Afr. J. Ophthalmol. 23, 139–141.

Salvaterra, P.M., Kitamoto, T., 2001. Drosophila cholinergic neurons and processes visualized with Gal4/UAS-GFP. Brain Res. Gene Expr. Patterns 1, 73–82.

Sanchez, A.D., Feldman, J.L., 2017. Microtubule-organizing centers: from the centrosome to non-centrosomal sites. Curr. Opin. Cell Biol. 44, 93–101.

Sanchez, G.M., Alkhori, L., Hatano, E., Schultz, S.W., Kuzhandaivel, A., Jafari, S., Granseth, B., Alenius, M., 2016. Hedgehog Signaling Regulates the Ciliary Transport of Odorant Receptors in Drosophila. Cell Rep. 14, 464–470.

Sánchez, I., Dynlacht, B.D., 2016. Cilium assembly and disassembly. Nat. Cell Biol. 18, 711–717.

Sarpal, R., Todi, S.V., Sivan-Loukianova, E., Shirolikar, S., Subramanian, N., Raff, E.C., Erickson, J.W., Ray, K., Eberl, D.F., 2003. Drosophila KAP interacts with the kinesin II motor subunit KLP64D to assemble chordotonal sensory cilia, but not sperm tails. Curr. Biol. CB 13, 1687–1696.

Satir, P., 2017. CILIA: before and after. Cilia 6, 1.

Satir, P., 2005. Tour of organelles through the electron microscope: a reprinting of Keith R. Porter's classic Harvey Lecture with a new introduction. Anat. Rec. A. Discov. Mol. Cell. Evol. Biol. 287, 1184–1185.

Satir, P., Christensen, S.T., 2007. Overview of structure and function of mammalian cilia. Annu. Rev. Physiol. 69, 377–400.

Satir, P., Guerra, C., Bell, A.J., 2007. Evolution and persistence of the cilium. Cell Motil. Cytoskeleton 64, 906–913.

Satir, P., Pedersen, L.B., Christensen, S.T., 2010. The primary cilium at a glance. J. Cell Sci. 123, 499–503.

Schindelin, J., Arganda-Carreras, I., Frise, E., Kaynig, V., Longair, M., Pietzsch, T., Preibisch, S., Rueden, C., Saalfeld, S., Schmid, B., Tinevez, J.-Y., White, D.J., Hartenstein, V., Eliceiri, K., Tomancak, P., Cardona, A., 2012. Fiji: an open-source platform for biological-image analysis. Nat. Methods 9, 676–682.

Schleicher, M., Jockusch, B.M., 2008. Actin: its cumbersome pilgrimage through cellular compartments. Histochem. Cell Biol. 129, 695–704.

Schneider, L., Clement, C.A., Teilmann, S.C., Pazour, G.J., Hoffmann, E.K., Satir, P., Christensen, S.T., 2005. PDGFRalphaalpha signaling is regulated through the primary cilium in fibroblasts. Curr. Biol. CB 15, 1861–1866.

Senthilan, P.R., Piepenbrock, D., Ovezmyradov, G., Nadrowski, B., Bechstedt, S., Pauls, S., Winkler, M., Möbius, W., Howard, J.,

Göpfert, M.C., 2012. Drosophila auditory organ genes and genetic hearing defects. Cell 150, 1042–1054.

Serwas, D., Su, T.Y., Roessler, M., Wang, S., Dammermann, A., 2017. Centrioles initiate cilia assembly but are dispensable for maturation and maintenance in C. elegans. J. Cell Biol. 216, 1659–1671.

Sharma, R.K., Duda, T., 2014. Membrane guanylate cyclase, a multimodal transduction machine: history, present, and future directions. Front. Mol. Neurosci. 7, 56.

Sheehan, P., Zhu, M., Beskow, A., Vollmer, C., Waites, C.L., 2016. Activity-Dependent Degradation of Synaptic Vesicle Proteins Requires Rab35 and the ESCRT Pathway. J. Neurosci. 36, 8668–8686.

Sherwin, T., Schneider, A., Sasse, R., Seebeck, T., Gull, K., 1987. Distinct localization and cell cycle dependence of COOH terminally tyrosinolated alpha-tubulin in the microtubules of Trypanosoma brucei brucei. J. Cell Biol. 104, 439–446.

Shiao, M.-S., Fan, W.-L., Fang, S., Lu, M.-Y.J., Kondo, R., Li, W.-H., 2013. Transcriptional profiling of adult Drosophila antennae by high-throughput sequencing. Zool. Stud. 52, 42.

Simonelli, F., Ziviello, C., Testa, F., Rossi, S., Fazzi, E., Bianchi, P.E., Fossarello, M., Signorini, S., Bertone, C., Galantuomo, S., Brancati, F., Valente, E.M., Ciccodicola, A., Rinaldi, E., Auricchio, A., Banfi, S., 2007. Clinical and molecular genetics of Leber's congenital amaurosis: a multicenter study of Italian patients. Invest. Ophthalmol. Vis. Sci. 48, 4284–4290.

Simonnet, M.M., Berthelot-Grosjean, M., Grosjean, Y., 2014. Testing Drosophila Olfaction with a Y-maze Assay. J. Vis. Exp. JoVE.

Singhvi, A., Liu, B., Friedman, C.J., Fong, J., Lu, Y., Huang, X.-Y., Shaham, S., 2016. A Glial K/Cl Transporter Controls

Neuronal Receptive-Ending Shape by Chloride Inhibition of an rGC. Cell 165, 936–948.

Sluder, G., 2014. One to only two: a short history of the centrosome and its duplication. Philos. Trans. R. Soc. Lond. B. Biol. Sci. 369.

Song, L., Dentler, W.L., 2001. Flagellar protein dynamics in Chlamydomonas. J. Biol. Chem. 276, 29754–29763.

Sonnen, K.F., Schermelleh, L., Leonhardt, H., Nigg, E.A., 2012. 3D-structured illumination microscopy provides novel insight into architecture of human centrosomes. Biol. Open 1, 965–976.

Sönnichsen, B., Koski, L.B., Walsh, A., Marschall, P., Neumann, B., Brehm, M., Alleaume, A.-M., Artelt, J., Bettencourt, P., Cassin, E., Hewitson, M., Holz, C., Khan, M., Lazik, S., Martin, C., Nitzsche, B., Ruer, M., Stamford, J., Winzi, M., Heinkel, R., Röder, M., Finell, J., Häntsch, H., Jones, S.J.M., Jones, M., Piano, F., Gunsalus, K.C., Oegema, K., Gönczy, P., Coulson, A., Hyman, A.A., Echeverri, C.J., 2005. Full-genome RNAi profiling of early embryogenesis in Caenorhabditis elegans. Nature 434, 462–469.

Sorokin, S., 1962. Centrioles and the formation of rudimentary cilia by fibroblasts and smooth muscle cells. J. Cell Biol. 15, 363–377.

Sorokin, S.P., 1968. Reconstructions of centriole formation and ciliogenesis in mammalian lungs. J. Cell Sci. 3, 207–230.

Stepanek, L., Pigino, G., 2016. Microtubule doublets are double-track railways for intraflagellar transport trains. Science 352, 721–724.

Stinchcombe, J.C., Randzavola, L.O., Angus, K.L., Mantell, J.M., Verkade, P., Griffiths, G.M., 2015. Mother Centriole Distal Appendages Mediate Centrosome Docking at the

Immunological Synapse and Reveal Mechanistic Parallels with Ciliogenesis. Curr. Biol. CB 25, 3239–3244.

Stubbs, J., Oishi, I., Belmonte, J.C.I., Kintner, C., 2008. The Forkhead protein, FoxJ1, specifies node-like cilia in Xenopus and Zebrafish embryos. Nat. Genet. 40, 1454–1460.

Sun, Y., Liu, L., Ben-Shahar, Y., Jacobs, J.S., Eberl, D.F., Welsh, M.J., 2009. TRPA channels distinguish gravity sensing from hearing in Johnston's organ. Proc. Natl. Acad. Sci. U. S. A. 106, 13606–13611.

Takao, D., Verhey, K.J., 2016. Gated entry into the ciliary compartment. Cell. Mol. Life Sci. CMLS 73, 119–127.

Tang, N., Marshall, W.F., 2012. Centrosome positioning in vertebrate development. J. Cell Sci. 125, 4951–4961.

Tanos, B.E., Yang, H.-J., Soni, R., Wang, W.-J., Macaluso, F.P., Asara, J.M., Tsou, M.-F.B., 2013. Centriole distal appendages promote membrane docking, leading to cilia initiation. Genes Dev. 27, 163–168.

Taschner, M., Bhogaraju, S., Lorentzen, E., 2012. Architecture and function of IFT complex proteins in ciliogenesis. Differ. Res. Biol. Divers. 83, S12-22.

Taschner, M., Kotsis, F., Braeuer, P., Kuehn, E.W., Lorentzen, E., 2014. Crystal structures of IFT70/52 and IFT52/46 provide insight into intraflagellar transport B core complex assembly. J. Cell Biol. 207, 269–282.

Taschner, M., Lorentzen, E., 2016. The Intraflagellar Transport Machinery. Cold Spring Harb. Perspect. Biol. 8.

Taschner, M., Weber, K., Mourão, A., Vetter, M., Awasthi, M., Stiegler, M., Bhogaraju, S., Lorentzen, E., 2016. Intraflagellar transport proteins 172, 80, 57, 54, 38, and 20 form a stable tubulin-binding IFT-B2 complex. EMBO J. 35, 773–790.

Thoma, C.R., Frew, I.J., Hoerner, C.R., Montani, M., Moch, H., Krek, W., 2007. pVHL and GSK3beta are components of a primary cilium-maintenance signalling network. Nat. Cell Biol. 9, 588–595.

Thompson, C.L., Wiles, A., Poole, C.A., Knight, M.M., 2016. Lithium chloride modulates chondrocyte primary cilia and inhibits Hedgehog signaling. FASEB J. 30, 716–726.

Tian, L., Hires, S.A., Mao, T., Huber, D., Chiappe, M.E., Chalasani, S.H., Petreanu, L., Akerboom, J., McKinney, S.A., Schreiter, E.R., Bargmann, C.I., Jayaraman, V., Svoboda, K., Looger, L.L., 2009. Imaging neural activity in worms, flies and mice with improved GCaMP calcium indicators. Nat. Methods 6, 875–881.

Todi, S.V., Sharma, Y., Eberl, D.F., 2004. Anatomical and Molecular Design of the Drosophila Antenna as a Flagellar Auditory Organ. Microsc. Res. Tech. 63, 388–399.

Toropova, K., Mladenov, M., Roberts, A.J., 2017. Intraflagellar transport dynein is autoinhibited by trapping of its mechanical and track-binding elements. Nat. Struct. Mol. Biol. 24, 461–468.

Toyama, B.H., Savas, J.N., Park, S.K., Harris, M.S., Ingolia, N.T., Yates, J.R., Hetzer, M.W., 2013. Identification of long-lived proteins reveals exceptional stability of essential cellular structures. Cell 154, 971–982.

Tran, P.V., Haycraft, C.J., Besschetnova, T.Y., Turbe-Doan, A., Stottmann, R.W., Herron, B.J., Chesebro, A.L., Qiu, H., Scherz, P.J., Shah, J.V., Yoder, B.K., Beier, D.R., 2008. THM1 negatively modulates mouse sonic hedgehog signal transduction and affects retrograde intraflagellar transport in cilia. Nat. Genet. 40, 403–410.

Trapnell, C., 2015. Defining cell types and states with single-cell genomics. Genome Res. 25, 1491–1498.

Trivedi, D., Colin, E., Louie, C.M., Williams, D.S., 2012. Live-cell imaging evidence for the ciliary transport of rod photoreceptor opsin by heterotrimeric kinesin-2. J. Neurosci. Off. J. Soc. Neurosci. 32, 10587–10593.

Tsujikawa, M., Malicki, J., 2004. Intraflagellar transport genes are essential for differentiation and survival of vertebrate sensory neurons. Neuron 42, 703–716.

Tucker, C.L., Ramamurthy, V., Pina, A.-L., Loyer, M., Dharmaraj, S., Li, Y., Maumenee, I.H., Hurley, J.B., Koenekoop, R.K., 2004. Functional analyses of mutant recessive GUCY2D alleles identified in Leber congenital amaurosis patients: protein domain comparisons and dominant negative effects. Mol. Vis. 10, 297–303.

Vaisse, C., Reiter, J.F., Berbari, N.F., 2017. Cilia and Obesity. Cold Spring Harb. Perspect. Biol. 9.

Vale, R.D., 2014. Preface: the role of reconstitution in cytoskeleton research. Methods Enzymol. 540, xix–xxiii.

van Breugel, M., Hirono, M., Andreeva, A., Yanagisawa, H., Yamaguchi, S., Nakazawa, Y., Morgner, N., Petrovich, M., Ebong, I.-O., Robinson, C.V., Johnson, C.M., Veprintsev, D., Zuber, B., 2011. Structures of SAS-6 suggest its organization in centrioles. Science 331, 1196–1199.

van Dam, T.J.P., Townsend, M.J., Turk, M., Schlessinger, A., Sali, A., Field, M.C., Huynen, M.A., 2013. Evolution of modular intraflagellar transport from a coatomer-like progenitor. Proc. Natl. Acad. Sci. U. S. A. 110, 6943–6948.

Verma, A., Perumalsamy, V., Shetty, S., Kulm, M., Sundaresan, P., 2013. Mutational screening of LCA genes emphasizing

RPE65 in South Indian cohort of patients. PloS One 8, e73172.

Vermehren-Schmaedick, A., Ainsley, J.A., Johnson, W.A., Davies, S.-A., Morton, D.B., 2010. Behavioral responses to hypoxia in Drosophila larvae are mediated by atypical soluble guanylyl cyclases. Genetics 186, 183–196.

Vermehren-Schmaedick, A., Scudder, C., Timmermans, W., Morton, D.B., 2011. Drosophila gustatory preference behaviors require the atypical soluble guanylyl cyclases. J. Comp. Physiol. A Neuroethol. Sens. Neural. Behav. Physiol. 197, 717–727.

Vieillard, J., Duteyrat, J.-L., Cortier, E., Durand, B., 2015. Imaging cilia in Drosophila melanogaster. Methods Cell Biol. 127, 279–302.

Vieillard, J., Paschaki, M., Duteyrat, J.-L., Augière, C., Cortier, E., Lapart, J.-A., Thomas, J., Durand, B., 2016. Transition zone assembly and its contribution to axoneme formation in Drosophila male germ cells. J Cell Biol 214, 875–889.

Vivier, E., van de Pavert, S.A., Cooper, M.D., Belz, G.T., 2016. The evolution of innate lymphoid cells. Nat. Immunol. 17, 790–794.

Wang, J., Silva, M., Haas, L., Morsci, N., Nguyen, K.C.Q., Hall, D.H., Barr, M.M., 2014. C. elegans ciliated sensory neurons release extracellular vesicles that function in animal communication. Curr. Biol. CB 24, 519–525.

Wang, W.-J., Soni, R.K., Uryu, K., Tsou, M.-F.B., 2011. The conversion of centrioles to centrosomes: essential coupling of duplication with segregation. J. Cell Biol. 193, 727–739.

Waters, A.M., Beales, P.L., 2011. Ciliopathies: an expanding disease spectrum. Pediatr. Nephrol. Berl. Ger. 26, 1039–1056.

Wei, Q., Zhang, Y., Li, Y., Zhang, Q., Ling, K., Hu, J., 2012. The BBSome controls IFT assembly and turnaround in cilia. Nat. Cell Biol. 14, 950–957.

Weleber, R.G., Francis, P.J., Trzupek, K.M., Beattie, C., 2013. Leber Congenital Amaurosis, in: Pagon, R.A., Adam, M.P., Ardinger, H.H., Wallace, S.E., Amemiya, A., Bean, L.J., Bird, T.D., Ledbetter, N., Mefford, H.C., Smith, R.J., Stephens, K. (Eds.), GeneReviews(®). University of Washington, Seattle, Seattle (WA).

Wells, W.A., 2005a. Microtubules get a name. J. Cell Biol. 168, 852–853.

Wells, W.A., 2005b. The discovery of tubulin. J. Cell Biol. 169, 552–552.

Wheatley, D.N., Wang, A.M., Strugnell, G.E., 1996. Expression of primary cilia in mammalian cells. Cell Biol. Int. 20, 73–81.

Wheway, G., Schmidts, M., Mans, D.A., Szymanska, K., Nguyen, T.-M.T., Racher, H., Phelps, I.G., Toedt, G., Kennedy, J., Wunderlich, K.A., Sorusch, N., Abdelhamed, Z.A., Natarajan, S., Herridge, W., van Reeuwijk, J., Horn, N., Boldt, K., Parry, D.A., Letteboer, S.J.F., Roosing, S., Adams, M., Bell, S.M., Bond, J., Higgins, J., Morrison, E.E., Tomlinson, D.C., Slaats, G.G., van Dam, T.J.P., Huang, L., Kessler, K., Giessl, A., Logan, C.V., Boyle, E.A., Shendure, J., Anazi, S., Aldahmesh, M., Al Hazzaa, S., Hegele, R.A., Ober, C., Frosk, P., Mhanni, A.A., Chodirker, B.N., Chudley, A.E., Lamont, R., Bernier, F.P., Beaulieu, C.L., Gordon, P., Pon, R.T., Donahue, C., Barkovich, A.J., Wolf, L., Toomes, C., Thiel, C.T., Boycott, K.M., McKibbin, M., Inglehearn, C.F., UK10K Consortium, University of Washington Center for Mendelian Genomics, Stewart, F., Omran, H., Huynen, M.A., Sergouniotis, P.I., Alkuraya, F.S., Parboosingh, J.S., Innes,

A.M., Willoughby, C.E., Giles, R.H., Webster, A.R., Ueffing, M., Blacque, O., Gleeson, J.G., Wolfrum, U., Beales, P.L., Gibson, T., Doherty, D., Mitchison, H.M., Roepman, R., Johnson, C.A., 2015. An siRNA-based functional genomics screen for the identification of regulators of ciliogenesis and ciliopathy genes. Nat. Cell Biol. 17, 1074–1087.

Wickham, H., 2016. ggplot2: Elegant Graphics for Data Analysis. Springer.

Williams, C.L., McIntyre, J.C., Norris, S.R., Jenkins, P.M., Zhang, L., Pei, Q., Verhey, K., Martens, J.R., 2014. Direct evidence for BBSome-associated intraflagellar transport reveals distinct properties of native mammalian cilia. Nat. Commun. 5, 5813.

Winey, M., O'Toole, E., 2014. Centriole structure. Philos. Trans. R. Soc. Lond. B. Biol. Sci. 369.

Wingfield, J.L., Mengoni, I., Bomberger, H., Jiang, Y.-Y., Walsh, J.D., Brown, J.M., Picariello, T., Cochran, D.A., Zhu, B., Pan, J., Eggenschwiler, J., Gaertig, J., Witman, G.B., Kner, P., Lechtreck, K., 2017. IFT trains in different stages of assembly queue at the ciliary base for consecutive release into the cilium. eLife 6.

Wisdom, K.M., Delp, S.L., Kuhl, E., 2015. Use it or lose it: multiscale skeletal muscle adaptation to mechanical stimuli. Biomech. Model. Mechanobiol. 14, 195–215.

Witman, G.B., Carlson, K., Berliner, J., Rosenbaum, J.L., 1972. Chlamydomonas flagella. I. Isolation and electrophoretic analysis of microtubules, matrix, membranes, and mastigonemes. J. Cell Biol. 54, 507–539.

Wojnacki, J., Quassollo, G., Marzolo, M.-P., Cáceres, A., 2014. Rho GTPases at the crossroad of signaling networks in mammals. Small GTPases 5.

Wong, S.Y., Seol, A.D., So, P.-L., Ermilov, A.N., Bichakjian, C.K., Epstein, E.H., Dlugosz, A.A., Reiter, J.F., 2009. Primary cilia can both mediate and suppress Hedgehog pathway–dependent tumorigenesis. Nat. Med. 15, 1055–1061.

Woodruff, J.B., Ferreira Gomes, B., Widlund, P.O., Mahamid, J., Honigmann, A., Hyman, A.A., 2017. The Centrosome Is a Selective Condensate that Nucleates Microtubules by Concentrating Tubulin. Cell 169, 1066–1077.e10.

Woodruff, J.B., Wueseke, O., Hyman, A.A., 2014. Pericentriolar material structure and dynamics. Phil Trans R Soc B 369, 20130459.

Wyatt, T.A., 2015. Cyclic GMP and Cilia Motility. Cells 4, 315–330.

Xiang, W., Guo, F., Cheng, W., Zhang, J., Huang, J., Wang, R., Ma, Z., Xu, K., 2017. HDAC6 inhibition suppresses chondrosarcoma by restoring the expression of primary cilia. Oncol. Rep.

Xu, Y., Xiao, X., Li, S., Jia, X., Xin, W., Wang, P., Sun, W., Huang, L., Guo, X., Zhang, Q., 2016. Molecular genetics of Leber congenital amaurosis in Chinese: New data from 66 probands and mutation overview of 159 probands. Exp. Eye Res. 149, 93–99.

Yang, J., Gao, J., Adamian, M., Wen, X.-H., Pawlyk, B., Zhang, L., Sanderson, M.J., Zuo, J., Makino, C.L., Li, T., 2005. The ciliary rootlet maintains long-term stability of sensory cilia. Mol. Cell. Biol. 25, 4129–4137.

Yang, T.T., Chong, W.M., Liao, J.-C., 2016. STED and STORM Superresolution Imaging of Primary Cilia, in: Cilia, Methods in Molecular Biology. Humana Press, New York, NY, pp. 169–192.

Yates, A., Akanni, W., Amode, M.R., Barrell, D., Billis, K., Carvalho-Silva, D., Cummins, C., Clapham, P., Fitzgerald, S., Gil, L.,

Girón, C.G., Gordon, L., Hourlier, T., Hunt, S.E., Janacek, S.H., Johnson, N., Juettemann, T., Keenan, S., Lavidas, I., Martin, F.J., Maurel, T., McLaren, W., Murphy, D.N., Nag, R., Nuhn, M., Parker, A., Patricio, M., Pignatelli, M., Rahtz, M., Riat, H.S., Sheppard, D., Taylor, K., Thormann, A., Vullo, A., Wilder, S.P., Zadissa, A., Birney, E., Harrow, J., Muffato, M., Perry, E., Ruffier, M., Spudich, G., Trevanion, S.J., Cunningham, F., Aken, B.L., Zerbino, D.R., Flicek, P., 2016. Ensembl 2016. Nucleic Acids Res. 44, D710-716.

Ye, F., Breslow, D.K., Koslover, E.F., Spakowitz, A.J., Nelson, W.J., Nachury, M.V., 2013. Single molecule imaging reveals a major role for diffusion in the exploration of ciliary space by signaling receptors. eLife 2.

Ye, J., Coulouris, G., Zaretskaya, I., Cutcutache, I., Rozen, S., Madden, T.L., 2012. Primer-BLAST: a tool to design target-specific primers for polymerase chain reaction. BMC Bioinformatics 13, 134.

Yorozu, S., Wong, A., Fischer, B.J., Dankert, H., Kernan, M.J., Kamikouchi, A., Ito, K., Anderson, D.J., 2009. Distinct sensory representations of wind and near-field sound in the Drosophila brain. Nature 458, 201–205.

Zägel, P., Koch, K.-W., 2014. Dysfunction of outer segment guanylate cyclase caused by retinal disease related mutations. Front. Mol. Neurosci. 7, 4.

Zampieri, F., Coen, M., Gabbiani, G., 2014. The prehistory of the cytoskeleton concept. Cytoskelet. Hoboken NJ 71, 464–471.

Zernant, J., Külm, M., Dharmaraj, S., den Hollander, A.I., Perrault, I., Preising, M.N., Lorenz, B., Kaplan, J., Cremers, F.P.M., Maumenee, I., Koenekoop, R.K., Allikmets, R., 2005. Genotyping microarray (disease chip) for Leber congenital

amaurosis: detection of modifier alleles. Invest. Ophthalmol. Vis. Sci. 46, 3052–3059.

Zhang, W., Cheng, L.E., Kittelmann, M., Li, J., Petkovic, M., Cheng, T., Jin, P., Guo, Z., Göpfert, M.C., Jan, L.Y., Jan, Y.N., 2015. Ankyrin Repeats Convey Force to Gate the NOMPC Mechanotransduction Channel. Cell 162, 1391–1403.

Zhang, W., Yan, Z., Jan, L.Y., Jan, Y.N., 2013. Sound response mediated by the TRP channels NOMPC, NANCHUNG, and INACTIVE in chordotonal organs of Drosophila larvae. Proc. Natl. Acad. Sci. U. S. A. 110, 13612–13617.

Zhang, Y., Kwon, S., Yamaguchi, T., Cubizolles, F., Rousseaux, S., Kneissel, M., Cao, C., Li, N., Cheng, H.-L., Chua, K., Lombard, D., Mizeracki, A., Matthias, G., Alt, F.W., Khochbin, S., Matthias, P., 2008. Mice lacking histone deacetylase 6 have hyperacetylated tubulin but are viable and develop normally. Mol. Cell. Biol. 28, 1688–1701.

Zitouni, S., Francia, M.E., Leal, F., Montenegro Gouveia, S., Nabais, C., Duarte, P., Gilberto, S., Brito, D., Moyer, T., Kandels-Lewis, S., Ohta, M., Kitagawa, D., Holland, A.J., Karsenti, E., Lorca, T., Lince-Faria, M., Bettencourt-Dias, M., 2016. CDK1 Prevents Unscheduled PLK4-STIL Complex Assembly in Centriole Biogenesis. Curr. Biol. CB 26, 1127–1137.

Zwicker, D., Decker, M., Jaensch, S., Hyman, A.A., Jülicher, F., 2014. Centrosomes are autocatalytic droplets of pericentriolar material organized by centrioles. Proc. Natl. Acad. Sci. U. S. A. 111, E2636-2645.